UNIVERSIDADE DE LISBOA

FACULDADE DE MEDICINA

Molecular mechanisms by which low doses of ionizing radiation promote neovascularization in ischemic tissues

Paula Alexandra Gomes de Oliveira

Orientadora: Professora Doutora Susana Constantino Rosa Santos

Tese especialmente elaborada para a obtenção do grau de Doutor em Ciências Biomédicas - Especialidade em Biologia Celular e Molecular

2017

UNIVERSIDADE DE LISBOA

FACULDADE DE MEDICINA

Molecular mechanisms by which low doses of ionizing radiation promote neovascularization in ischemic tissues

Paula Alexandra Gomes de Oliveira

Orientadora: Professora Doutora Susana Constantino Rosa Santos

Tese especialmente elaborada para a obtenção do grau de Doutor em Ciências Biomédicas - Especialidade em Biologia Celular e Molecular

Júri:

Presidente: Doutor José Luís Bliebernicht Ducla Soares, Professor Catedrático em regime de *tenure* e Vice-Presidente do Conselho Científico da Faculdade de Medicina da Universidade de Lisboa, Presidente do Júri

Vogais: Doutora Raquel Ângela Silva Soares Lino, Professora Catedrática da Faculdade de Medicina da Universidade do Porto;
Doutora Maria José Cardoso Oliveira, Professora Auxiliar Convidada da Faculdade de Ciências da Universidade do Porto;
Doutor Cláudio Areias Franco, Investigador do Instituto de Medicina Molecular, unidade de investigação associada à Faculdade de Medicina da Universidade de Lisboa;
Doutora Maria Isabel de Freitas Ferreira Queimado Monteiro Grillo, Professora Associada Convidada Aposentada da Faculdade de Medicina da Universidade de Lisboa;
Doutor Sérgio Jerónimo Rodrigues Dias, Professor Associado Convidado da Faculdade de Medicina da Universidade de Lisboa;
Doutora Susana Constantino Rosa Santos, Professora Auxiliar da Faculdade de Medicina da Universidade de Lisboa; *(Orientadora)*

Bolsa de Doutoramento SFRH/BD/80483/2011 financiada pela Fundação para a Ciência e Tecnologia

2017

Preface

The work presented in this Thesis is derived from my Ph.D. research, made possible primarily by the Ph.D. fellowship ref. SFRH/BD/80483/2011, from *Fundação para a Ciência e a Tecnologia* (FCT), *Ministério da Ciência, Tecnologia e Ensino Superior* (MCTES), Portugal. This study, carried out between 2012 and 2016, was integrated in the Ph.D. program of *Centro Académico de Medicina de Lisboa* (CAML), which is shared between *Instituto de Medicina Molecular* (IMM, Lisbon, Portugal), *Faculdade de Medicina da Universidade de Lisboa* (FMUL, Lisbon, Portugal) and Hospital Santa Maria, Centro Hospitalar Lisboa Norte (HSM-CHLN, Lisbon, Portugal). The work took place at the Angiogenesis Lab, at *Centro Cardiovascular da Universidade de Lisboa* (CCUL), under the supervision of Prof. Susana Constantino (CCUL/FMUL).

This thesis is constituted by five chapters, which are preceded by a summary, both in Portuguese and in English. Chapter I consists of a general introduction to blood vessels, with particular emphasis on the angiogenic process, approached from the early embryonic development to adulthood, in physiology and pathology, arteriogenesis and postnatal neovascularization. A brief overview about the cellular and molecular effects of ionizing radiation is also presented. Chapter II specifically indicates the main objectives of the research proposal that led to the work presented in this thesis. Chapter III and IV include the experimental work developed through the research project. Chapter III, **Low-dose ionizing radiation induces therapeutic neovascularization in a pre-clinical model of hindlimb ischemia**, includes already published work (presented in word format) in Cardiovascular Research journal. Chapter IV, **Low-dose ionizing radiation promotes neovascularization in experimentally induced diabetic mice subjected to hindlimb ischemia**, includes results from ongoing work that is currently being developed in our lab and has not yet been published. Both results chapters include an abstract, a specific introduction, the results obtained in the work developed, and a focused discussion, as well as the methods and the references. In Chapter V, conclusions are integrated and discussed, generating new testable hypotheses which comprise the foreseen future directions of our research in this field.

As opiniões expressas nesta publicação são da exclusiva responsabilidade do seu autor.

A impressão desta Tese foi aprovada pelo Conselho Científico da Faculdade de Medicina de Lisboa em reunião de 18 de Julho de 2017.

Acknowledgements

Ao longo deste doutoramento muitas foram as pessoas com quem me cruzei e que contribuíram para o sucesso deste trabalho. Nesta secção da minha tese quero deixar um agradecimento especial a todos os que considerei fundamentais para a realização deste trabalho. Foram anos de muita aprendizagem e crescimento científico, mas principalmente humano. Agora sei com mais certeza que não há caminho, o caminho faz-se a andar e sem dúvida que a vida se resolve sozinha!

Começo por agradecer à minha orientadora, a Professora Susana Constantino, por me ter recebido na Unidade de Angiogénese e por ter acreditado em mim dando-me a oportunidade de crescer a nível científico. Obrigada pelo apoio, profissional, mas também pessoal, que sempre demonstrou ao longo destes anos permitindo-me desenvolver este trabalho com espírito crítico e perfecionismo.

À Fundação para a Ciência e Tecnologia, pela minha bolsa de doutoramento SFRH/BD/80483/2011, financiada por fundos nacionais do Ministério da Ciência, Tecnologia e Ensino Superior.

Ao serviço de Radioterapia, do Hospital de Santa Maria, sem o qual não teria sido possível realizar este trabalho. Gostaria de agradecer particularmente o apoio da Doutora Isabel Monteiro Grilo, na qualidade de ex-diretora do serviço de Radioterapia, que abraçou este projeto e possibilitou o seu início, da Doutora Marília Jorge, também na qualidade de ex-diretora do serviço, e que proporcionou a continuidade do trabalho apoiando-o incondicionalmente, e da Doutora Filomena Pina, na qualidade de atual diretora do serviço de Radioterapia, que sempre demonstrou interesse no trabalho possibilitando também a sua continuidade. Obrigada à Doutora Esmeralda Poli, na qualidade de responsável da Unidade de Física Médica, e à sua equipa por todo o apoio. Obrigada à técnica Ana Duarte pela ajuda no planeamento e dosimetria. Obrigada à técnica coordenadora Isabel Diegues e a toda a sua equipa pela ajuda nas sessões de irradiação ao longo destes anos.

Ao biotério de Roedores do Instituto de Medicina Molecular, com especial agradecimento à Joana, Dolores, Iolanda e Carlos, por se mostrarem sempre disponíveis e por todo o apoio ao longo destes anos.

Ao Laboratório de Histologia Patologia Comparada do Instituto de Medicina Molecular, Tânia, Andreia, Ana e Bruna, obrigada pelo apoio e pela ajuda nas muitas urgências que surgiram.
Um agradecimento especial para ti Andreia! Conhecemo-nos através de um crióstato e um músculo congelado mas hoje somos muito mais. Obrigada por sempre arranjares um tempinho para os meus cortes, pelas dicas de trabalho, mas principalmente pela amizade, pelas conversas tanto sérias como triviais. É tão bom partilhar histórias de crianças e melhor ainda vê-los juntos!

Ao serviço de Citometria de Fluxo do Instituto de Medicina Molecular, Maria Soares e Ana Vieira, obrigada pelo apoio e ensinamentos sobre FACS.

Ao serviço de Bioimagem do Instituto de Medicina Molecular, Rino, António e Ana, obrigada por todo o apoio em todos os microscópios que usei. Foram incansáveis na procura da melhor imagem.

Ao Professor João O'Neill, da Faculdade de Ciências Médicas da Universidade Nova de Lisboa, obrigada por todo o apoio e dedicação na implementação da técnica de diafanização em pequenos animais possibilitando a obtenção de excelentes imagens. Foi um prazer conhecer o seu laboratório e o trabalho que tem vindo a realizar.

A todos os membros da Unidade de Agiogénese que conheci ao longo destes anos e com quem partilhei o meu dia: André, Adriana, Andreia, Carolina, Joana, Liliana, Teresa Freitas (tem sido um apoio para mim desde o primeiro dia, obrigada por partilhar o dia comigo), Carolina Cardina (tens um lugar especial no meu coração), Rita (gostei muito de te conhecer).

Um especial agradecimento à Raquel, foi contigo que tudo começou, deste-me as primeiras introduções sobre o mundo da angiogénese e foi tão bom partilhar o laboratório e o dia contigo. A tua boa disposição era contagiante, tive saudades tuas ao longo deste tempo.
Augusto, também para ti um especial obrigada, pela disponibilidade imediata sempre que programávamos isquémias, claro que tínhamos de começar o dia sempre de madrugada mas a boa disposição compensava e o tempo passava sem darmos conta.
Filipa, foste a minha companheira de laboratório durante estes anos, partilhávamos o gosto em ter tudo arrumado. Um grande obrigada, pela disponibilidade que sempre tiveste para me ajudar e lembro-me particularmente duma noite complicada em que fizeste de babysistter e saíste-te muito bem, o miúdo gosta de ti! Obrigada também pelos cafés, pelas conversas e pelos olhares!
Ana, a tua chegada ao grupo é recente, mas sinto que foste fundamental. Muito obrigada pela disponibilidade e apoio, pelas conversas otimistas e pelas correções na escrita desta tese.

Ao meu colega e amigo Daniel pela amizade e companheirismo ao longo dos muitos anos que nos conhecemos. Obrigada pela ajuda, principalmente na formatação desta tese.

À minha amiga Sónia, para mim um modelo de perfecionismo e de rigor. Muito me ensinaste ao longo destes anos, ensinamentos científicos, mas também de vida. E quando a vida complicou tu descobriste a farmácia onde estava aquele leite tão difícil de encontrar… Obrigada por tudo, mantem-te aí!

À minha amiga Filomena, conhecemo-nos há muitos anos e tem sido muito bom saber que te tenho no laboratório/gabinete ao lado. Foram muitas as nossas partilhas ao longo dos últimos anos, científicas, mas também pessoais. Obrigada por me inspirares e por tantas vezes me dizeres para continuar!

Aos meus pais, Hortense e Ivo, pelo exemplo de vida e pelos valores com que me educaram, pelo incentivo e apoio em todos os meus desafios. Pelo imenso amor, por cuidarem sempre tão bem, por estarem sempre presentes, pela ajuda constante, pelas conversas que me levam ou trazem. Um obrigada nunca será suficiente, tentarei sempre fazer o meu melhor!

Ao meu marido Ricardo, mais uma etapa que concluímos juntos. Sabemos que somos uma boa equipa, rearranjamos os dias e modificamos as noites, mas conseguimos. Obrigada pelo amor, carinho e dedicação à nossa família, por tornares tudo mais fácil, por estares disponível sempre que precisei/precisamos. *Love you!*

Ao meu querido filho Martim, que enche os meus dias de luz e de um amor sem fim. Nesta nossa dança muito me tens ensinado, nasceste no início deste doutoramento e tens sido a melhor companhia, meu menino doce de abraço apertado e gargalhada fácil. Quando nos despedimos de manhã dizes "*mãe, faz coisas bonitas no teu trabalho*", a mãe tentará sempre fazer coisas bonitas!

A ti, meu querido Martim, eu dedico esta tese e de agora em diante *"vou pedir ao tempo que me dê mais tempo para olhar para ti…" (Mariza - o tempo não pára)*

Resumo

O sistema circulatório ou cardiovascular é formado pelo coração e vasos sanguíneos e a sua função é levar oxigénio e nutrientes aos órgãos e tecidos do corpo. A doença cardiovascular, de que é exemplo a doença arterial periférica (DAP) é uma das principais causas de mortalidade e morbilidade na população mundial. Estima-se que mais de 25 milhões de pessoas na Europa e nos Estados Unidos apresentem DAP, e a sua incidência tende a aumentar. Importantes fatores de risco para a DAP são a diabetes, tabagismo, hipertensão e dislipidemia. A DAP caracteriza-se por uma obstrução do lúmen arterial, resultando num défice de fluxo sanguíneo aos tecidos cuja principal consequência é a presença de sintomas característicos de isquemia. A manifestação mais frequente de DAP é a claudicação intermitente, que é caracterizada por desconforto muscular no membro inferior, produzido pelo exercício, e que alivia com o repouso. A claudicação tem um impacto negativo na qualidade de vida dos doentes, quer a nível profissional, quer interferindo com as suas atividades sociais. A isquemia crítica dos membros inferiores é a manifestação clínica mais grave da DAP, que descreve doentes com dor em repouso ou com lesões tróficas cutâneas, sejam elas úlceras ou gangrena. Aproximadamente 1% dos doentes com DAP apresentam o estado avançado da doença. As limitações dos procedimentos de revascularização, resultantes da extensão e distribuição anatómica da doença arterial, e do tratamento farmacológico, são bem conhecidas. Assim, a amputação surge como última alternativa terapêutica, apesar das taxas de morbilidade e mortalidade associadas. Na última década vários estudos têm vindo a ser desenvolvidos com o objetivo de encontrar tratamentos alternativos, incluindo a angiogénese terapêutica.

A angiogénese terapêutica, a qual pode ser alcançada através da administração local de fatores de crescimento pró-angiogénicos na forma de proteína recombinante ou de células progenitoras endoteliais (CEPs) ou mesmo recorrendo à terapia génica, oferece uma possibilidade de recuperação para estes pacientes. Apesar dos estudos pré-clínicos e de alguns ensaios clínicos em fase I/II mostrarem-se bastante promissores, a progressão desses ensaios clínicos para terapias angiogénicas não têm revelado um efeito benéfico em doentes com isquemia crítica dos membros inferiores. Também o pouco conhecimento sobre os agentes angiogénicos envolvidos, nomeadamente a dose, a frequência e o método de administração têm contribuído para o fracasso dos ensaios clínicos.

No passado, o nosso grupo de investigação demonstrou que baixas doses de radiação ionizante (BDRI) promovem angiogénese durante o desenvolvimento embrionário e no processo de regeneração da barbatana caudal do *peixe zebra*. Assim, de acordo com os nossos resultados as BDRI induzem angiogénese *in vivo*, mas não existe prova de que produzam angiogénese terapêutica em doentes com doença isquémica, sendo este o propósito deste trabalho de doutoramento. Assim, o presente trabalho tem como objetivo:

1) identificar os mecanismos celulares e moleculares pelos quais as BDIR poderão promover angiogénese terapêutica;
2) avaliar se as BDRI promovem a vascularização pós-natal pelo aumento de CEPs em circulação e sua incorporação em locais de neovascularização nos tecidos isquémicos;
3) demonstrar que as BDRI promovem neovascularização num modelo experimental de diabetes.

Um modelo animal de isquémia foi desenvolvido usando fêmeas de ratinhos C57BL/6 e recorrendo a várias técnicas de biologia celular e molecular, nomeadamente RT-PCR, imunohistoquímica, imunofluorescência, citometria de fluxo, ELISA, microscopia de microdissecção a laser e diafanização.

Neste estudo, após a indução de isquémia unilateral, os ratinhos C57BL/6 foram irradiados ou não com 0.3 Gy, durante quatro dias consecutivos.

Os resultados demonstraram que as BDRI, aumentam significativamente a perfusão sanguínea no membro inferior do ratinho sujeito a isquémia, assim como a densidade capilar e a formação de colaterais. Foi também avaliada a vasculatura no membro inferior contralateral que apesar de irradiado não foi sujeito a isquémia. Neste caso particular, nem a densidade capilar, nem a formação de colaterais registaram alterações quando comparadas com animais não irradiados. Estas observações sugerem que em condições não patológicas as BDRI não têm efeito na vascularização.

De forma a validar os mecanismos moleculares no nosso modelo isquémico, foram selecionados os melhores candidatos associados a uma resposta pró-angiogénica a partir de uma análise de expressão gênica por microarrays. Os nossos resultados mostraram que a expressão de vários genes pró-angiogénicos nomeadamente, *Vegfr2, Vegfr1, Fgf2, Angpt2, Pdgfc, Tgfb2, Hgf* e *Met* está induzida em células endoteliais isoladas de músculos

de ratinhos sujeitos a isquémia e comparadas com a expressão em células endoteliais isoladas dos músculos não isquémicos contralaterais. Desta forma, as BDRI sugerem conferir uma resposta pró-angiogénica após indução de isquémia.

Neste trabalho foi também demonstrado que as BDRI aumentam significativamente tanto a concentração de VEGF, PIGF e G-CSF como de CEPs em circulação e medeiam a incorporação destas células nos músculos isquémicos.

Este trabalho revela ainda que não existe diferença de morbilidade nem de mortalidade em ratinhos irradiados quando comparados com ratinhos não irradiados, sendo eles acompanhados durante 52 semanas após exposição a BDRI.

Para complementar este trabalho e sendo a diabetes um importante fator de risco no contexto da DAP, foi observado que em resposta à indução de isquémia as BDRI, administradas durante quatro dias consecutivos, aumentam significativamente a perfusão sanguínea, a densidade capilar e a formação de colaterais num modelo experimental diabético. No entanto estes dados resultam de um estudo preliminar, sendo crucial o aumento do número de animais.

Em conclusão, o presente trabalho demonstra que BDIR induzem angiogénese terapêutica num modelo experimental de isquémia do membro inferior. Este trabalho é relevante pois propõe o uso de BDIR como uma estratégia inovadora e não invasiva no tratamento da isquémia crítica do membro inferior.

Palavras-chave

Neovascularização; Radiação ionizante; Isquémia do membro inferior; Células endoteliais progenitoras; Diabetes

Abstract

Peripheral arterial disease (PAD) is mainly caused by an obstructive artherosclerosis, which results in a mismatch between oxygen supply and demand. Diabetes is an important risk factor for PAD and it is present in almost 50% of the patients with limb ischemia. Critical limb ischemia (CLI) is the end stage of PAD, being characterized by severe obstruction of blood flow to the affected extremity, which results in ischemic rest pain, ulcers or gangrene. Despite substantial evidence of their efficacy in preclinical studies, as well as some promising phase I/II clinical trials, larger randomized clinical trials on angiogenic therapies for CLI have been unsatisfactory.

Here, we investigated the ability of low-dose ionizing radiation (LDIR) to stimulate therapeutic neovascularization, in murine models, in a context of hindlimb ischemia (HLI), conjugated or not with diabetes.

We demonstrate that 0.3 Gy, administered for four consecutive days, significantly improves blood perfusion in the murine ischemic limb by stimulating angiogenesis and arteriogenesis, as assessed by laser Doppler flow, capillary density and collateral vessel formation. LDIR significantly increased the circulating levels of VEGF, PlGF and G-CSF, as well as the number of circulating endothelial progenitor cells (EPCs), mediating their incorporation into ischemic muscles. These effects were dependent upon LDIR exposition on the ischemic niche (thigh and shank regions). In irradiated ischemic muscles, these effects were independent of the recruitment of monocytes and macrophages. Also, the vasculature in an irradiated non-ischemic bed was not affected and after 52-week LDIR exposure no differences in the incidence of morbidity and mortality were seen. Additionally, in diabetic mice, our data suggest that 0.3 Gy applied during four consecutive days significantly promote blood perfusion, capillary and collateral vessel densities in response to HLI induction. These findings disclose an innovative and non-invasive strategy to induce therapeutic angiogenesis in a murine model of severe HLI, emerging as a novel approach in the treatment of CLI.

Keywords

Neovascularization; Hindlimb ischemia; Ionizing radiation; Endothelial progenitor cell; Diabetes

Abbreviations

AKT	protein kinase B
ALK	activin receptor-like kinase
ANGPT	angiopoietin
BM-MNCs	bone marrow-derived mononuclear cells
BM-MSCs	bone marrow-derived mesenchymal stem cells
CLI	critical limb ischemia
CoCl2	cobalt chloride
COUP-TFII	chicken ovalbumin upstream promoter transcription factor II
CVD	collateral vessel density
CXCR4	cell-derived factor-1 receptor
DLL4	delta-like-4
DNA	deoxyribonucleic acid
ECs	endothelial cells
ECM	extracellular matrix
ELISA	enzyme linked immunosorbent assay
EPCs	endothelial progenitor cells
ERK	extracellular signal-regulated kinase
FACS	fluorescence activated cell sorting
FAK	focal adhesion kinase
FGF	fibroblast growth factor
FGFR	fibroblast growth factor receptor
Fox c	forkhead C
FSS	fluid shear stress
G-CSF	granulocyte-colony stimulating factor
Gy	Gray
HGF	hepatocyte growth factor
HLI	hindlimb ischemia
HMVEC-L	lung microvascular endothelial cells
i.p.	intraperitoneal
ICAM	intercellular adhesion molecule

IL	interleukin
iMM	Instituto de Medicina Molecular
LCM	laser capture microdissection microscope
LDIR	low-doses ionizing radiation
LFA	lymphocyte function-associated antigen
Mac1	macrophage 1 antigen
MAPK	mitogen-activated protein kinase
MCP1	monocyte chemoattractant protein 1
MET	hepatocyte growth factor receptor
MMPs	matrix metalloproteinases
MSCs	mesenchymal stem cells
NO	nitric oxide
NOS	nitric oxide synthase
NRPs	neuropilins
PAD	peripheral arterial disease
PB-MNCs	peripheral blood-derived mononuclear cells
PCA	principal component analysis
PDGF	platelet-derived growth factor
PDGFR	platelet-derived growth factor receptor
PECAM-1	platelet endothelial cell adhesion molecule 1
PI3K	phosphatidylinositl-3-kinase
PIGF	placental growth factor
PSGL-1	P-selectin glycoprotein ligand 1
PTK/ZK	PTK787/ZK222584
ROI	region of interest
RT-PCR	real-time polymerase chain reaction
S1PR	sphingosine-1-phosphatase receptor
SDF-1	cell-derived factor-1
SMCs	smooth muscle cells
STZ	streptozotocin
TACT	Therapeutic Angiogenesis Using Cell Transplantation
TGFβ	transforming growth factor β

TGFβR	transforming Growth Factor Receptor β
TIE2	tyrosine-protein kinase receptor for ANG
TNFα	tumor necrosis factor α
TPS	treatment planning system
TSP1	thrombospondin 1
uPA	urokinase-type plasminogen activator
VCAM	vascular cell adhesion molecule
VE-cadherin	vascular endothelial cadherin
VEGF	vascular endothelial growth factor
VEGFR	vascular endothelial growth factor receptor

Table of contents

Chapter I

Introduction

1. Blood vessels: Structure and Function

Contrarily to primitive and smaller organisms, the complex body architecture of vertebrates requires an efficient circulatory system, able to distribute oxygen and nutrients to tissues and remove carbon dioxide and other metabolic waste products throughout the body.

The circulatory system carries out two main networks: the blood-vascular and the lymphatic systems, both formed by endothelial cells (EC). The cardiovascular system allows blood to circulate and transport nutrients, oxygen, carbon dioxide and other molecules throughout all cells in the body[1], while the lymphatic system drains extravassed fluid, the lymph, from the extracellular space and returns it into the venous circulation. The lymphatic vasculature is also essential for the immune defense, since any foreign material present in the lymph is filtered through the chain of lymph nodes[2]. Both networks are essential for homeostasis of a healthy organism, and their malformation or dysfunction contributes to many diseases[1].

Blood vessels are divided into three main groups: arteries, veins, and capillaries[3]. Briefly, blood full of oxygen and nutrients is pumped from the heart to the tissues, through the arteries that ramify into smaller arterioles and into capillary beds, while blood enriched in carbon dioxide and waste returns to the heart through venules and veins[1].

Arteries and veins are further divided according to their caliber, into large, medium and small blood vessels. The microvasculature composed of the smallest vessels (arterioles, venules and capillaries) is a very dynamic and complex system, capable of constant change, while the larger blood vessels are more permanent structures with reduced plasticity[3]. Capillaries, the most abundant vessels in our body, are also one of the most important vessels of the cardiovascular system, since their thin walls allow the exchange of oxygen and nutrients between blood and tissues[3]. Capillaries are composed of endothelial cells surrounded by basement membrane and a sparse layer of pericytes embedded within the EC basement membrane. Pericytes, due to their contractile fibers, possess a cell body with prominent nucleus and a small content of cytoplasm. They are functionally significant, since when vessels lose pericytes, they become hemorrhagic and hyper dilated, leading to conditions such as edema, diabetic retinopathy, and even embryonic lethality[4]. Capillaries in different tissues exhibit different cellular morphology, associated with distinct levels of

permeability (Figure 1): (a) **continuous capillaries**, characterized by an uninterrupted endothelium and a continuous basement membrane, that exist, for instance, in muscle, lung or the nervous system; (b) **fenestrated capillaries**, characterized by a continuous basement membrane with fenestrae or pores in the endothelium that allow the rapid passage of macromolecules and exist, for example, in the kidney, intestines or endocrine glands and (c) **discontinuous capillaries**, characterized by large openings in the endothelium and a discontinuous or absent basement membrane that exist, for instance, in the liver and spleen[5].

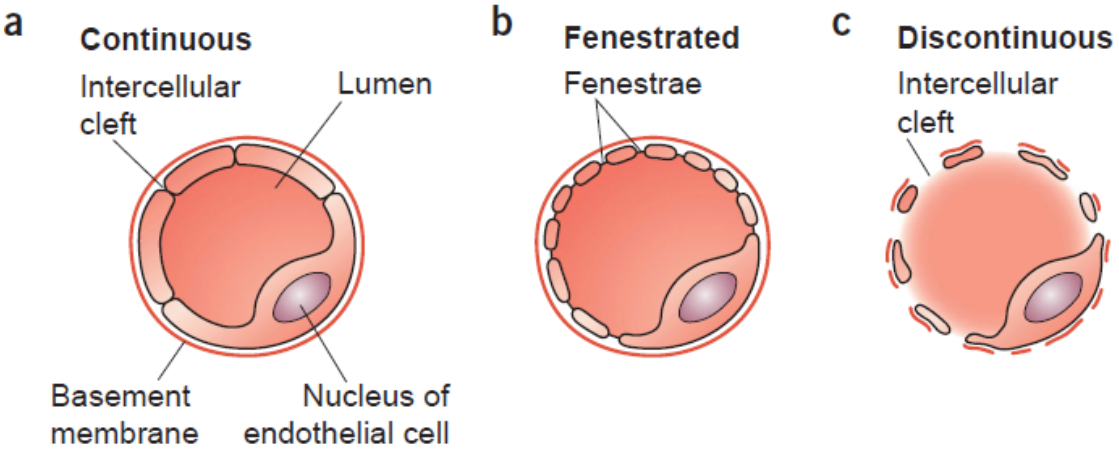

Figure 1 - Capillary wall morphology. **(a)** Continuous capillaries have no openings in their wall and are lined continuously with the EC body. **(b)** Fenestrated capillaries have small openings, called fenestrae that are covered by a small, non-membranous, permeable diaphragm and allow the rapid passage of macromolecules. The basement membrane of ECs is continuous over the fenestrae. **(c)** Discontinuous capillaries have a large lumen, many fenestrations with no diaphragm and a discontinuous or absent basal lamina. Adapted from reference[5].

In contrast, the walls of larger vessels (arteries and veins) have three specialized layers (Figure 2). The ***tunica intima*** consists of an endothelium, a basement membrane and an internal elastic layer. The ***tunica media*** is composed of a thick layer of smooth muscle cells (SMCs) with reticular fibers, elastin and proteoglycans and external elastic lamina, while the ***tunica adventitia*** consists of connective tissue with both elastic and collagenous fibers and external elastic lamina[5,6]. Arterioles and venules have an increased coverage of mural cells when compared to capillaries.

The advential layer has its own blood supply, known as vasa vasorum. SMCs and elastic laminae contribute to the vessel tone and mediate the control of vessel diameter and blood flow. Although the walls of arteries and veins are composed of these same layers, they present some differences as a result of the pressure and direction of the blood flow. Arteries are more robust, with a strong elastic vessel wall to cope with the high arterial blood pressure downstream of the heart. Since veins conduct blood back to the heart, blood flows with a lower pressure in veins and consequently their wall is thinner than the one of arteries. Veins have additional semi-lunar valves, which prevent the blood from flowing backwards[5].

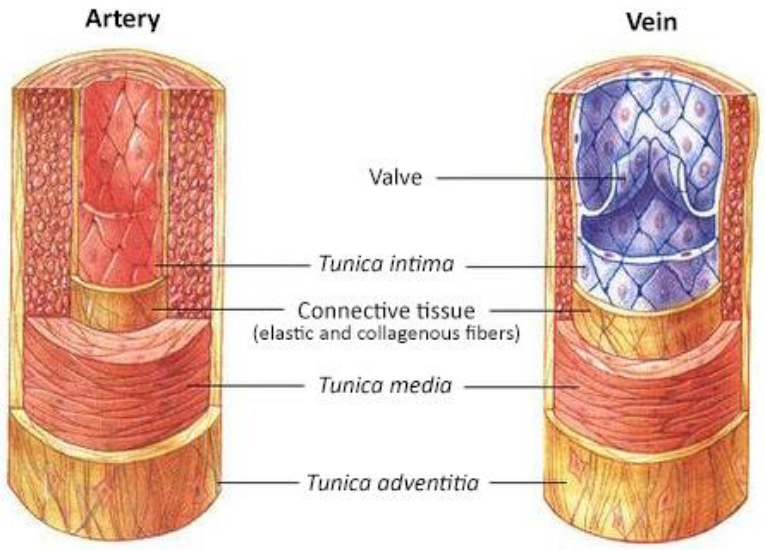

Figure 2 - Morphology and wall composition of large blood vessels. Adapted from reference[7].

1.1. Endothelial Cell Specification

Although arteries and veins are both formed from primitive blood vessels, different hemodynamic changes and physiology lead to their distinct morphology and physiology factors, in a process known as arteriovenous differentiation[1,2,8]. Hemodynamic forces such as blood flow rate, direction, and pressure are key factors driving the differentiation of vessels into arteries and veins. However, studies have demonstrated that arteries and veins possess distinct molecular identities from a very early stage, suggesting that genetics have a critical role in dictating arterial/venous fate[9]. Although the molecular processes

underlying arteriovenous differentiation are not fully understood, increasing evidence suggests that this process is regulated by the concerted action of different molecules.

The first discovered specific markers that distinguish arteries from veins were two members of the Eph-Ephrin subclass of receptor tyrosine kinases, ephrinB2 and EphB4[9]. EphrinB2 is a transmembrane ligand and is specifically expressed in endothelial precursors that produce arteries, whereas Ephb4, the receptor for Ephrin B2, is found preferentially in veins[10]. Mice deficient in Ephrin B2 and Ephb4 have similar defects in the remodeling of primary capillary vessels into a mature vascular network[8].

It is known that Notch pathway is directly involved in the differentiation of the arterial branch[1]. In mice, the receptors Notch1 and Notch2 and the ligands Jagged1, Jagged2 and delta-like-4 (DLL4) are all expressed in arterial but not in venous ECs. Notch4$^{-/-}$ and Notch1$^{-/-}$ mice exhibit abnormal vascular development, whereas Dll4$^{-/-}$ mice are not viable, presenting severe vascular defects and showing reduced EphrinB2 expression and increased EphB4 expression, consistent with a failure in arterial differentiation. These data suggest that Notch activity is important for the promotion of arterial cell fate[9,11]. Upstream from Notch pathway are Foxc1 and Foxc2 (forkhead C1 and C2) that control arterial specification by regulating the expression of the Notch ligand Dll4. Mice with inactivated Foxc1 and Foxc2 develop arterial-venous malformations[10].

Additionally, COUP-TFII (chicken ovalbumin upstream promoter transcription factor II) is specifically expressed in venous endothelium. COUP-TFII mutant mice show ectopic expression of arterial markers such as neuropilin 1 (NRP1), Notch1 and EphrinB2 in veins. These studies suggest that COUP-TFII is a crucial regulator of venous cell fate by inhibiting the expression of NRP1 and Notch signaling[8,12].

The expansion of larger arteries and veins occurs by acquisition of additional layers of mural cells, extracellular matrix (ECM) and elastic laminae to provide the required viscoelastic properties. Homotypic and heterotypic junctions facilitate cell-to-cell communication and regulate vessel permeability. Vascular endothelial cadherin is an important component of EC-EC junctions, whereas neural cadherin facilitates EC-mural cell communication. Gap junctions (made of connexins) also facilitate communication between ECs and between ECs and perivascular cells. Tight junctions (formed by occludins, claudins and zona occludens) contribute to the blood tissue barrier in the brain and retinal capillaries[6].

2. Vasculogenesis

Vasculogenesis is a fundamental process by which new blood vessels are formed, characterized by the differentiation of precursor cells into endothelial cells and the *de novo* formation of a vascular network.

2.1. Vasculogenesis during embryo development

The development of the vascular system is one of the earliest events in organogenesis[13]. In vertebrates, one of the mechanisms by which the vascular development proceeds is via **vasculogenesis**, the process of *de novo* blood formation, characterized by the formation of vessels directly from angioblastic precursors[14].

In the early phase of vasculogenesis, hemangioblasts undergo their first critical steps of differentiation within the blood islands, being committed to differentiate into angioblasts and primitive haematopoietic cells. The angioblasts aggregate in the periphery and the hematopoietic precursors accumulate at the center of the blood islands in the yolk sac and embryo[15,16]. The angioblasts migrate to discrete locations, differentiate *in situ* and assemble into solid endothelial cords, later forming a plexus with endocardial tubes[13].

Vascular endothelial growth factor (VEGF) and their receptors, vascular endothelial growth factor receptor 1 and 2 (VEGFR1 and VEGFR2), are key players in embryonic vessel formation. Particularly, VEGFA is required for the chemotaxis and differentiation of endothelial precursor cells, EC proliferation and angiogenic remodeling[1]. Genetic studies show that the deficiency in one of these VEGF/VEGFR molecules is lethal in mice, due to failed development of the vasculature[2,16]. The lethality resulting from the loss of a single allele is indicative of a dependent regulation of embryonic vessel development by VEGFA[2]. The existence of a precursor for these cells types (haemangioblast) is suggested by defects in both the haematopoietic and angioblastic lineages of embryos lacking VEGFR2. Moreover, in the absence of the VEGFR1 mice produce angioblasts but their assembly into functional blood vessels is impaired[17].

2.2. Postnatal Vasculogenesis

Until the late 1990s, it was generally accepted that after birth, new blood vessels were developed only by angiogenesis. However, new findings indicate that vasculogenesis is not

restricted to early embryogenesis[18]. Asahara et al., pioneer in the scientific field of adult vasculogenesis, isolated mononuclear cells from adult peripheral blood and found that those cells had the same characteristics as the embryonic angioblasts, contributing to the revascularization of the ischemic tissue[19]. These cells were termed "endothelial progenitor cells" (EPCs). Thus, a new concept, describing postnatal neovascularization as a combination of vasculogenesis and angiogenesis, in which EPCs play a crucial role, emerged[18].

2.2.1. EPCs phenotypic identification and characterization

The identification of EPCs can be based on their cellular origin, isolation methods and surface marker expression[20]. Although the analysis of cell surface markers is currently the most used methodology[21], EPCs identification is controversial, since there is no unique protein marker that defines them[22]. The analyzed markers are usually shared with cells from hematopoietic lineage and mature ECs[23]. Therefore, EPCs combine stem cell markers, such as CD133, c-kit and Sca-1 and endothelial markers, such as VEGFR2, CD31, VE-cadherin and von Willebrand factor[20,24]. CD34 represents a link between precursor and mature cells, since it is expressed in both cell types. On the other hand, CD133 allows the distinction between progenitor and mature cells, since it is not present on mature ECs[22].

Beyond the controversy about the phenotypic identification of EPCs, the heterogeneity of cultured cells has also been a concern. Many studies reported EPCs after using different sources of the cells or method for culture[22,25-27]. For instance, human $CD34^+$ cells isolated from peripheral blood, umbilical cord blood or bone marrow can all differentiate into ECs. Moreover, studies show that when total mononuclear cells, isolated from peripheral blood, are cultured *in vitro*, two types of cell populations that appear sequentially can be observed[26]. The first population, "Early EPCs", comes after 4-7 days of plating on fibronectin-coated surface with the addition of endothelial growth media, as spindle-shaped cells. "Early EPCs" gradually loose CD45 and CD31 expression and gain low-level expression of VEGFR2 and VE-Cadherin. However, they lose this low-level expression of VEGFR2 and VE-cadherin after 3 weeks, dying after that[26]. These cells play a role in vasculogenesis by secreting large quantities of angiogenic factors, which act through paracrine mechanisms[28]. On the other hand, when blood-derived mononuclear cells are maintained in culture for 2-3 weeks "late EPCs" can be observed[22]. "Late EPCs" have a

higher and longer sustained expression of VEGFR2 and VE-cadherin[26], much higher proliferation potential and are able to differentiate into ECs and promote vascular tube formation[22]. Thus, "late EPCs" enhance neovasculogenesis, by providing a sufficient number of ECs based on their high proliferation potency[26]. These two type of cells have the ability to absorb acetylated low-density lipoprotein and bind lectin *Ulex europaeus* agglutinin I[29]. Despite such differences in genetic and functional *in vitro* aspects, they equally contribute to neovasculogenesis[26].

2.2.2. Mobilization and Recruitment of EPCs

Under physiological conditions, levels of EPCs in the peripheral circulation are low and these cells reside in the bone marrow niche in a quiescent state[30]. The mobilization of EPCs from the bone marrow into the peripheral circulation is promoted by several growth factors, chemokines and cytokines which are produced in response to a physiological stress (tissue hypoxia and trauma) (Figure 3)[31].

One of the most important factors in EPCs mobilization is VEGF. When VEGF interacts with its receptor, VEGFR2, it activates nitric oxide synthase (NOS) in the bone marrow, which produces nitric oxide (NO), a key player for matrix metalloproteinase 9 (MMP) 9 activation. Activated MMP-9 contributes to the transformation of membrane-bound Kit ligand to a soluble form (sKitL) and consequently detaches EPCs from the bone marrow niche to the peripheral circulation[28].

Once in circulation, homing of EPCs is activated in response to chemokine gradients that are formed in the tissue undergoing active remodeling. The major chemokine that regulates activation and homing of EPCs is the stromal cell-derived factor1 (SDF1)[32,33]. In response to an ischemic stimulus, released SDF1 interacts with its receptor (CXCR4), and initiates, not only the mobilization of EPCs from bone marrow, but also their adhesion to ischemic areas. The SDF-1/CXCR4 interaction upregulates the P-selectin glycoprotein ligand 1 (PSGL1) expression on the surface of EPCs, which is the major ligand of P-selectin. The binding contributes to the adhesion of EPCs to the sites of vessel damage and enhances their pro-angiogenic capacity. However, in the absence of injury, the effect of SDF1 is abolished. After homing into the injured vessel wall, EPCs will contribute to new vessel formation and remodeling, but the mechanism behind the functional activity of EPCs is still under investigation. Besides differentiating into ECs, EPCs also produce multiple paracrine

factors, such as VEGF, SDF1, hepatocyte growth factor (HGF), angiopoetin1 (ANGPT1), insulin-like growth factor 1, monocyte chemoattractant protein1 (MCP1) and platelet-derived growth factor (PDGF). These factors can assist different cell types in promoting angiogenesis and tissue regeneration, reflecting the indirect contribution of EPCs to neovascularization[34].

EPCs are mobilized from bone marrow into the peripheral circulation and recruited into sites of vessel injury to participate in blood vessel formation, in both physiological and pathological conditions. However, the mechanisms of mobilization and recruitment are still incompletely understood and require further analysis. Nevertheless, several studies suggest that EPCs play a critical role in postnatal neovascularization and vascular homeostasis[30].

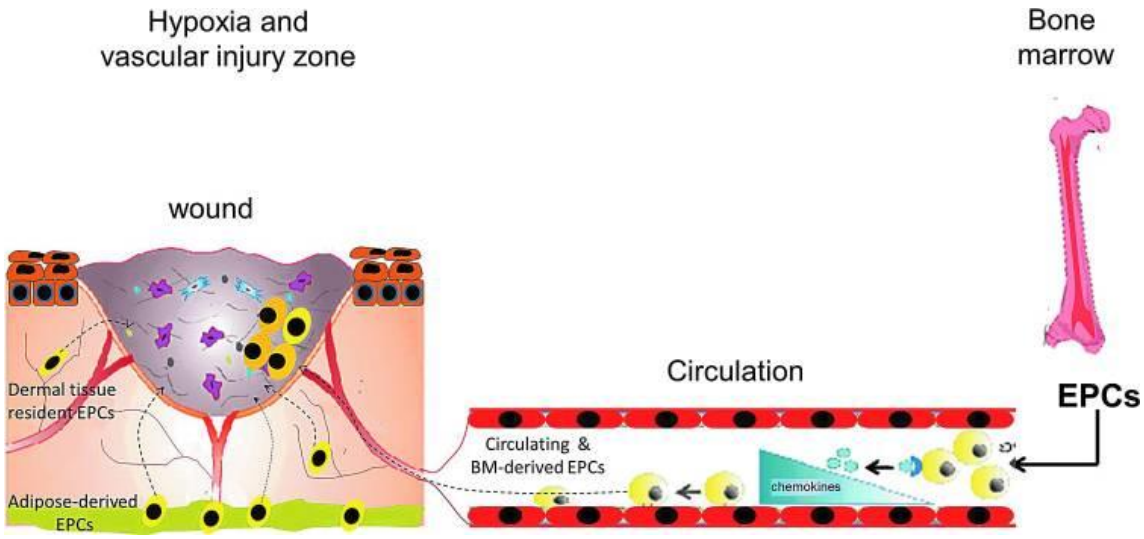

Figure 3 - EPCs mobilize in response to hypoxia induced by trauma or vascular injury. In normal homeostatic conditions, EPCs reside within a stem cell niche in the bone marrow. Peripheral tissue hypoxia under trauma, wound healing or vascular injury conditions results in increased production of EPC-mobilizing chemokines and growth factors to a concentration greater than that in the bone marrow, causing EPC release and mobilization into the peripheral circulation. Once in circulation, EPCs respond to chemokine signaling in the tissues by undergoing active remodeling and homing to the injury site. Concomitantly, circulating progenitor cells, tissue-resident, and adipose-derived stem cells respond to the chemokine signaling, homing to the active tissue-remodeling site. Adapted from reference[20].

3. Arteriogenesis

Arteriogenesis, defined as the formation of mature arteries from pre-existing arterioles after an arterial occlusion, needs to be activated to confer proper tissue function[35] (Figure 4).

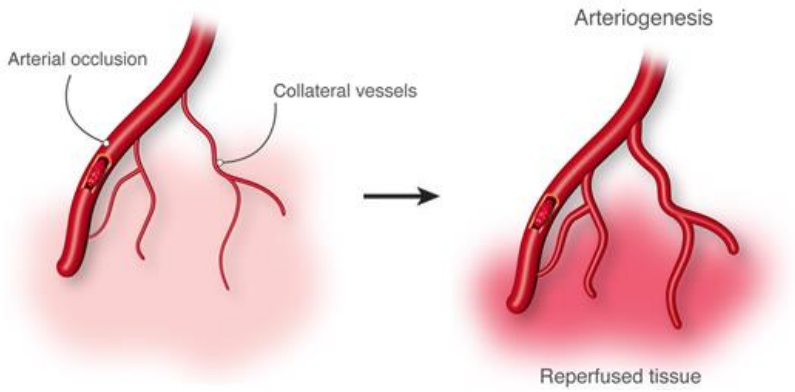

Figure 4 - Arteriogenesis. Arterial occlusion induces a pressure gradient followed by a redistribution of perfusion, an increase in collateral flow and a subsequent outgrowth of the collateral arteriole. Adapted from reference[36].

The driving force for arteriogenesis is altered fluid shear stress (FSS), which appears within the collateral arteriole after a blood flow increase. However, the large pressure difference in the pre-existing arterioles connecting upstream with downstream branches, relative to the point of occlusion, also contributes to initiate a complex cascade of molecular and cellular events leading to increased vessel lumen and wall thickness[37]. The primary physiological response to FSS is the activation of ECs in the collateral wall. After an arterial occlusion, the ECs of collateral vessels appear swollen, as opposed to the completely flat inner surface of normal arteries[38]. The endothelial activation is indicated by several processes that condition for the attraction of circulating cells: upregulated genes that encode for chemoattractant or activated cytokines, including growth factors or adhesion molecules[37]. Thus, changes in the expression and conformation of adhesion molecules converts the collateral endothelium from a quiescent vessel layer with very low adhesion tendency into a highly activated one, which is now supporting attraction, adhesion and invasion of leukocytes[37]. Also, several molecules involved in cell proliferation and migration were found up-regulated, including MMP2, MMP9, urokinase-type plasminogen activator (uPA), focal adhesion kinase (FAK) and integrins (α5β1 and αvβ3)[38]. Moreover, after an arterial obstruction, the altered FSS induces at least two signaling pathways: (1) the

attraction, adhesion and invasion of monocytes that are required for structural remodeling and (2) the pathway that causes ECs and SMCs to enter the cell cycle, leading to proliferation. Thus, in response to altered FSS, NO and VEGF are induced and, together with calcium-activated ion channels, interfere with osmotic regulation of the endothelium[38,39]. This occurs along with monocyte adhesion, since the activated endothelium produces MCP1, leading to the recruitment of monocytes to the sites of proliferation[40]. After the initial monocyte-endothelium interaction, which is mediated by several selectins, the tight monocyte adhesion to the endothelium is triggered by macrophage-1 antigen (Mac1) and lymphocyte function-associated antigen (LFA). These integrins interact with their corresponding adhesion molecules (intercellular adhesion molecule 1 and 2 (ICAM1), (ICAM2) and vascular cell adhesion molecule 1 (VCAM1), (respectively) on the endothelial cell surface[41]. After adhesion, migration into deeper parts of the collateral wall and surrounding areas can be observed. During migration, monocytes should overcome barriers, like the internal elastic lamina and ECM. However, as monocytes are producers of proteases, such as MMPs and uPA, they enable the proteolytic degradation of these barriers and could therefore create a gap by which monocytes could invade the vascular wall. At the same time, these events may also generate a proliferation signal for SMC[37]. Furthermore, lymphocytes (natural killer family, CD4 and CD8 cells) also play a role in arteriogenesis. Studies from Stephen Epstein´s group showed that in mice with a genetic deficiency in the T-cell marker CD4, arteriogenesis was inhibited in the hindlimb ischemia model, but could be rescued by an injection of purified CD4 positive cells. Additionally, the lack of CD4 positive T-cells led to a reduced inflammatory response in the same model including a consistent reduction in the number of monocytes[37]. As mentioned before, remodeling from a small pre-existing arteriole to a large collateral artery is facilitated by a complex cascade of processes. The signaling cascade uses the mitogen activated protein kinases with activation of the RAS-ERK- and the Rho pathway[41]. ECs mitosis precedes that of SMCs by a few hours and growth factors are released from monocytes such as MMPs, u-PA and fibroblast growth factor 2 (FGF2) during that time[38]. Also, degradation of extracellular structures leads to the release of additional matrix-bound growth factors. The increase in cell mitosis in SMCs occurs together with a morphological change: their transformation from a contractile into a proliferative/synthetic phenotype. Elastin is present in the elastic lamina, preventing SMCs proliferation, but its degradation products

stimulate SMCs proliferation[41]. Subsequently, SMCs migrate and rearrange accordingly to the increasing vessel lumen and wall thickness. The controlled destruction of the vascular scaffolding paves the way for the expansion and outward growth of collateral vessels. Moreover, apoptosis of SMCs may facilitate the renewal of the vascular wall[38]. Finally, remodeling enters in a maturation state when both elastic lamina and ECM components are rearranged. In this process, laminin and collagen IV are crucial since they promote the differentiation and inhibit the proliferation of SMCs[37].

4. Angiogenesis

After the formation of a primitive vascular plexus during vasculogenesis, the growth, expansion and remodeling of primitive vessels into a mature vascular network (including arteries, veins, and capillaries) is initiated. This process, named angiogenesis, occurs by intussusception, in which interstitial tissue columns are inserted into the lumen of pre-existing vessels, inducing partition of the vessel lumen, or by sprouting of new vessels from the ends and sides of the pre-existing ones[17,42-44].

The sprouting angiogenesis is facilitated by hypoxia, which regulates the expression of several genes involved in vessel formation, patterning and maturation, such as NOS, VEGF and ANGPT2[6]. The existing vessels dilate and become leaky in response to NO and VEGF, respectively. At the same time, redistribution of intercellular adhesion molecules (platelet endothelial cell adhesion molecule 1(PECAM1), vascular endothelial cadherin (VE cadherin)) and alteration in cell membrane structure occur[16]. Consequently, the extracellular matrix ECM dissolves in response to activation of MMPs (MMP2, MMP3 and MMP9) and suppression of protease inhibitors. Degradation of ECM also results in the release of growth factors, including FGF2, VEGF and insulin-like growth factor, which otherwise remain stored within the matrix. As the physical barriers are dissolved, ECs can migrate to distant sites, through interactions between integrins (αvβ3 and α5β1) and the matrix proteins, and proliferate in response to VEGF and other endothelial mitogens (ANGPTs, FGFs and PDGF)[6,16].

The different steps of angiogenic process are explained in Figure 5. Briefly, the ECs, also known as “tip cells”, become selected to lead the tip in the presence of factors such as: VEGF receptors, NRPs and NOTCH ligands. The neighbors of the “tip cell” assume positions

as “stalk cells”, which divide to support sprout elongation and establish the lumen[3,44,45]. At this point, the vessel sprouting remodels into a highly organized vascular network of larger vessels ramifying into smaller ones[160]. Then, the maturation process begins, described as the stepwise transition from an actively growing vascular bed to a quiescent functional network. This process involves the suppression of endothelial proliferation and sprouting, and the stabilization of existing vascular tubes through the recruitment of mural cells. Pericytes establish direct cell-cell contact with ECs in capillaries and immature vessels, whereas SMCs cover large diameter vessels (arteries and veins) and are separated from ECs by a matrix[1]. During this process, the pericytes and SMCs contribute to the deposition of ECM. This is critical for normal vessel growth and maintenance by providing the solid scaffold through which new vessels may migrate and store growth factors and pro-enzymes involved in vessel development. Thus, the recruitment of these mural cells is crucial for the maturation and stability of the new vasculature[44].

The regulation of the angiogenic process involves at least four molecular pathways: (1) PDGF/platelet-derived growth factor receptor (PDGFR); (2) ANGPT1/Tie2; (3) Transforming growth factor β (TGFβ) and (4) Sphingosine 1 phosphatase receptor (S1PR) signaling. The PDGF/PDGFR signaling is an important regulator of this process. PDGFβ is secreted by ECs in response to VEGF, recruiting pericytes and SMC and allowing their proliferation and migration during vascular maturation[6]. *Pdgf* mutations leads to poorly covered vessels with excessive endothelial sprouting, microaneurysms, leakage and haemorrhaging[1].

Also, critical for vessel formation and stability are ANGPT1 and ANGPT2 and their Tie receptors. The Tie2 receptor is expressed in ECs and is stimulated by ANGPT1 and ANGPT2, expressed by mural cells and ECs, respectively[1,46]. ANGPT1 stabilizes nascent vessels and makes them leak-resistant through the communication between ECs and mural cells[6]. In agreement with this, mouse mutants for Tie2 or ANGPT1 have similar behaviors, presenting severe vascular defects, and are unable to recruit pericytes[47]. The role of ANGPT2 is dependent on the presence or absence of VEGF. When VEGF is present, ANGPT2 promotes blood vessel growth and sprouting; the absence of VEGF leads to endothelial cell death and vessel regression[48,49].

Additionally, TGFβ1 is also involved in the stabilization of immature vasculature. It is a multifunctional cytokine that promotes the maturation of vessels through the stimulation of SMC differentiation and ECM deposition, while inhibiting ECs proliferation and

migration. TGFβ1 is expressed in ECs and mural cells and can be either pro or anti-angiogenic, depending on context and concentration [6]. Loss of function of TGFβR2 in mice causes vessel fragility due to impaired mural cells development[50].

Also, S1PR signaling controls EC/mural cell interaction. Endothelial-derived S1P binds to G protein-coupled S1PRs and triggers cytoskeletal, adhesive and junctional changes, affecting cell migration, proliferation and survival. Disruption on S1PR1 or loss of both S1PR2 and S1PR3 in mice causes defective coverage of vascular SMCs[50].

In the end of the maturation process ECs acquire highly specialized characteristics to provide the functional needs within specific tissues and organs[16]. This process includes arterio-venous determination, formation of homotypic and heterotypic junctions and ECs differentiation to form organ-specific capillary structures[6].

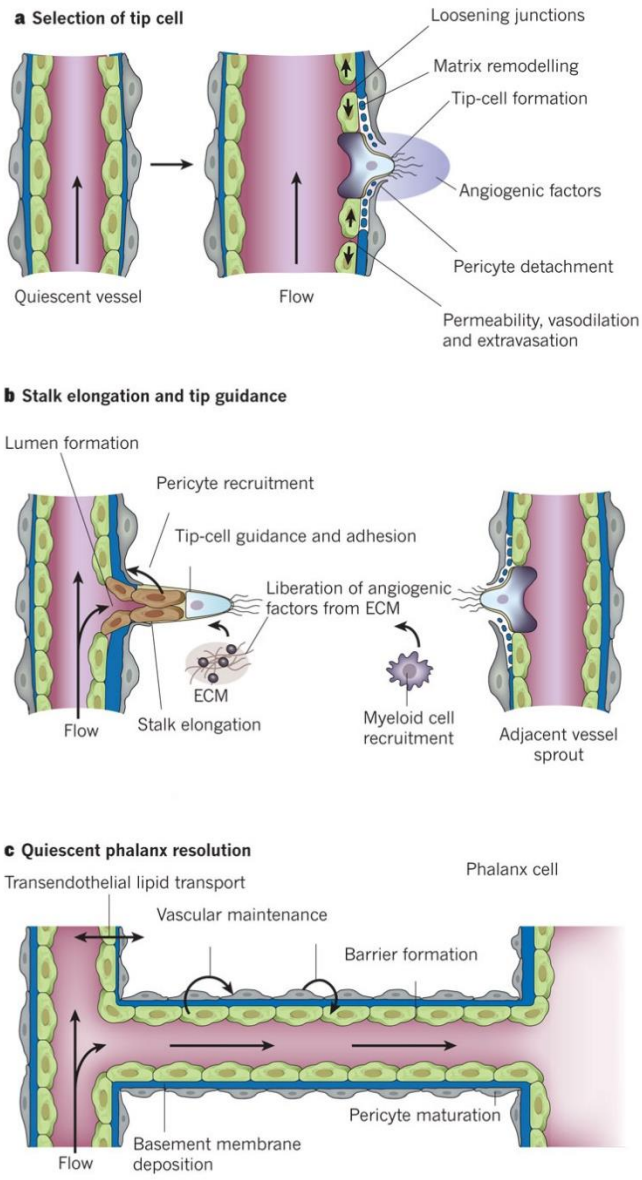

Figure 5 - Angiogenesis. **(a)** After stimulation with angiogenic factors, the quiescent vessel dilates and an EC tip cell is selected to ensure branch formation. Tip cell formation requires degradation of the basement membrane, pericyte detachment and loosening of endothelial cell junctions. Increased permeability permits extravasation of plasma proteins to deposit a provisional matrix layer, and proteases remodel the pre-existing interstitial matrix, all enabling cell migration. **(b)** Tip cells navigate in response to guidance signals and adhere to the ECM to migrate. Stalk cells behind the tip cell proliferate, elongate and form a lumen, and sprouts fuse to establish a perfused neovessel. Proliferating stalk cells attract pericytes and deposit basement membranes to become stabilized. **(c)** After fusion of neighboring branches, lumen formation allows perfusion of the neovessel, which resumes quiescence by the promotion of a phalanx phenotype, re-establishment

of junctions, deposition of basement membrane, maturation of pericytes and production of vascular maintenance signals. Adapted from reference[45].

4.1 Physiological Angiogenesis

After birth, angiogenesis still contributes to organ growth, but once the new vessels are assembled, the ECs become notably resistant to exogenous factors and most blood vessels remain quiescent[16,43]. Accordingly, in adults and in physiological conditions, angiogenesis occurs only in specific situations, such as wound healing, regeneration of the endometrium during the menstrual cycle or in the placenta during pregnancy[6,51].

Quiescent ECs retain their remarkable ability to divide rapidly in response to a physiological stimulus, such as hypoxia, low pH or shear stress, and therefore influence the formation, maturation and remodeling of small and large vessels[6,51]. Thus, in physiological situations, it is reasonable to assume that molecules involved in vessel formation and maturation during embryonic development are also involved in the postnatal period, but their precise role is not yet known because most knockout mice die pre- or perinatally[6].

4.1.1 Angiogenic Regulators

In multicellular organisms, the process of angiogenesis is regulated by a complex and tight balance between pro- and anti-angiogenic molecules[43]. Physiologically, the body controls angiogenesis through a series of “on” and “off” regulatory switches. The main “on” switches are known as angiogenesis growth factors and the main “off” switches are known as endogenous angiogenesis inhibitors. A selective list of the main stimulators and inhibitors that take part in the angiogenic process is shown in Table 1 and some of these factors will be briefly detailed below [52].

Table 1 - List of the main angiogenic stimulators and inhibitors. Adapted from reference[52].

Angiogenic Stimulators	Angiogenic Inhibitors
Angiogenin	Angioarrestin
Angiopoietin-1	Angiostatin
Fibroblast growth factors	Endostatin
Granulocyte colony-stimulating factor (G-CSF)	Fibronectin fragment
Hepatocyte growth factor	Heparinases
Interleukin-8	Interferon alpha/ beta/gamma
Placental growth factor	Interferon inducible protein
Platelet-derived endothelial cell growth factor	Interleukin-12
Platelet-derived growth factor-BB	Metalloproteinase inhibitors
Pleiotrophin	Plasminogen activator inhibitor
Progranulin	Retinoids
Transforming growth factor alpha and beta	Thrombospondin-1
Tumor necrosis factor-alpha	Vasculostatin
Vascular endothelial growth factor	Vasostatin

Vascular Endothelial Growth Factor

VEGF family consist of six members: VEGFA, also called VEGF, VEGFB, VEGFC, VEGFD, PIGF and virus VEGF (VEGFE)[53]. VEGF was the first identified and the most studied of the VEGF family members[54]. VEGF is expressed in different tissues including brain, kidney, liver, spleen and by many different cell types[55]. Several *in vitro* studies have shown that VEGF stimulates microvascular EC proliferation, enhancing migration and inhibiting apoptosis. Additionally, VEGF induces the growth of new capillaries from preexisting vasculature. *In vivo* studies also showed that VEGF regulates vascular permeability, which is important for the initiation of angiogenesis[56-59]. VEGF causes vasodilatation by inducing endothelial nitric oxide synthase and thus increasing NO production[60], and it also plays a crucial role in several angiogenic processes, namely wound healing, ovulation, maintenance of blood pressure, menstruation and pregnancy[61]. In humans, VEGF is expressed in almost every solid tumors as well as in some hematological malignances[62].

Different growth factors and cytokines such as PDGF, tumor necrosis factor α (TNFα), TGFβ and interleukin 1β (IL1β) induce transcription of VEGF mRNA, thus VEGF may function as a mediator for indirect action of angiogenic factors[53]. VEGF levels can also be regulated by tissue oxygen tension, since exposure to hypoxia induces VEGF expression. In contrast, normoxia downregulates VEGF production and even causes regression of some newly formed blood vessels[63].

The expression of VEGF has been shown to be associated with significant steps in angiogenesis and physiological vasculogenesis. According to this, several *in vivo* studies demonstrate that, in mice, deletion of the VEGF gene leads to embryonic death, resulting in vascular defects and cardiovascular abnormalities[64].There are currently six isoforms of VEGF resulting from alternative splicing of a single gene ($VEGF_{121}$, $VEGF_{145}$, $VEGF_{165}$, $VEGF_{183}$, $VEGF_{189}$ and $VEGF_{206}$). Some of these isoforms remain associated with cells or membranes, while others are extracellularly released. Despite this difference, all of them have identical biological activities[65,66].

Two high affinity binding sites for VEGF have been identified on vascular endothelium: VEGFR1 (Flt1) and VEGFR2 (KDR or Flk1). An additional member of this family, VEGFR3 (Flt4) is not a receptor for VEGF but binds VEGFC and VEGFD[55]. All VEGF receptors have seven immunoglobulin domains in their extracellular part and an intracellular tyrosine kinase domain[65]. Also, all VEGF receptors are expressed in high levels during embryogenesis, and in adults VEGFR1 and VEGFR2 are mainly expressed in the blood vascular system, whereas VEGFR3 is restricted to the lymphatic endothelium[67]. Knockout mice for VEGFR1 or VEGFR2 are embryonically lethal, being the blood vessels completely absent, which suggest that both receptors are essential for normal development of the embryonic vasculature[68,69].

Neuropilin, another receptor for VEGF, was primarily identified as a receptor for members of the collapsing/semaphoring family on neuronal cells, but it is also expressed on ECs. Neuropilin is an isoform specific receptor that binds to $VEGF_{165}$[65].

VEGFR1 strongly interacts with VEGF, but this interaction plays a minor role in angiogenesis. However, interaction of VEGFR2 with VEGF is a major contributor to the mitogenic, chemotactic, angiogenic and increased permeability effects of VEGF[70]. Once VEGF binds to the extracellular domain of the receptor, after the dimerization and auto-phosphorylation of the intracellular receptor tyrosine kinases, a cascade of downstream proteins are activated[54].

Due to the key role of VEGF in angiogenesis, the use of anti-VEGF drugs has been applied in many different fields of medicine, such as prevention of angiogenesis associated with tumors and induction of neovasculature in ischemic diseases[3].

Angiopoietins

ANGPT family consists of four ligands: ANGPT1, 2, 3 and 4; and two tyrosine kinase receptors, TIE1 and TIE2[45].

ANGs are paracrine growth factors that act as ligands for the TIE receptors, specifically on ECs, and are involved in the maintenance, growth and stabilization of the vessels[71,72]. The most important and well characterized ANGPTs that play a role in angiogenesis are ANGPT1 and ANGPT2. Both ANGPT1 and ANGPT2 bind to TIE2 receptors, but only the binding of ANGPT1 results on signal transduction and regulation of blood vessel maturation[55]. Thus, the interaction between ANGPT1 and TIE2 receptor induces the remodeling and stabilization of blood vessels. ANGPT1 is expressed by mural and tumor cells, whereas ANGPT2 is released from angiogenic tip cells. In confluent endothelium, ANGPT1 induces the maintenance of quiescent endothelial cells through cell-cell junction. Also, ANGPT1 stimulates mural coverage and basement membrane deposition, thereby promoting vessel tightness[45]. Studies have shown that knockout mice for ANGPT1 or TIE2 exhibit similar phenotypes, with prominent endocardial and myocardial defects. The primary vasculature of these mice develops normally, but the stabilization and remodeling of the vessels fails, leading to embryonic death[65]. On the other hand, overexpression of ANGPT1 in transgenic mice causes excessive hypervascularization, namely a greater number of blood vessels with large diameters[73]. Concerning ANGPT2, its role in angiogenesis is more complex. ANGPT2 can act as a pro- or anti-angiogenic factor, dependent on co-stimulatory molecules, such as VEGF. At first, ANGPT2 was considered as a natural antagonist of ANGPT1, since it blocks ANGPT1-induced TIE2 autophosphorylation in ECs[49]. However, recent new studies suggest that in the presence of VEGF, ANGPT2 mediates an increase in the capillary diameter, induces migration and proliferation of ECs and stimulates sprouting of new blood vessels, while in its absence, ANGPT2 causes apoptosis of ECs and regression of blood vessels[74].

Despite the current difficulty to understand ANGPT2 activity, the selective inhibition of ANGPT2 may have clinical value. Several studies have shown ANGPT2 upregulation in some diseases that involve pathogenic angiogenesis including cancer, rheumatoid arthritis,

osteoarthritis and psoriasis[75-77]. Additionally, various agents that block either TIE2 or ANGPT2 are being evaluated in early-phase clinical trials[45]. Regarding TIE1 receptor, since no ligand has been identified, it may act as a negative regulator of TIE2, but its role remains undefined.

Fibroblast Growth Factors

FGFs are soluble growth factors that stimulate EC proliferation and migration, as well as production of collagenase and the plasminogen activator[54]. FGF family is known to contain at least 20 factors, numbered FGF1 to FGF20, and 4 different tyrosine kinase receptors (FGFR), numbered FGFR1 to FGFR4.

The most studied forms are FGF1 (acid FGF) and FGF2 (basic FGF), which were among the first growth factors that were known to stimulate angiogenesis.

They are both secreted by a wide range of cell types and bind to all four FGFR[65]. In addition, FGFs also bind, with high affinity, to heparin sulfate proteoglycans (HSPGs), which act as co-receptors. HSPGs are located on cell surface and within the ECM, modulating the effects of FGF both *in vitro* and *in vivo*[78,79]. Heparin induces oligomerization of FGF2, which might be important for receptor dimerization and activation. FGFR activation will then trigger an intracellular signal cascade leading to multiple biological responses, including ECs proliferation, migration, differentiation, protease production and angiogenesis[55].

FGFs stimulate angiogenesis directly by activating their receptors on ECs or indirectly by inducing the release of angiogenic factors from other cell types. For instance, in the heart, FGF-mediated signaling induces vessel growth by stimulating the release of hedgehog, ANGPT2 and VEGFB.

FGF1 and FGF2 knockout mice develop and grow normally without any evident pathological phenotype, being their organogenesis and life span unaffected. However, mice lacking FGF2 show neuronal defects and exhibit delays in wound healing, suggesting that FGF2 might regulate sprouting of new sites of tissue repair[80,81]. Additionally, tube formation stimulated by VEGF is totally abolished when neutralizing antibodies against FGF2 are added to the system, showing that in this particular setting, VEGF requires the presence of FGF2 to promote vessel assembly[82]. FGF signaling also contributes to the proliferation of tumor cells, either by an autocrine or paracrine mechanism[82,83].

Moreover, disruption of the genes encoding FGFR1 or FGFR2 leads to embryonic death, which makes impossible to define the role of these receptors in the later stages of development and in angiogenesis[84,85].

Transforming Growth Factor β

TGFβs are a family of homodimeric cytokines that include TGFβ1, 2, 3, 4 and 5. TGFβ binds to two different types of serine-threonine kinase receptors, known as type I (TGFβR1) and type II (TGFβR2). TGFβR1 and TGFβR2 are interdependent, meaning that TGFβR1 requires TGFβR2 to bind to TGFβ and TGFβR2 requires TGFβR1 for signaling. ECs also present another specific type III (co)receptor, endoglin, which is upregulated during angiogenesis.
TGFβ helps to control many different cellular processes, including angiogenesis[3]. TGFβs are normally found in the ECM of many different cells types. In the microvasculature both EC and pericytes express TGFβRs and produce TGFβ, suggesting an auto- or paracrine loop for TGFβ[86].
An interesting property of TGFβ is that it is secreted as inactive precursors which need to become activated[87]. *In vitro* studies have shown their activation by heat, acidification and proteases[88]. Additionally, *in vivo,* activation of TGFβ by proteases could be a regulatory mechanism for TGFβ-mediated activity[89].
To date, both pro- and anti-angiogenic properties have been attributed to TGFβ, depending on the context. At low doses (<0.5 ng/ml), TGFβ helps to initiate the angiogenic switch by upregulating angiogenic factors and proteinases. However, at high doses, it inhibits EC growth, promotes basement membrane reformation and stimulates SMCs differentiation and recruitment[71].
Additionally, TGFβ reduces the degradation of the perivascular ECM by the induction of protease inhibitors and the reduction of proteases. On the other hand, TGFβ stimulates angiogenesis *in vivo*, leading to the formation of highly vascular granulation tissue two or three days after mice being subcutaneously injected[90].
Since TGFβ is not an EC mitogen, angiogenesis is indirectly stimulated through the recruitment of inflammatory cells, which in turn release pro-angiogenic cytokines[65]. TGFβ is highly chemotactic for monocytes, which under the influence of TGFβ are able to infiltrate a wound site and produce angiogenic factors[91]. However, a direct action is also possible through the binding of the two types of TGFβR1: ALK1 and ALK5 (activin receptor-

like kinase 1 and 5, respectively) and consequent activation of pro-angiogenic or maturation-specific genes[92].

Genetic studies in mice have shown that the loss of TGFβ leads to leaky vessels and lack of their structural integrity, leading to premature death[93]. TGFβ1 inactivation is lethal due to defects in the hematopoietic system and yolk sac vasculature[94].

TGFβ is also associated with pathological conditions, such as human hereditary hemorrhagic telangiectasia, which is characterized by vascular malformations. Genetic studies have shown that this disorder is caused by mutations in the genes that encode endoglin or ALK1 and ALK5, receptors of the TGFβ family. Studies in mice have shown that the loss of the TGFβRs results in arteriovenous malformations.

Platelet-derived growth factor

PDGF comprises four members: PDGF A, B, C and D, that exist at homo- or heterodimeric versions of PDGF. PDGF receptors (PDGFRs) are composed of two single α and β subunits and occur also as a homo- or heterodimers. PDGF was initially isolated from platelets, but fibroblasts, ECs, keratinocytes and various other cell types also express PDGF under certain conditions[65]. PDGF is an important signaling molecule with several different roles in angiogenesis. In ECs, PDGFRβ interacts with PDGFBB, and when the receptors are stimulated *in vitro*, the DNA synthesis increases and the angiogenic sprouting occurs[3,54]. Furthermore, PDGFB is mitogenic for SMCs and pericytes and induces the expression of VEGF and VEGFR2 in cardiac ECs[95,96]. Additionally, pericyte proliferation and migration in a growing blood vessel is enhanced by interaction with PDGF, although the initial recruitment of pericytes to growing vessels is PDGF independent[97]. The interaction of PDGF with its receptor on pericytes increases the expression of ANGPT1, which leads to a signaling cascade that facilitates the interaction between pericytes and ECs. This interaction is important to maintain the stability of newly formed capillary walls[98].

Knockout mice for the genes encoding PDGFB and PDGFRβ die prenatally from edema and hemorrhage caused by the absence of vascular mural cells. The large increase in the permeability of blood vessels found in mice deficient for PDGFB and PDGFRβ indicates that PDGF is essential for vessel stabilization[99]. Furthermore, PDGF appears to play an important role in pericyte recruitment in tumors. The inhibition of PGDFR reduces tumor growth by causing pericyte detachment, what leads to immature vessels prone to regression.

Paradoxically, others studies have shown that the overexpression of PDGFB in mice inhibits tumor growth by promoting pericyte recruitment and inducing EC growth arrest[45].

Hepatocyte Growth Factor

HGF is mapped to an heavy α chain and a light β chain[100]. The inactive pre-pro-HGF becomes active after two cleavage processes in the ECM[101].

HGF is a multifunctional cytokine produced by cells of mesenchymal origin; however, HGF was purified for the first time from rat platelets and it was described as a potent mitogenic factor for mature rat hepatocytes *in vitro*[102-105].

Additionally, HGF binds exclusively to the product of the cMET proto-oncogene[106-108]. The MET receptor comprises a ligand-binding extracellular domain, a transmembrane region and a cytoplasmic domain with tyrosine kinase activity[109]. HGF/MET binding promotes its dimerization and autophosphorylation of tyrosine residues, and the downstream signaling pathways generate diverse cellular responses, such as proliferation, survival, motility, invasion and stimulation of angiogenesis[110,111]. In the angiogenic context, the ligand–receptor interaction stimulates ECs to proliferate and migrate *in vitro*, induces blood vessel formation *in vivo*, and induces VEGF expression in human tumor cells[112,113]. Furthermore, the expression of HGF can be upregulated by several growth factors, cytokines and prostaglandins.

Several studies involving disruption of HGF or MET showed that these knockouts are embryonically lethal, with impaired development in the liver and placenta, indicating that HGF signals are essential for organ development[114,115]. On the other hand, overexpression of the receptor has been implicated in different types of tumors[116]. Thus, the significant role of the HGF/MET pathway in diverse biological and physiological processes, such as organogenesis, morphogenesis, tissue regeneration and carcinogenesis is evident. Moreover, the one-to-one ligand-receptor relationship makes the HGF/MET axis an attractive target for drug development, either by activation or inhibition of this pathway[100].

Endostatin

Endostatin is an anti-angiogenic 20-kDa internal fragment of the C-terminal of collagen XVIII[117]. Collagen XVIII is a component of basement membranes with structural properties

of both a collagen and a protheoglycan. Proteolytic cleavage within its C-terminal domain releases an endostatin fragment[118]. It was originally isolated from a hemangioendothelioma cell line for its ability to inhibit proliferation[119]. Endostatin interacts with many different cell surface proteins, including integrins and glypicans, and these interactions result in altered ECs adhesion and migration. *In vitro* studies have shown inhibition of ECs migration, proliferation and tube formation by endostatin[3]. Endostatin reduces ECs proliferation by arresting the EC cell cycle, through the downregulation of cyclin-D1 promotor transcriptional activity. Moreover, inhibition of angiogenesis via endostatin *in vivo* leads to a reduction of tumor growth, which is partially accomplished by the reduction of VEGF expression. Endostatin has the ability to block existing VEGF from interacting with its receptor VEGFR2[117]. Recent studies have also shown that endostatin disturbs the survival/death balance via activation of the pro-apoptotic pathway through the induction of caspase-9 activation[3].

Physiological function of collagen XVIII/endostatin has recently been uncovered through the identification of inactivating mutations in the human collagen XVIII/endostatin gene (COLI18A1) in patients with Knobloch syndrome, characterized by age-dependent vitreoretinal degeneration and occipital encephalocele. The essential role of collagen XVIII/endostatin in ocular development and in the maintenance of the visual function is further demonstrated in the ocular abnormities seen in mice lacking collagen XVIII/endostatin gene[118]. Furthermore, studies in mice lacking collagen XVIII and its proteolytically derived product endostatin show delayed regression of blood vessels in the vitreous along the surface of the retina vessels. These findings suggest that collagen XVIII/endostatin is critical for normal blood vessel formation in the eye[120].

Thrombospondin-1

Thrombospondin1 (TSP1), a 142 kDa secreted glycoprotein, initially isolated from human platelets, was the first endogenous protein with anti-angiogenic properties to be identified[121,122]. TSP1, a member of a large family of matricellular proteins, plays an important role in genesis and remodelling of multiple tissues including cartilage and vasculature[123]. TSP1 is found in the extra- and pericellular matrix and regulate the extracellular milieu through a direct interaction with extracellular matrix proteins[124]. TSP1 modulates expression of several genes involved in angiogenesis including TGFβ, VEGF and

its receptors, plasminogen activator, MMPs and CD36, inducing a quiescent state and a differentiated phenotype of vascular ECs[125]. TSP1 promotes the migration of SMCs but suppresses chemotaxis and motility of the ECs, stimulates matrix assembly through binding to other matrix proteins, such as fibronectin and collagen and regulates matrix digestion by MMPs and plasmin. Finally, TSP1 stimulates apoptosis of ECs but promotes the survival of SMCs[123]. The interaction of TSP1 with its receptor CD36 inhibits cell migration and induces apoptosis through down-regulation of Bcl2 and activation of caspases and the JNK-MAP kinase pathway[125]. Animal studies shown that TSP1 inhibits EC migration and neovascularization in the rat cornea[122]. Also, the expression of TSP1 in various tumor cell lines prevents their aggressive growth and neovascularization when implanted in mice[125]. Moreover, in a context of retinal vasculature and neovascularization, studies with TSP1 deficient mice showed an increased retinal vascular density and a reduced number of apoptotic nuclei during remodelling and maturation in TSP1 deficient mice when compared to the normal one[125].

Tumstatin

Tumstatin is a 28 kDa cleaved fragment of type IV collagen, a basement membrane collagen found in the kidney, lung and other vascular basement membranes[126].

Tumstatin influences the sprouting and proliferation of ECs by interacting with their specific receptor and thus resulting in changes in the intracellular signaling and inducing anti-angiogenic effects. Tumstatin inhibits angiogenesis by inducing apoptosis and inhibits EC proliferation through its binding to αvβ3 integrin[124].

Mice model studies have shown that administration of exogenous tumstatin inhibits tumor growth. However, tumstatin deficient mice had a much greater micro-vessel density near implanted murine tumors and a 300% increase in overall tumor growth[3]. Moreover, mice with a genetic deletion on tumstatin gene showed accelerated tumor growth associated with enhanced pathological angiogenesis, while angiogenesis associated with development and tissue repair were unaffected[127]. Animal studies determining the viability of tumstatin as an anti-angiogenic drug showed a reduction of over 90% in tumor size when compared with the controls[3].

4.2. Pathological Angiogenesis

In physiological conditions, the angiogenic balance is sustained by the activity of stimulators (pro-angiogenic factors) and inhibitors (anti-angiogenic factors). However, the loss of this balance becomes a critical factor in certain pathological conditions such as cancer, atherosclerosis, ischemia and diabetic retinopathy[51]. When more angiogenic growth factors than angiogenesis inhibitors are produced, the balance is tipped in favor of blood vessel growth, implicated in diseases like cancer[51,128]. Tumor vessels are architecturally different from normal ones, having an abnormal structure and function with apparently chaotic organization[16]. Vessels vary from abnormally wide, irregular and tortuous serpentine-like shape to thin channels with small or compressed lumens[129]. Every layer of the tumor vessel wall is abnormal: ECs form an imperfect lining, with wide junctions at some locations and stacked layers of ECs at others. ECs may contain many fenestrations, vesicle vacuolar organelles or both. The expression of adhesion molecules is also more heterogeneous than in normal tissue. Because of the abnormal organization and structure of tumor vessels, the blood flow is chaotic and the vessels are leaky. The resulting irregular perfusion impairs oxygen, nutrient and drug delivery[6,50].

On the other hand, when angiogenesis inhibitors are more produced than angiogenic growth factors, angiogenesis does not occur, resulting in ECs dysfunction, vessel malformation or regression and situations like ischemia or atherosclerosis may take place[51,128].

Both situations lead to an uncontrolled angiogenesis process. In this work, we will give especial attention to critical limb ischemia (CLI).

4.2.1. Critical Limb Ischemia

CLI is the most severe manifestation of peripheral arterial disease (PAD)[130]. PAD can be anatomically defined as an obstructive arterial disease or functionally as an arterial narrowing, causing a mismatch between oxygen supply and demand[131]. Thus, PAD is a medical condition that involves an obstruction in arteries that provide blood flow to the arms or legs, due to atherosclerosis[132,133]. CLI patients typically present chronic ischemic rest pain or ischemic skin lesions, either ulcers or gangrene and this condition is estimated to develop in 500 to 1000 individual per million per year[134,135]. Almost 50% of patients with

CLI have diabetes, which is a metabolic disorder of multifactorial etiology. Diabetes is characterized by chronic hyperglycemia and changes in the metabolism of carbohydrates, lipids and proteins, resulting in relative to absolute impairment in insulin secretion and/or reduction in its biological activity[136].

Patients with CLI have high mortality rates because the atherosclerotic disease is a systemic disease that does not localize to an isolated vessel segment. So, CLI is a chronic and complex process that affects the macrovascular and microvascular systems, as well as surrounding tissues[137]. This usually results from the presence of multilevel occlusive disease or occlusion of critical collaterals[134]. Additionally, CLI leads to alterations in structure and function of ECs. This endothelial dysfunction leads to micro thrombosis within the capillaries and exacerbates edema formation in their extremity. Furthermore, endothelial trauma results in increased free radical production, inappropriate platelet activation, and leukocyte adhesion, all of which lead to micro thrombi formation[137]. Capillary microscopy has shown initial tissue edema and pericapillary hemorrhage, followed by a reduction in the number of perfused capillaries, resulting in ischemic areas[134]. Once the diagnosis is confirmed, the goals for treating CLI are to relieve ischemic pain, heal ischemic ulcers and prevent limb loss. For that, it is crucial to control the risk factors such as hypertension, diabetes, dyslipidemia and smoking, thereby changing the life style and prolonging the survival of the patient[137,138]. Revascularization of ischemic areas may be the solution, but important issues must be considered, including the presence of comorbidity and arterial anatomy. It is mandatory to perform a risk-benefit analysis to determine the optimal therapy. A significant improvement in blood flow may diminish the symptoms of rest pain, but pulsatile flow to the foot is generally necessary for the treatment of ischemic ulcers or gangrene[134,137]. In patients not eligible for arterial reconstruction, pharmacotherapy using antiplatelet agents and vasodilators are the only option[138]. In these cases, prostanoids are the only vasoactive drugs with proven efficacy. Most studies have found that parenteral administration of either prostaglandin E1 or Iloprost reduces pain, ulcer size, and/or the need for amputation. However, amputation continues to be the recommended solution to the disabling symptoms, despite its associated morbidity and mortality rates. Only 50% of patients who are not candidates for revascularization will be alive without a major amputation one year after the onset of CLI. Furthermore, one-third of amputated patients die within one year, one-third achieve partial autonomy and only one-third obtain

complete autonomy[134]. Many clinical studies are being carried on with the goal of increasing or stimulating angiogenesis in patients with PAD or CLI[137].

5. Pro-angiogenic therapy

Pro-angiogenic therapy is introduced as a novel strategy for the treatment of vascular insufficiency[139]. There are three major disorders for which pro-angiogenesis therapy is clinically indicated: chronic wound, CLI and ischemic heart disease[52].

To successfully apply it, several conditions should be met: (1) newly formed blood vessels must be functional and supply the ischemic region with oxygenated blood; (2) the functional blood vessels must remain stable; and (3) the neovascularization in ischemic tissue should be tightly regulated to attain maximum efficiency. Thus, the aim of pro-angiogenic therapy is to deliver highly effective angiogenic factors to the ischemic region, in order to increase the perfusion and function of an organ or tissue[140].

Several approaches have been considered to increase angiogenesis, including the evaluation of different angiogenic growth factors, of different treatment modalities and routes of administration (recombinant protein versus gene transfer) and of cellular techniques[141].

5.1. Local administration of pro-angiogenic growth factors

Angiogenic growth factors have the ability to increase collateral vessels and augment tissue perfusion and oxygenation, limiting ischemic lesions in a variety of animal models of coronary or limb ischaemia[142]. The beneficial effects of growth factors in animal ischemic models led to a great expectation of its use for the treatment of CLI[130]. During the past decade, numerous clinical trials have been encouraged in a context of therapeutic angiogenesis and despite claims of success in an early state, clinical trials failed to conclusively show a clinical benefit[143,144]. VEFG family are among the most powerful growth factors that modulate vascular biology and have received much attention regarding their potential therapeutic effect in CLI. Others angiogenic growth factors, like members of the HGF, FGF, PDGF or TGFβ are also under study[131,135,137,138,144-146]. Unfortunately, the results have been quite disappointing and numerous reasons have been pointed out to explain this[130,145].

Part of this failure can be attributed to the lack of efficiency of the delivery procedure. For example, naked DNA is poorly taken-up, but different types of DNA vector have been successfully used to increase the efficiency of gene transfer. However, even the best methods of gene transfer still encounter significant problems to achieve effective transfection rates that could result in clinically significant levels of protein production[141]. Another problem can be dose-response: low doses for longer-term administration have shown a better prognosis with fewer side effects, when compared with higher doses[147]. Moreover, blood vessel growth is a process too complex to be stimulated effectively by the administration of a single angiogenic cytokine. So, combining factors that are pro-angiogenic, such as VEGF or FGF2, with pro-maturation factors, such as ANGPT1 or PDGFBB, that mediate pericytes recruitment, could prevent hyperpermeability and also stabilize the nascent vasculature[140]. Additionally, potential patient-related issues, such as the existence of co-morbidities, the use of other medications, circulation of angiogenic inhibitors and lack of target receptor expression in target tissues could contribute to the ineffective response to angiogenic stimulation[148]. Alternatively, the increase of cellular recruitment with the induction of local production by a cocktail of growth factors has been explored. Thus, *in vitro* studies have shown that the administration of MCP1, which increases the recruitment of monocytes to ischemic tissue, improves collateral flow in a rabbit model of hindlimb ischemia[141].

5.2 Cell-based therapeutic strategy

An alternative strategy to achieve angiogenesis is through cell therapy, in which transplanted cells can be integrated into the neovasculature of the ischemic tissue to increase its density and perfusion[145]. Moreover, transplanted cells can secrete multiple endogenous growth factors, meaning that these cells will induce vascular growth in a paracrine manner[148]. The potential of EPCs therapy in hindlimb ischemia disease is currently being extensively studied[149]. In the process of neovascularization, EPCs can differentiate into ECs. Thus, EPCs from bone marrow or peripheral blood are expanded and concentrated *ex vivo* and then re-administrated into the ischemic region. This approach accelerates the process of neovascularization and could be an alternative to angiogenic factors[140,142]. The transplantation of EPCs significantly improved blood flow recovery and capillary density in several animal models of hindlimb ischemia[33]. Moreover, studies from

Asahara *at al* showed *in vivo* mobilization and incorporation of autologous EPCs application into sites of tissue ischemia and neovascularization in a rabbit model of hindlimb ischemia[139,150]. Also, EPCs transplantation induces blood flow recovery in the ischemic hindlimbs of both diabetic mice and rats, suggesting that EPC-mediated neovascularization can still occur under disease conditions[33]. These encouraging results from preclinical studies have rapidly led to several clinical trials, in which bone marrow-derived mononuclear cells (BM-MNCs) were administrated to patients with CLI[151]. Moreover, recent evidences indicate that BM-MNCs promote collateral vessel formation in patient with CLI[144]. A variety of cell types has been studied in cell therapy, including unselected BM-MNC or peripheral blood-derived mononuclear cells (PB-MNCs), which comprise a heterogeneous mix of blood cells and nonhematopoietic stromal cells (mesenchymal stem cells (MSCs) and EPCs) and selected EPCs isolated and purified from BM-MNCs or PB-MNCs[145,149].

The first report on the use of BM-MNC in limb ischemia was the Therapeutic Angiogenesis Using Cell Transplantation (TACT) study, in which an intramuscular injection of autologous BM-MNC significantly improved the leg pain scale, ulcer size and pain-free walking distance, for at least 2 years. Also, a 3 years' follow-up assessment showed significantly lower amputation rates[144,149]. In the last decade, several trials have been performed, indicating that the use of BM-MNCs or PB-MNCs in cell therapy is a feasible, relatively safe and potentially effective therapeutic strategy for CLI patients[144,152].

Also, a randomized controlled trial comparing BM-MNCs and bone marrow-derived mesenchymal stem cells (BM-MSCs) demonstrated a significant improvement in pain-free walking time in both groups after 6 months. Additionally, the patients administrated with BM-MSC had significantly greater collateral blood vessel scores than patients administrated with BM-MNCs[153]. Others cell types, such as adipose-derived regenerative cells, are currently being explored. Clinical studies using these cells are now required to determine whether these cells provide advantages for CLI treatment[145]. However, more clinical trials are needed to clarify the still open issues, including the selection of optimal cell type, isolation method, cell number, route of administration and paracrine stimulation mechanisms[151].

Particularly for CLI, it is disappointing that after extensive preclinical investigation and two decades of clinical trials of angiogenic or cell therapies, none has been approved.

5.3 The use of ionizing radiation as a novel approach

Ionizing radiation is a type of energy released by atoms that travels in the form of electromagnetic waves (gamma or X-rays) or particles (electrons, neutrons, beta or alpha particles). Exposure to ionizing radiation comes mainly in the form of natural background radiation (from the earth, cosmic rays and the radioactivity naturally contained in the human body), but also from human-made sources, ranging from nuclear power generation to medical uses of radiation for diagnosis or treatment, prominently X-rays[154].

Radiotherapy is the treatment of diseases by using ionizing radiation. It is a widely applied and highly effective therapeutic modality for the majority of the solid malignant neoplasms, being applied alone or associated with chemotherapy and/or surgery[155]. It is classically delivered in fractionated schemes of typically of 1.8 to 2.0 Gy/daily dose, repeated until a potentially curative tumor specific dose has accumulated.

In addition to treatment of malignant diseases, ionizing radiation therapy can also be used for successful treatment of benign or non-malignant conditions, namely a variety of inflammatory and painful joint disease (such as heel spurs, osteoarthritis, tendonitis)[156]. Several studies demonstrate that ionizing radiation can differently modulate the inflammatory process. For instance, low-dose ionizing radiation (LDIR) (<1 Gy) attenuates a pre-existing inflammation, while doses exceeding 1 Gy may act as an initiator of the inflammatory process[157]. It was also demonstrated that ionizing radiation can attenuate the pathology of autoimmune diseases in animal models. In a mice model of rheumatoid arthritis, a suppression of IL6 and IL7 production and up-regulation of regulatory T cells was demonstrated after repeated irradiation with 0.5 Gy. Studies using a mice model of multiple sclerosis showed suppression of pro-inflammatory cytokines, reduction of $CD8^+$ T cells and induction of regulatory T cells after exposure to 0.5 Gy once per week during 4 weeks[156].

In a scenario of hindlimb ischemia, Heissig *at al* revealed that doses of ionizing radiation between 2 and 10 Gy increases vasculogenesis in ischemic tissues[158]. This study shows that increased recruitment and activation of mast cells following ionizing radiation exposure alters the ischemic microenviroment and promotes vascular regeneration in an ischemic model. Therefore, these data showed a novel strategy of neovascularization and suggest another therapeutic use for ionizing radiation. Moreover, Thanik *at al* showed that a single dose of 5 Gy delivered to an ischemic full-thickness cutaneous flap improves vascularity in

two ways: (1) through upregulation of HIF1, leading to increased angiogenic and vasculogenic pathways and (2) by direct upregulation of MMP9, which mobilizes EPCs from bone marrow into the peripheral circulation[159]. This study suggests that ionizing radiation creates a stimulus for systemic response, leading to pro-angiogenic effects.

Furthermore, *in vitro* studies from our research group demonstrated that LDIR, lower than 0.8 Gy, enhances the migration of lung microvascular endothelial cells (HMVEC-L), without affecting their proliferation or survival. LDIR-induced endothelium activation occurs through the phosphorylating VEGFR2, which is a critical player in the angiogenic process. Using a zebrafish model, our group also showed that LDIR accelerates vessel formation by inducing angiogenic sprouting in embryos and increasing vessel density in adults. This knowledge was extended to different mouse models, where LDIR was found to promote angiogenesis and accelerate tumor growth and metastasis[160].

Overall, the results of these investigations may help to support the use of ionizing radiation, particularly LDIR, as an option for the treatment of ischemic diseases, namely in a setting of CLI[156].

6. References

1 Adams, R. H. & Alitalo, K. Molecular regulation of angiogenesis and lymphangiogenesis. *Nature reviews. Molecular cell biology* **8**, 464-478, doi:10.1038/nrm2183 (2007).

2 Eichmann, A. *et al.* Vascular development: from precursor cells to branched arterial and venous networks. *The International journal of developmental biology* **49**, 259-267, doi:10.1387/ijdb.041941ae (2005).

3 Nussenbaum, F. & Herman, I. M. Tumor angiogenesis: insights and innovations. *Journal of oncology* **2010**, 132641, doi:10.1155/2010/132641 (2010).

4 Hellstrom, M. *et al.* Lack of pericytes leads to endothelial hyperplasia and abnormal vascular morphogenesis. *The Journal of cell biology* **153**, 543-553 (2001).

5 Cleaver, O. & Melton, D. A. Endothelial signaling during development. *Nature medicine* **9**, 661-668, doi:10.1038/nm0603-661 (2003).

6 Jain, R. K. Molecular regulation of vessel maturation. *Nature medicine* **9**, 685-693, doi:10.1038/nm0603-685 (2003).

7 Shier, D., Butler, J. L., Lewis, R. *Hole's Human Anatomy and Physiology*. 1024 pages (McGraw-Hill Education, 1996).

8 Kume, T. Specification of arterial, venous, and lymphatic endothelial cells during embryonic development. *Histology and histopathology* **25**, 637-646 (2010).

9 Swift, M. R. & Weinstein, B. M. Arterial-venous specification during development. *Circulation research* **104**, 576-588, doi:10.1161/CIRCRESAHA.108.188805 (2009).

10 Lin, F. J., Tsai, M. J. & Tsai, S. Y. Artery and vein formation: a tug of war between different forces. *EMBO reports* **8**, 920-924, doi:10.1038/sj.embor.7401076 (2007).

11 Torres-Vazquez, J., Kamei, M. & Weinstein, B. M. Molecular distinction between arteries and veins. *Cell and tissue research* **314**, 43-59, doi:10.1007/s00441-003-0771-8 (2003).

12 Fish, J. E. & Wythe, J. D. The molecular regulation of arteriovenous specification and maintenance. *Developmental dynamics : an official publication of the American Association of Anatomists* **244**, 391-409, doi:10.1002/dvdy.24252 (2015).

13 Coultas, L., Chawengsaksophak, K. & Rossant, J. Endothelial cells and VEGF in vascular development. *Nature* **438**, 937-945, doi:10.1038/nature04479 (2005).

14 Udan, R. S., Culver, J. C. & Dickinson, M. E. Understanding vascular development. *Wiley interdisciplinary reviews. Developmental biology* **2**, 327-346, doi:10.1002/wdev.91 (2013).

15 Beck, L., Jr. & D'Amore, P. A. Vascular development: cellular and molecular regulation. *FASEB journal : official publication of the Federation of American Societies for Experimental Biology* **11**, 365-373 (1997).

16 Conway, E. M., Collen, D. & Carmeliet, P. Molecular mechanisms of blood vessel growth. *Cardiovascular research* **49**, 507-521 (2001).

17 Risau, W. Mechanisms of angiogenesis. *Nature* **386**, 671-674, doi:10.1038/386671a0 (1997).

18 Kassmeyer, S., Plendl, J., Custodis, P. & Bahramsoltani, M. New insights in vascular development: vasculogenesis and endothelial progenitor cells. *Anatomia, histologia, embryologia* **38**, 1-11, doi:10.1111/j.1439-0264.2008.00894.x (2009).

19 Asahara, T. *et al.* Isolation of putative progenitor endothelial cells for angiogenesis. *Science* **275**, 964-967 (1997).

20 Balaji, S., King, A., Crombleholme, T. M. & Keswani, S. G. The Role of Endothelial Progenitor Cells in Postnatal Vasculogenesis: Implications for Therapeutic Neovascularization and Wound Healing. *Advances in wound care* **2**, 283-295, doi:10.1089/wound.2012.0398 (2013).

21 Kachamakova-Trojanowska, N., Bukowska-Strakova, K., Zukowska, M., Dulak, J. & Jozkowicz, A. The real face of endothelial progenitor cells - Circulating angiogenic cells as endothelial prognostic marker? *Pharmacological reports : PR* **67**, 793-802, doi:10.1016/j.pharep.2015.05.017 (2015).

22 Resch, T., Pircher, A., Kahler, C. M., Pratschke, J. & Hilbe, W. Endothelial progenitor cells: current issues on characterization and challenging clinical applications. *Stem cell reviews* **8**, 926-939, doi:10.1007/s12015-011-9332-9 (2012).

23 Ribatti, D., Vacca, A., Nico, B., Roncali, L. & Dammacco, F. Postnatal vasculogenesis. *Mechanisms of development* **100**, 157-163 (2001).

24 Murasawa, S. & Asahara, T. Endothelial progenitor cells for vasculogenesis. *Physiology* **20**, 36-42, doi:10.1152/physiol.00033.2004 (2005).

25 Duan, H., Cheng, L., Jianwang, Hu, L. & Lu, G. Angiogenic potential difference between two types of endothelial progenitor cells from human umbilical cord blood. *Cell Biology International* **30**, 1018-1027, doi:10.1016/j.cellbi.2006.08.002 (2006).

26 Hur, J. *et al.* Characterization of Two Types of Endothelial Progenitor Cells and Their Different Contributions to Neovasculogenesis. *Arteriosclerosis, thrombosis, and vascular biology* **24**, 288-293, doi:10.1161/01.atv.0000114236.77009.06 (2003).

27 Young, P. P., Vaughan, D. E. & Hatzopoulos, A. K. Biologic properties of endothelial progenitor cells and their potential for cell therapy. *Progress in cardiovascular diseases* **49**, 421-429, doi:10.1016/j.pcad.2007.02.004 (2007).

28 Hristov, M., Erl, W. & Weber, P. C. Endothelial progenitor cells: mobilization, differentiation, and homing. *Arteriosclerosis, thrombosis, and vascular biology* **23**, 1185-1189, doi:10.1161/01.ATV.0000073832.49290.B5 (2003).

29 George, A. L. *et al.* Endothelial progenitor cell biology in disease and tissue regeneration. *Journal of hematology & oncology* **4**, 24, doi:10.1186/1756-8722-4-24 (2011).

30 Li, D. W., Liu, Z. Q., Wei, J., Liu, Y. & Hu, L. S. Contribution of endothelial progenitor cells to neovascularization (Review). *International journal of molecular medicine* **30**, 1000-1006, doi:10.3892/ijmm.2012.1108 (2012).

31 Hillen, F. & Griffioen, A. W. Tumour vascularization: sprouting angiogenesis and beyond. *Cancer metastasis reviews* **26**, 489-502, doi:10.1007/s10555-007-9094-7 (2007).

32 Caiado, F. & Dias, S. Endothelial progenitor cells and integrins: adhesive needs. *Fibrogenesis & tissue repair* **5**, 4, doi:10.1186/1755-1536-5-4 (2012).

33 Szmitko, P. E. *et al.* Endothelial progenitor cells: new hope for a broken heart. *Circulation* **107**, 3093-3100, doi:10.1161/01.CIR.0000074242.66719.4A (2003).

34 Asahara, T., Kawamoto, A. & Masuda, H. Concise review: Circulating endothelial progenitor cells for vascular medicine. *Stem cells* **29**, 1650-1655, doi:10.1002/stem.745 (2011).

35 Jazwa, A. *et al.* Limb ischemia and vessel regeneration: Is there a role for VEGF? *Vascular pharmacology* **86**, 18-30, doi:10.1016/j.vph.2016.09.003 (2016).

36 Cochain, C. & Zernecke, A. Stimulating arteriogenesis but not atherosclerosis: IFN-alpha/beta receptor subunit 1 as a novel therapeutic target. *Cardiovascular research* **107**, 200-202, doi:10.1093/cvr/cvv174 (2015).

37 Heil, M., Eitenmuller, I., Schmitz-Rixen, T. & Schaper, W. Arteriogenesis versus angiogenesis: similarities and differences. *Journal of cellular and molecular medicine* **10**, 45-55 (2006).

38 Cai, W. & Schaper, W. Mechanisms of arteriogenesis. *Acta biochimica et biophysica Sinica* **40**, 681-692 (2008).

39 Schaper, W. Collateral circulation: past and present. *Basic research in cardiology* **104**, 5-21, doi:10.1007/s00395-008-0760-x (2009).

40 van Royen, N. *et al.* Stimulation of arteriogenesis; a new concept for the treatment of arterial occlusive disease. *Cardiovascular research* **49**, 543-553 (2001).

41 Heil, M. & Schaper, W. Influence of mechanical, cellular, and molecular factors on collateral artery growth (arteriogenesis). *Circulation research* **95**, 449-458, doi:10.1161/01.RES.0000141145.78900.44 (2004).

42 Burri, P. H., Hlushchuk, R. & Djonov, V. Intussusceptive angiogenesis: its emergence, its characteristics, and its significance. *Developmental dynamics : an official publication of the American Association of Anatomists* **231**, 474-488, doi:10.1002/dvdy.20184 (2004).

43 Carmeliet, P. & Jain, R. K. Angiogenesis in cancer and other diseases. *Nature* **407**, 249-257, doi:10.1038/35025220 (2000).

44 Herbert, S. P. & Stainier, D. Y. Molecular control of endothelial cell behaviour during blood vessel morphogenesis. *Nature reviews. Molecular cell biology* **12**, 551-564, doi:10.1038/nrm3176 (2011).

45 Carmeliet, P. & Jain, R. K. Molecular mechanisms and clinical applications of angiogenesis. *Nature* **473**, 298-307, doi:10.1038/nature10144 (2011).

46 Loughna, S. & Sato, T. N. Angiopoietin and Tie signaling pathways in vascular development. *Matrix biology : journal of the International Society for Matrix Biology* **20**, 319-325 (2001).

47 Suri, C. *et al.* Requisite role of angiopoietin-1, a ligand for the TIE2 receptor, during embryonic angiogenesis. *Cell* **87**, 1171-1180 (1996).

48 Bergers, G. & Song, S. The role of pericytes in blood-vessel formation and maintenance. *Neuro-oncology* **7**, 452-464, doi:10.1215/S1152851705000232 (2005).

49 Maisonpierre, P. C. *et al.* Angiopoietin-2, a natural antagonist for Tie2 that disrupts in vivo angiogenesis. *Science* **277**, 55-60 (1997).

50 Potente, M., Gerhardt, H. & Carmeliet, P. Basic and therapeutic aspects of angiogenesis. *Cell* **146**, 873-887, doi:10.1016/j.cell.2011.08.039 (2011).

51 Carmeliet, P. Angiogenesis in life, disease and medicine. *Nature* **438**, 932-936, doi:10.1038/nature04478 (2005).

52 Prabhu, V. V., Chidambaranathan, N. & Gopal, V. A Historical Review on Current Medication and Therapies for Inducing and Inhibiting Angiogenesis. *Journal of chemical and pharmaceutical research* **3**, 526-533 (2011).

53 Veikkola, T. & Alitalo, K. VEGFs, receptors and angiogenesis. *Seminars in cancer biology* **9**, 211-220, doi:10.1006/scbi.1998.0091 (1999).

54 Otrock, Z. K., Mahfouz, R. A., Makarem, J. A. & Shamseddine, A. I. Understanding the biology of angiogenesis: review of the most important molecular mechanisms. *Blood cells, molecules & diseases* **39**, 212-220, doi:10.1016/j.bcmd.2007.04.001 (2007).

55 Liekens, S., De Clercq, E. & Neyts, J. Angiogenesis: regulators and clinical applications. *Biochemical pharmacology* **61**, 253-270 (2001).

56 Conn, G. *et al.* Purification of a glycoprotein vascular endothelial cell mitogen from a rat glioma-derived cell line. *Proceedings of the National Academy of Sciences of the United States of America* **87**, 1323-1327 (1990).

57 Dimmeler, S., Dernbach, E. & Zeiher, A. M. Phosphorylation of the endothelial nitric oxide synthase at ser-1177 is required for VEGF-induced endothelial cell migration. *FEBS letters* **477**, 258-262 (2000).

58 Dvorak, H. F., Brown, L. F., Detmar, M. & Dvorak, A. M. Vascular permeability factor/vascular endothelial growth factor, microvascular hyperpermeability, and angiogenesis. *The American journal of pathology* **146**, 1029-1039 (1995).

59 Gerber, H. P. *et al.* Vascular endothelial growth factor regulates endothelial cell survival through the phosphatidylinositol 3'-kinase/Akt signal transduction

pathway. Requirement for Flk-1/KDR activation. *The Journal of biological chemistry* **273**, 30336-30343 (1998).

60 Hood, J. D., Meininger, C. J., Ziche, M. & Granger, H. J. VEGF upregulates ecNOS message, protein, and NO production in human endothelial cells. *Am J Physiol* **274**, H1054-1058 (1998).

61 Brown, L. F. *et al.* Expression of vascular permeability factor (vascular endothelial growth factor) by epidermal keratinocytes during wound healing. *The Journal of experimental medicine* **176**, 1375-1379 (1992).

62 Ferrara, N., Gerber, H. P. & LeCouter, J. The biology of VEGF and its receptors. *Nature medicine* **9**, 669-676, doi:10.1038/nm0603-669 (2003).

63 Richard, D. E., Berra, E. & Pouyssegur, J. Angiogenesis: how a tumor adapts to hypoxia. *Biochem Biophys Res Commun* **266**, 718-722 (1999).

64 Carmeliet, P. *et al.* Abnormal blood vessel development and lethality in embryos lacking a single VEGF allele. *Nature* **380**, 435-439 (1996).

65 Distler, J. H. W. *et al.* Angiogenic and angiostatic factors in the molecular control of angiogenesis. *Q J Nucl Med* **47**, 149-161 (2003).

66 Hughes, S., Yang, H. & Chan-Ling, T. Vascularization of the human fetal retina: roles of vasculogenesis and angiogenesis. *Investigative ophthalmology & visual science* **41**, 1217-1228 (2000).

67 Veikkola, T., Karkkainen, M., Claesson-Welsh, L. & Alitalo, K. Regulation of angiogenesis via vascular endothelial growth factor receptors. *Cancer research* **60**, 203-212 (2000).

68 Fong, G. H., Zhang, L., Bryce, D. M. & Peng, J. Increased hemangioblast commitment, not vascular disorganization, is the primary defect in flt-1 knock-out mice. *Development* **126**, 3015-3025 (1999).

69 Shalaby, F. *et al.* Failure of blood-island formation and vasculogenesis in Flk-1-deficient mice. *Nature* **376**, 62-66 (1995).

70 Eichmann, A. *et al.* Ligand-dependent development of the endothelial and hemopoietic lineages from embryonic mesodermal cells expressing vascular endothelial growth factor receptor 2. *Proceedings of the National Academy of Sciences of the United States of America* **94**, 5141-5146 (1997).

71 Carmeliet, P. Angiogenesis in health and disease. *Nature medicine* **9**, 653-660, doi:10.1038/nm0603-653 (2003).

72 Klagsbrun, M. & Moses, M. A. Molecular angiogenesis. *Chemistry & biology* **6**, R217-224, doi:10.1016/S1074-5521(99)80081-7 (1999).

73 Suri, C. *et al.* Increased vascularization in mice overexpressing angiopoietin-1. *Science* **282**, 468-471 (1998).

74 Lobov, I. B., Brooks, P. C. & Lang, R. A. Angiopoietin-2 displays VEGF-dependent modulation of capillary structure and endothelial cell survival in vivo. *Proceedings of the National Academy of Sciences of the United States of America* **99**, 11205-11210, doi:10.1073/pnas.172161899 (2002).

75 Fearon, U. *et al.* Angiopoietins, growth factors, and vascular morphology in early arthritis. *The Journal of rheumatology* **30**, 260-268 (2003).

76 Hangai, M. *et al.* Angiopoietin-1 upregulation by vascular endothelial growth factor in human retinal pigment epithelial cells. *Investigative ophthalmology & visual science* **42**, 1617-1625 (2001).

77 Kuroda, K., Sapadin, A., Shoji, T., Fleischmajer, R. & Lebwohl, M. Altered expression of angiopoietins and Tie2 endothelium receptor in psoriasis. *The Journal of investigative dermatology* **116**, 713-720, doi:10.1046/j.0022-202x.2001.doc.x (2001).

78 Ornitz, D. M. FGFs, heparan sulfate and FGFRs: complex interactions essential for development. *BioEssays : news and reviews in molecular, cellular and developmental biology* **22**, 108-112, doi:10.1002/(SICI)1521-1878(200002)22:2<108::AID-BIES2>3.0.CO;2-M (2000).

79 Vlodavsky, I., Bar-Shavit, R., Ishai-Michaeli, R., Bashkin, P. & Fuks, Z. Extracellular sequestration and release of fibroblast growth factor: a regulatory mechanism? *Trends in biochemical sciences* **16**, 268-271 (1991).

80 Miller, D. L., Ortega, S., Bashayan, O., Basch, R. & Basilico, C. Compensation by fibroblast growth factor 1 (FGF1) does not account for the mild phenotypic defects observed in FGF2 null mice. *Molecular and cellular biology* **20**, 2260-2268 (2000).

81 Ortega, S., Ittmann, M., Tsang, S. H., Ehrlich, M. & Basilico, C. Neuronal defects and delayed wound healing in mice lacking fibroblast growth factor 2. *Proceedings of*

the National Academy of Sciences of the United States of America **95**, 5672-5677 (1998).

82 Javerzat, S., Auguste, P. & Bikfalvi, A. The role of fibroblast growth factors in vascular development. *Trends in molecular medicine* **8**, 483-489 (2002).

83 Beenken, A. & Mohammadi, M. The FGF family: biology, pathophysiology and therapy. *Nature reviews. Drug discovery* **8**, 235-253, doi:10.1038/nrd2792 (2009).

84 Deng, C. X. *et al.* Murine FGFR-1 is required for early postimplantation growth and axial organization. *Genes & development* **8**, 3045-3057 (1994).

85 Xu, X. *et al.* Fibroblast growth factor receptor 2 (FGFR2)-mediated reciprocal regulation loop between FGF8 and FGF10 is essential for limb induction. *Development* **125**, 753-765 (1998).

86 Sato, Y. & Rifkin, D. B. Inhibition of endothelial cell movement by pericytes and smooth muscle cells: activation of a latent transforming growth factor-beta 1-like molecule by plasmin during co-culture. *The Journal of cell biology* **109**, 309-315 (1989).

87 Lyons, R. M., Keski-Oja, J. & Moses, H. L. Proteolytic activation of latent transforming growth factor-beta from fibroblast-conditioned medium. *The Journal of cell biology* **106**, 1659-1665 (1988).

88 Lawrence, D. A., Pircher, R. & Jullien, P. Conversion of a high molecular weight latent beta-TGF from chicken embryo fibroblasts into a low molecular weight active beta-TGF under acidic conditions. *Biochem Biophys Res Commun* **133**, 1026-1034 (1985).

89 Klagsbrun, M. & D'Amore, P. A. Regulators of angiogenesis. *Annual review of physiology* **53**, 217-239, doi:10.1146/annurev.ph.53.030191.001245 (1991).

90 Roberts, A. B. *et al.* Transforming growth factor type beta: rapid induction of fibrosis and angiogenesis in vivo and stimulation of collagen formation in vitro. *Proceedings of the National Academy of Sciences of the United States of America* **83**, 4167-4171 (1986).

91 Wahl, S. M. *et al.* Transforming growth factor type beta induces monocyte chemotaxis and growth factor production. *Proceedings of the National Academy of Sciences of the United States of America* **84**, 5788-5792 (1987).

92 Bertolino, P., Deckers, M., Lebrin, F. & ten Dijke, P. Transforming growth factor-beta signal transduction in angiogenesis and vascular disorders. *Chest* **128**, 585S-590S, doi:10.1378/chest.128.6_suppl.585S (2005).

93 van den Driesche, S., Mummery, C. L. & Westermann, C. J. Hereditary hemorrhagic telangiectasia: an update on transforming growth factor beta signaling in vasculogenesis and angiogenesis. *Cardiovascular research* **58**, 20-31 (2003).

94 Goumans, M. J., Lebrin, F. & Valdimarsdottir, G. Controlling the angiogenic switch: a balance between two distinct TGF-b receptor signaling pathways. *Trends in cardiovascular medicine* **13**, 301-307 (2003).

95 Battegay, E. J., Rupp, J., Iruela-Arispe, L., Sage, E. H. & Pech, M. PDGF-BB modulates endothelial proliferation and angiogenesis in vitro via PDGF beta-receptors. *The Journal of cell biology* **125**, 917-928 (1994).

96 Edelberg, J. M. *et al.* PDGF mediates cardiac microvascular communication. *The Journal of clinical investigation* **102**, 837-843, doi:10.1172/JCI3058 (1998).

97 Hellstrom, M., Kalen, M., Lindahl, P., Abramsson, A. & Betsholtz, C. Role of PDGF-B and PDGFR-beta in recruitment of vascular smooth muscle cells and pericytes during embryonic blood vessel formation in the mouse. *Development* **126**, 3047-3055 (1999).

98 Lindblom, P. *et al.* Endothelial PDGF-B retention is required for proper investment of pericytes in the microvessel wall. *Genes & development* **17**, 1835-1840, doi:10.1101/gad.266803 (2003).

99 Lindahl, P., Johansson, B. R., Leveen, P. & Betsholtz, C. Pericyte loss and microaneurysm formation in PDGF-B-deficient mice. *Science* **277**, 242-245 (1997).

100 Fajardo-Puerta, A. B., Mato Prado, M., Frampton, A. E. & Jiao, L. R. Gene of the month: HGF. *Journal of clinical pathology*, doi:10.1136/jclinpath-2015-203575 (2016).

101 Jiang, W., Hiscox, S., Matsumoto, K. & Nakamura, T. Hepatocyte growth factor/scatter factor, its molecular, cellular and clinical implications in cancer. *Critical reviews in oncology/hematology* **29**, 209-248 (1999).

102 Gohda, E. *et al.* Purification and partial characterization of hepatocyte growth factor from plasma of a patient with fulminant hepatic failure. *The Journal of clinical investigation* **81**, 414-419, doi:10.1172/JCI113334 (1988).

103 Nakamura, T., Nawa, K. & Ichihara, A. Partial purification and characterization of hepatocyte growth factor from serum of hepatectomized rats. *Biochem Biophys Res Commun* **122**, 1450-1459 (1984).

104 Nakamura, T., Nawa, K., Ichihara, A., Kaise, N. & Nishino, T. Purification and subunit structure of hepatocyte growth factor from rat platelets. *FEBS letters* **224**, 311-316 (1987).

105 Russell, W. E., McGowan, J. A. & Bucher, N. L. Partial characterization of a hepatocyte growth factor from rat platelets. *Journal of cellular physiology* **119**, 183-192, doi:10.1002/jcp.1041190207 (1984).

106 Bottaro, D. P. *et al.* Identification of the hepatocyte growth factor receptor as the c-met proto-oncogene product. *Science* **251**, 802-804 (1991).

107 Dean, M. *et al.* The human met oncogene is related to the tyrosine kinase oncogenes. *Nature* **318**, 385-388 (1985).

108 Naldini, L. *et al.* Hepatocyte growth factor (HGF) stimulates the tyrosine kinase activity of the receptor encoded by the proto-oncogene c-MET. *Oncogene* **6**, 501-504 (1991).

109 Matsumoto, K., Kataoka, H., Date, K. & Nakamura, T. Cooperative interaction between alpha- and beta-chains of hepatocyte growth factor on c-Met receptor confers ligand-induced receptor tyrosine phosphorylation and multiple biological responses. *The Journal of biological chemistry* **273**, 22913-22920 (1998).

110 Peschard, P. & Park, M. Escape from Cbl-mediated downregulation: a recurrent theme for oncogenic deregulation of receptor tyrosine kinases. *Cancer cell* **3**, 519-523 (2003).

111 Ponzetto, C. *et al.* A novel recognition motif for phosphatidylinositol 3-kinase binding mediates its association with the hepatocyte growth factor/scatter factor receptor. *Molecular and cellular biology* **13**, 4600-4608 (1993).

112 Dong, G. *et al.* Hepatocyte growth factor/scatter factor-induced activation of MEK and PI3K signal pathways contributes to expression of proangiogenic cytokines interleukin-8 and vascular endothelial growth factor in head and neck squamous cell carcinoma. *Cancer research* **61**, 5911-5918 (2001).

113 Grant, D. S. *et al.* Scatter factor induces blood vessel formation in vivo. *Proceedings of the National Academy of Sciences of the United States of America* **90**, 1937-1941 (1993).

114 Schmidt, C. *et al.* Scatter factor/hepatocyte growth factor is essential for liver development. *Nature* **373**, 699-702, doi:10.1038/373699a0 (1995).

115 Uehara, Y. *et al.* Placental defect and embryonic lethality in mice lacking hepatocyte growth factor/scatter factor. *Nature* **373**, 702-705, doi:10.1038/373702a0 (1995).

116 Maroun, C. R. & Rowlands, T. The Met receptor tyrosine kinase: a key player in oncogenesis and drug resistance. *Pharmacology & therapeutics* **142**, 316-338, doi:10.1016/j.pharmthera.2013.12.014 (2014).

117 Javaherian, K., Lee, T. Y., Tjin Tham Sjin, R. M., Parris, G. E. & Hlatky, L. Two Endogenous Antiangiogenic Inhibitors, Endostatin and Angiostatin, Demonstrate Biphasic Curves in their Antitumor Profiles. *Dose-response : a publication of International Hormesis Society* **9**, 369-376, doi:10.2203/dose-response.10-020.Javaherian (2011).

118 Marneros, A. G. & Olsen, B. R. Physiological role of collagen XVIII and endostatin. *FASEB journal : official publication of the Federation of American Societies for Experimental Biology* **19**, 716-728, doi:10.1096/fj.04-2134rev (2005).

119 Zatterstrom, U. K., Felbor, U., Fukai, N. & Olsen, B. R. Collagen XVIII/endostatin structure and functional role in angiogenesis. *Cell structure and function* **25**, 97-101 (2000).

120 Fukai, N. *et al.* Lack of collagen XVIII/endostatin results in eye abnormalities. *The EMBO journal* **21**, 1535-1544, doi:10.1093/emboj/21.7.1535 (2002).

121 Klenotic, P. A. *et al.* Molecular basis of antiangiogenic thrombospondin-1 type 1 repeat domain interactions with CD36. *Arteriosclerosis, thrombosis, and vascular biology* **33**, 1655-1662, doi:10.1161/ATVBAHA.113.301523 (2013).

122 Lawler, P. R. & Lawler, J. Molecular basis for the regulation of angiogenesis by thrombospondin-1 and -2. *Cold Spring Harbor perspectives in medicine* **2**, a006627, doi:10.1101/cshperspect.a006627 (2012).

123 Mirochnik, Y., Kwiatek, A. & Volpert, O. V. Thrombospondin and apoptosis: molecular mechanisms and use for design of complementation treatments. *Current drug targets* **9**, 851-862 (2008).

124 Sund, M. *et al.* Function of endogenous inhibitors of angiogenesis as endothelium-specific tumor suppressors. *Proceedings of the National Academy of Sciences of the United States of America* **102**, 2934-2939, doi:10.1073/pnas.0500180102 (2005).

125 Wang, S., Wu, Z., Sorenson, C. M., Lawler, J. & Sheibani, N. Thrombospondin-1-deficient mice exhibit increased vascular density during retinal vascular development and are less sensitive to hyperoxia-mediated vessel obliteration. *Developmental dynamics : an official publication of the American Association of Anatomists* **228**, 630-642, doi:10.1002/dvdy.10412 (2003).

126 Maeshima, Y. *et al.* Tumstatin, an endothelial cell-specific inhibitor of protein synthesis. *Science* **295**, 140-143, doi:10.1126/science.1065298 (2002).

127 Hamano, Y. *et al.* Physiological levels of tumstatin, a fragment of collagen IV alpha3 chain, are generated by MMP-9 proteolysis and suppress angiogenesis via alphaV beta3 integrin. *Cancer cell* **3**, 589-601 (2003).

128 Pandya, N. M., Dhalla, N. S. & Santani, D. D. Angiogenesis--a new target for future therapy. *Vascular pharmacology* **44**, 265-274, doi:10.1016/j.vph.2006.01.005 (2006).

129 Carmeliet, P. & Jain, R. K. Principles and mechanisms of vessel normalization for cancer and other angiogenic diseases. *Nature reviews. Drug discovery* **10**, 417-427, doi:10.1038/nrd3455 (2011).

130 van Weel, V., van Tongeren, R. B., van Hinsbergh, V. W., van Bockel, J. H. & Quax, P. H. Vascular growth in ischemic limbs: a review of mechanisms and possible therapeutic stimulation. *Annals of vascular surgery* **22**, 582-597, doi:10.1016/j.avsg.2008.02.017 (2008).

131 Ho, T. K., Rajkumar, V., Black, D. C., Abraham, D. & Baker, D. Critical Limb Ischemia Classification and Therapeutic Angiogenesis. *International Journal of Angiology* **14**, 49-59, doi:10.1007/s00547-005-2030-1 (2005).

132 Gornik, H. L. & Beckman, J. A. Cardiology patient page. Peripheral arterial disease. *Circulation* **111**, e169-172, doi:10.1161/01.CIR.0000160581.58633.8B (2005).

133 Ouriel, K. Peripheral arterial disease. *Lancet* **358**, 1257-1264, doi:10.1016/S0140-6736(01)06351-6 (2001).

134 Minar, E. Critical limb ischaemia. *Hamostaseologie* **29**, 102-109 (2009).

135 Zhou, B., Poon, M. C., Pu, W. T. & Han, Z. C. Therapeutic neovascularization for peripheral arterial diseases: advances and perspectives. *Histology and histopathology* **22**, 677-686 (2007).

136 Kolluru, G. K., Bir, S. C. & Kevil, C. G. Endothelial dysfunction and diabetes: effects on angiogenesis, vascular remodeling, and wound healing. *International journal of vascular medicine* **2012**, 918267, doi:10.1155/2012/918267 (2012).

137 Varu, V. N., Hogg, M. E. & Kibbe, M. R. Critical limb ischemia. *Journal of vascular surgery* **51**, 230-241, doi:10.1016/j.jvs.2009.08.073 (2010).

138 Suzuki, H. & Iso, Y. Clinical application of vascular regenerative therapy for peripheral artery disease. *BioMed research international* **2013**, 179730, doi:10.1155/2013/179730 (2013).

139 Asahara, T. *et al.* Bone marrow origin of endothelial progenitor cells responsible for postnatal vasculogenesis in physiological and pathological neovascularization. *Circulation research* **85**, 221-228 (1999).

140 Cao, Y., Hong, A., Schulten, H. & Post, M. J. Update on therapeutic neovascularization. *Cardiovascular research* **65**, 639-648, doi:10.1016/j.cardiores.2004.11.020 (2005).

141 Collinson, D. J. & Donnelly, R. Therapeutic angiogenesis in peripheral arterial disease: can biotechnology produce an effective collateral circulation? *European journal of vascular and endovascular surgery : the official journal of the European Society for Vascular Surgery* **28**, 9-23, doi:10.1016/j.ejvs.2004.03.021 (2004).

142 Ferrara, N. & Kerbel, R. S. Angiogenesis as a therapeutic target. *Nature* **438**, 967-974, doi:10.1038/nature04483 (2005).

143 Simons, M. Angiogenesis: where do we stand now? *Circulation* **111**, 1556-1566, doi:10.1161/01.CIR.0000159345.00591.8F (2005).

144 Davies, M. G. Critical limb ischemia: cell and molecular therapies for limb salvage. *Methodist DeBakey cardiovascular journal* **8**, 20-27 (2012).

145 Cooke, J. P. & Losordo, D. W. Modulating the vascular response to limb ischemia: angiogenic and cell therapies. *Circulation research* **116**, 1561-1578, doi:10.1161/CIRCRESAHA.115.303565 (2015).

146 Sanada, F. *et al.* Therapeutic Angiogenesis by Gene Therapy for Critical Limb Ischemia: Choice of Biological Agent. *Immunology, endocrine & metabolic agents in medicinal chemistry* **14**, 32-39, doi:10.2174/1871522213999131231105139 (2014).

147 Lei, Y., Haider, H., Shujia, J. & Sim, E. S. Therapeutic angiogenesis. Devising new strategies based on past experiences. *Basic research in cardiology* **99**, 121-132, doi:10.1007/s00395-004-0447-x (2004).

148 Dragneva, G., Korpisalo, P. & Yla-Herttuala, S. Promoting blood vessel growth in ischemic diseases: challenges in translating preclinical potential into clinical success. *Disease models & mechanisms* **6**, 312-322, doi:10.1242/dmm.010413 (2013).

149 Sukmawati, D. & Tanaka, R. Introduction to next generation of endothelial progenitor cell therapy: a promise in vascular medicine. *American journal of translational research* **7**, 411-421 (2015).

150 Takahashi, T. *et al.* Ischemia- and cytokine-induced mobilization of bone marrow-derived endothelial progenitor cells for neovascularization. *Nature medicine* **5**, 434-438, doi:10.1038/7434 (1999).

151 Lawall, H., Bramlage, P. & Amann, B. Treatment of peripheral arterial disease using stem and progenitor cell therapy. *Journal of vascular surgery* **53**, 445-453, doi:10.1016/j.jvs.2010.08.060 (2011).

152 Raval, Z. & Losordo, D. W. Cell therapy of peripheral arterial disease: from experimental findings to clinical trials. *Circulation research* **112**, 1288-1302, doi:10.1161/CIRCRESAHA.113.300565 (2013).

153 Lu, D. *et al.* Comparison of bone marrow mesenchymal stem cells with bone marrow-derived mononuclear cells for treatment of diabetic critical limb ischemia and foot ulcer: a double-blind, randomized, controlled trial. *Diabetes research and clinical practice* **92**, 26-36, doi:10.1016/j.diabres.2010.12.010 (2011).

154 Wrixon, A. D. B., I. Radiation, People and The Environment *International Atomic Energy Agency (IAEA)* (2004).

155 Das, S. K. Challenges of ionizing radiation in tumor treatment and role of angiogenesis. *Indian journal of biochemistry & biophysics* **51**, 527-530 (2014).

156 Manda, K., Glasow, A., Paape, D. & Hildebrandt, G. Effects of ionizing radiation on the immune system with special emphasis on the interaction of dendritic and T cells. *Frontiers in oncology* **2**, 102, doi:10.3389/fonc.2012.00102 (2012).

157 Frey, B., Hehlgans, S., Rodel, F. & Gaipl, U. S. Modulation of inflammation by low and high doses of ionizing radiation: Implications for benign and malign diseases. *Cancer letters* **368**, 230-237, doi:10.1016/j.canlet.2015.04.010 (2015).

158 Heissig, B. *et al.* Low-dose irradiation promotes tissue revascularization through VEGF release from mast cells and MMP-9-mediated progenitor cell mobilization. *The Journal of experimental medicine* **202**, 739-750 (2005).

159 Thanik, V. D. *et al.* Cutaneous low-dose radiation increases tissue vascularity through upregulation of angiogenic and vasculogenic pathways. *Journal of vascular research* **47**, 472-480, doi:10.1159/000313875 (2010).

160 Sofia Vala, I. *et al.* Low doses of ionizing radiation promote tumor growth and metastasis by enhancing angiogenesis. *PloS one* **5**, e11222, doi:10.1371/journal.pone.0011222 (2010).

Chapter II

Aims

Aims

Lower limb ischemia is a major health problem. Critical limb ischemia (CLI) is the term used for patients with chronic ischemic rest pain, ulcers, or gangrene attributed to inadequate blood flow or arterial occlusive disease. Because of the absence of effective treatment in the advanced stages of disease, amputation is undertaken, even though it is associated with morbidity and mortality. Therefore, the need for alternative treatment strategies in CLI patients is compelling and therapeutic angiogenesis is a promising tool to treat these patients. Recently, our lab found that LDIR, lower or equal to 0.8 Gy, activates VEGFR2, induces the production of VEGF in hypoxia and promotes angiogenesis *in vivo*.

The overall goal of the work presented in this thesis is to study the effects of LDIR on neovascularization. For that, a mouse model of hindlimb ischemia was developed using C57BL/6 female mice. The major objectives of this *thesis* are:

1) to identify the cellular and molecular mechanisms by which LDIR is able to promote therapeutic angiogenesis;

2) to evaluate if LDIR promotes postnatal vascularization by augmenting the systemic circulation of EPCs and/or by homing and incorporation into sites of neovascularization in ischemic tissues;

3) to demonstrate that LDIR promotes neovascularization in the setting of experimentally induced diabetic mice.

The first two aims will be addressed in Chapter III. The last aim will be addressed in Chapter IV. Several cellular and molecular techniques, namely RT-PCR, immunohistochemistry, immunofluorescence, flow cytometry, ELISA, laser capture microdissection and diaphonization were used along these chapters.

In this thesis, we propose an innovative and non-invasive strategy to induce therapeutic neovascularization in a mouse model of hindlimb ischemia. LDIR may therefore have a clinical significant impact in the treatment of PAD.

Chapter III

Low-dose ionizing radiation induces therapeutic neovascularization in a pre-clinical model of hindlimb ischemia.

Augusto Ministro[†], Paula de Oliveira[†], Raquel J. Nunes, André dos Santos Rocha, Adriana Correia, Tânia Carvalho, José Rino, Pedro Faísca, Jorg D. Becker, J. Goyri-O'Neill, Filomena Pina, Esmeralda Poli, Bruno Silva-Santos, Fausto Pinto, Marc Mareel, Karine Serre and Susana Constantino Rosa Santos[*]

† Equal first authorship

* Corresponding author

Adapted from *Cardiovascular Research* (2017) vol. 113 (7) 783-794

Abstract

Aims We have previously shown that low-dose ionizing radiation (LDIR) induces angiogenesis but there is no evidence that it induces neovascularization in the setting of peripheral arterial disease. Here, we investigated the use of LDIR as an innovative and non-invasive strategy to stimulate therapeutic neovascularization using a model of experimentally induced hindlimb ischemia (HLI).

Methods and results After surgical induction of unilateral HLI, both hindlimbs of female C57BL/6 mice were sham-irradiated or irradiated with four daily fractions of 0.3 Gy, in consecutive days and allowed to recovered. We demonstrate that LDIR, significantly improved blood perfusion in the murine ischemic limb by stimulating neovascularization, as assessed by laser Doppler flow, capillary density and collateral vessel formation. LDIR significantly increased the circulating levels of VEGF, PlGF and G-CSF, as well as the number of circulating endothelial progenitor cells (EPCs) mediating their incorporation to ischemic muscles. These effects were dependent upon LDIR exposition on the ischemic niche (thigh and shank regions). In irradiated ischemic muscles, these effects were independent of the recruitment of monocytes and macrophages. Importantly, LDIR induced a durable and simultaneous up-regulation of a repertoire of pro-angiogenic factors and their receptors in endothelial cells (ECs), as evident in ECs isolated from the irradiated gastrocnemius muscles by laser capture microdissection. This specific mechanism was mediated via vascular endothelial growth factor (VEGF) receptor signaling, since VEGF receptor inhibition abrogated the LDIR-mediated gene up-regulation and impeded the increase in capillary density. Finally, the vasculature in an irradiated non-ischemic bed was not affected and after 52-wk of LDIR exposure no differences in the incidence of morbidity and mortality were seen.

Conclusions These findings disclose an innovative, non-invasive strategy to induce therapeutic neovascularization in a mouse model of hindlimb ischemia, emerging as a novel approach in the treatment of critical limb ischemia patients.

Introduction

Critical limb ischemia (CLI) is the end stage of peripheral arterial disease, and severe obstruction of blood flow to the affected extremity results in ischemic rest pain, ulcers or gangrene. Surgical revascularization remains the cornerstone of therapy for limb salvage but ~30% of CLI patients require amputation in the first year, procedure associated with high morbidity and mortality. Therapeutic angiogenesis became a promising treatment for limb preservation through the revascularization of ischemic tissues by local administration of pro-angiogenic growth factors [1-3]. Several clinical trials showed that therapeutic angiogenesis could be extended to CLI patients [4]. However, the initial enthusiasm was tempered by the less successful more recent, randomized and placebo-controlled studies with larger numbers of patients [4]. Several factors could contribute to this: (i) formation of a functional vascular network requires the concurrent use of multiple angiogenic factors, and not a monotherapy-based approach; (ii) instability of currently used factors to achieve long-term benefits; and (iii) dysfunction of endothelial cells (ECs) that may not respond [5, 6]. To solve this, cell-based therapeutic strategies were developed. Although clinical trials showed that autologous bone marrow-derived mononuclear cells, including endothelial progenitor cells (EPCs), increased collateral vessel formation and had clinical benefits [4], there are still major challenges that include determination of optimal cell phenotype, preparation protocols, dosing, route and frequency of administration. Moreover, endothelial dysfunction is associated with a scarce viable and functional EPC population [7]. We previously showed that low-dose ionizing radiation (LDIR) (< 0.8 Gy) induces a pro-angiogenic phenotype in ECs *in vitro,* and promote angiogenesis *in vivo* during regeneration [8]. Herein we aimed at testing an innovative non-invasive strategy, using LDIR to induce therapeutic neovascularization in CLI. Using a model of experimentally induced hindlimb ischemia (HLI), we show that LDIR improves limb reperfusion by enhancing collateral formation through EPC recruitment to sites of arteriogenesis. The effects of LDIR depend on exposure of the ischemic niche, but not on the local recruitment of myeloid cells. Moreover, LDIR induces capillary density in the gastrocnemius muscle by simultaneous activation of a repertoire of pro-angiogenic factors in a mechanism dependent of the vascular endothelial growth factor (VEGF) receptor signaling. No effects on resting vasculature were observed, disclosing the possibility of using LDIR as a non-invasive and effective therapeutic tool in lower limb vascular insufficiency.

Methods

Expanded method descriptions are available in Supplementary material online.

Study Approval

All animal procedures were performed according to Directive 2010/63/EU. The procedures were approved by the institutional Animal Welfare Body, licensed by DGAV, the Portuguese competent authority for animal protection (license number 023861/2013).

***In vitro* experiments**

Lung human microvascular endothelial cells (HMEC-L) were purchased from Lonza and cultured according to manufacturer's instructions. Cells were used at passages 4-6. Affymetrix GeneChip HuGene 1.0 ST Arrays were used.

***In vivo* experiments**

Twenty–two-week-old female C57BL/6 mice, purchased from Charles River Laboratories, Spain, were used in all experiments. Nine-week-old female C57Bl/6-Tg(CAG-EGFP)10sb/J mice were used as a donor in bone marrow transplantation model (Instituto Gulbenkian de Ciência). Unilateral HLI was induced by surgery. Ionizing radiation was delivered using a linear accelerator operating at a dose rate of 500 MU/min. In most experiments the dose of 0.3 Gy was administered for four consecutive days, starting 12 hours after ischemia induction. Blood flow was assessed by laser Doppler perfusion imaging. Capillary and collateral densities were assessed after immunohistochemistry and diaphonization, respectively. Capillaries were microdissected using a Zeiss PALM MicroBeam Laser Microdissection System. The immune cell infiltrate and EPCs were assessed by FACS. In plasma, cytokines were assessed by ELISA. RNA extraction, cDNA synthesis and qRT-PCR was performed using the primers described in the supplementary material online**.** After 52 weeks post-HLI, body weights were recorded, urine, blood and different organs collected and analyzed.

Statistics

Experimental results are shown as the mean ± SEM. Data were analyzed with SPSS 20.0 software for windows. Statistical test employed are detailed described in figure legends. For GeneChip data analysis, probe sets showing differential expression were determined using one-way Analysis of Variance (ANOVA).

Results

LDIR increases perfusion recovery and capillary and collateral densities

We used a previously established mouse model of HLI [9] to assess the effect of LDIR in the restoration of blood flow to ischemic muscle. After surgical induction of unilateral HLI, both hindlimbs were sham-irradiated or irradiated with four daily fractions of 0.3 Gy, in consecutive days (as illustrated in *Figure 1A*) and perfusion was measured overtime. As shown in *Figure 1B* and quantified in *Figure 1C*, a dramatic reduction in blood flow was observed in the ischemic limb immediately after surgery, in comparison to the contralateral limb, and as expected, a gradual improvement in perfusion was seen overtime. Strikingly, a significant improvement in blood flow recovery was seen in the LDIR group, at days 15 and 45 post-HLI, comparing with sham-irradiated mice. This demonstrates a benefit of LDIR in the setting of HLI.

Lower numbers of fractions (1 x 0.3 Gy; 2 x 0.3 Gy or 3 x 0.3 Gy) or lower dose per fraction (4 x 0.1 Gy) were also evaluated but failed to show an effect (Supplementary material online, *Figure S1A* and *B*). We also evaluated the effect of the same fraction over 7 days (7 x 0.3 Gy), but no benefit was seen comparing within the 4-day (Supplementary material online, *Figure S1C*).

Subsequently, we quantified capillary density and collateral vessel development in hindlimb muscles, since blood flow recovery depends on both angiogenesis and arteriogenesis. Consistently, HLI increases capillary density *per se*, assessed through quantification of CD31-positive capillaries on histological sections of gastrocnemius muscle. Importantly, this effect is further amplified after LDIR exposure and a significant increase in capillary density is observed in irradiated ischemic muscle versus the sham-irradiated ischemic ones at days 15 and 45 post-HLI (*Figure 1D and 1E*). Of note, while the capillary density did not significantly increase between days 15 and 45 in the sham-irradiated ischemic muscles, a significant increase is observed for the irradiated ones.

The collateral vessel density (CVD) was evaluated, at days 15 and 90 post-HLI. Mice were diaphonized and an equivalent ROI, corresponding to 20% of the limb area, was selected for CVD quantification (*Figure 1F*). A greater increase in CVD was observed for the ischemic limbs of LDIR mice, versus the sham-irradiated ones (*Figure 1G*). Noteworthy, no difference in these parameters was seen in non-ischemic muscle, LDIR and sham-irradiated, showing that irradiation *per se* does not have an effect on resting vasculature.

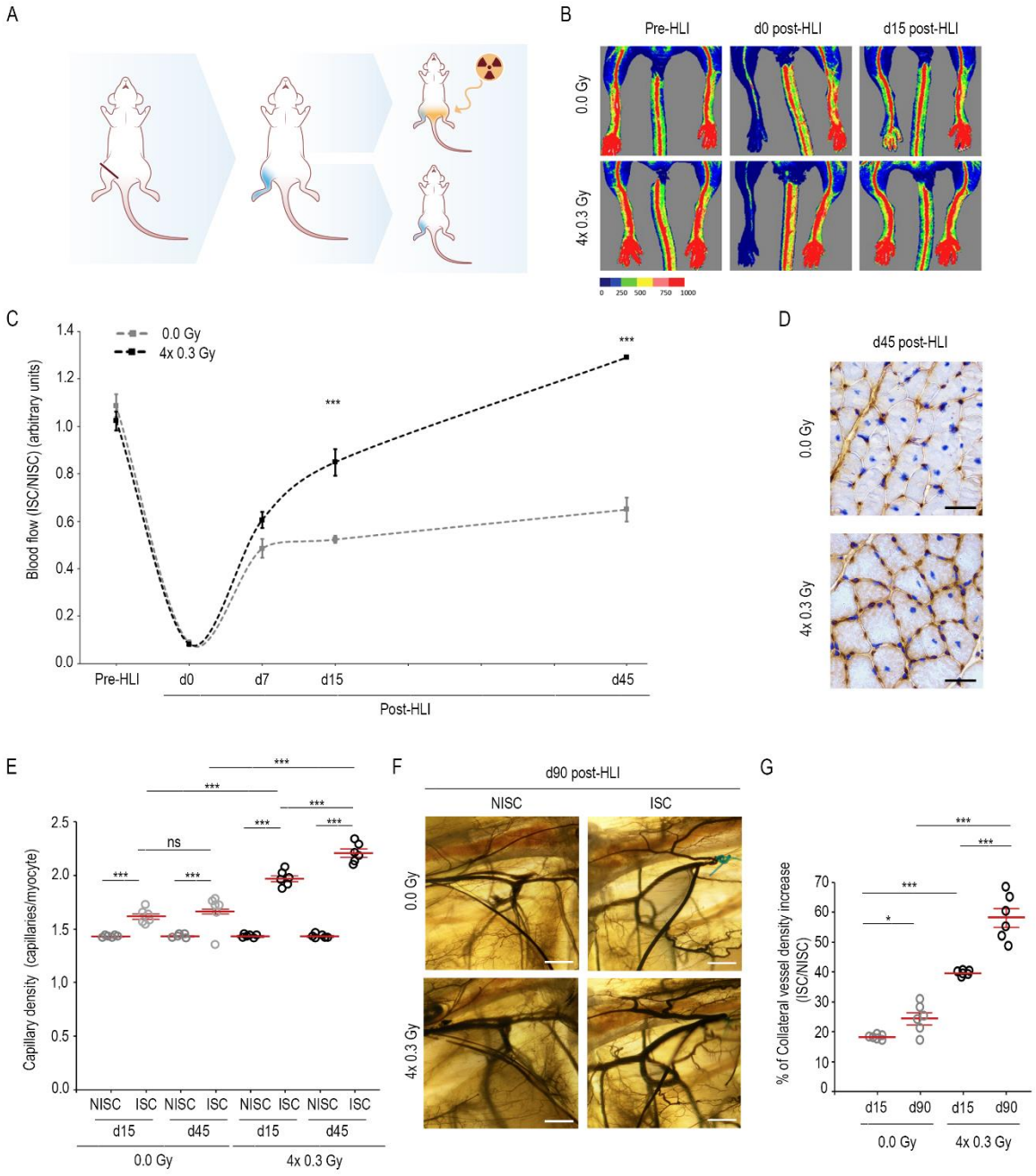

Figure 1. LDIR increases perfusion recovery, capillary and collateral densities.

After surgical induction of unilateral HLI, both hindlimbs of C57BL/6 mice were sham-irradiated or irradiated with four daily fractions of 0.3 Gy, in consecutive days and allowed to recover. (**A**) A schematic illustration of our experimental design. After unilateral HLI (represented by a thick brown line), the flow to the ischemic limb is dramatically decreased (in blue). Both hindlimbs are irradiated (in orange) or sham-irradiated. (**B**) Representative laser Doppler flow images pre-HLI, and at days 0 (d0) and 15 (d15) post-HLI induction. (**C**) Quantitative evaluation of blood flow expressed as a ratio of ISC to NISC limb demonstrated significantly enhanced limb blood perfusion in irradiated

mice vs sham-irradiated ones both at days 15 (d15) and 45 (d45) post-HLI. Between-group changes were assessed by two-way repeated measurements ANOVA followed by Bonferroni post-hoc test (n=12 mice per group). Means ± SEM are shown. (**D**) Representative sections from sham-irradiated and irradiated ischemic gastrocnemius muscles at day 45 post-HLI. Capillaries and myocytes were identified by CD31 immunohistochemistry and haematoxylin, respectively. Scale bar, 150µm. (**E**) Quantitative analysis revealed increased capillary density (capillaries/myocyte) in irradiated ischemic gastrocnemius muscles compared to sham-irradiated ischemic ones at days 15 and 45 post-HLI. Mixed ANOVA followed by Bonferroni post-hoc test was conducted with a within-subject factor of ISC and between-subject factors of day and irradiation (n=6 mice per group). (**F**) Illustrative images of selected regions of interest (ROI) for sham-irradiated and irradiated mice. ISC and NISC limbs at day 90 post-HLI are shown. Scale bar, 300µm. (**G**) Data are represented as the percentage of collateral vessel density (CVD) increase of the ISC limb relatively to the NISC one. At days 15 and 90 post-HLI, irradiated mice presented significantly higher CVD increase (%) versus sham-irradiated mice. Two-way ANOVA was conducted followed by Bonferroni post-hoc test with a between-subject factors of day and irradiation (n=6 mice per group). (**E**, **G**) Individual data and means ± SEM (in red) are shown. *P < 0.05; *** P < 0.001; ns, non-significant. HLI, hindlimb ischemia; ISC, ischemic; NISC, non-ischemic; Pre-HLI, before hindlimb ischemia.

LDIR modulates the expression of endothelial genes involved in an angiogenic response *in vitro*

Previously, using human lung microvascular ECs (HMVEC-L) we showed that 0.3 Gy leads to rapid phosphorylation of the VEGF receptor 2 (VEGFR2) [8], a key signal transduction mediator.in the angiogenic process. Consequently, signaling pathways such as PI3K/AKT and ERK/MAPK are activated and gene expression modulated. To assess the effect of LDIR on the EC gene expression profile, HMVEC-L were exposed to a single dose of 0.3 Gy, RNA was extracted at 4 hours post-LDIR and a global gene expression analysis was performed; sham-irradiated HMVEC-L were used as control. Principal component analysis (PCA) revealed a separation of all HMVEC-L based on the irradiation status (*Figure 2A*). Two thousand three hundred and seventy-four genes were differentially expressed in LDIR vs control HMVEC-L, at a cutoff corresponding to a P value<0.03 (*Figure 2B*).

Particular attention was paid to growth factors and receptors associated with angiogenesis, VEGF receptor 1 (VEGFR1) and VEGFR2, angiopoietin-2 (ANGPT2), transforming growth factor beta (TGF-β), platelet derived growth factor (PDGF) and fibroblast growth factor-2

(FGF-2), and their expression was validated by quantitative RT-PCR. Hepatocyte growth factor (HGF) and its receptor, MET, were also validated, as the use of HGF has been proposed in the setting of therapeutic angiogenesis, and clinical trials with HGF gene therapy are ongoing [4]. HMVEC-L were irradiated with a single dose of 0.3 Gy and screened at 4, 8 and 12 hours post-LDIR. Gene expression increased at 4 hours post-LDIR, compared with sham-irradiated HMVEC-L, with exception of *Tgfb2* whose increase was significant at 8 hours post-LDIR. Expression levels of all genes returned to baseline at 12 hours post-LDIR (*Figure 2C*). We tried to modulate gene expression by increasing total dose (or number of fractions), using daily 0.3 Gy.fractions during 2, 3 and 4 consecutive *d*ays; and cells were screened at 4, 8 and 12 hours after the last irradiation. Regardless of total dose, gene expression pattern and magnitude were similar to that observed after the single irradiation dose experiment (*Figure 2D-F*).

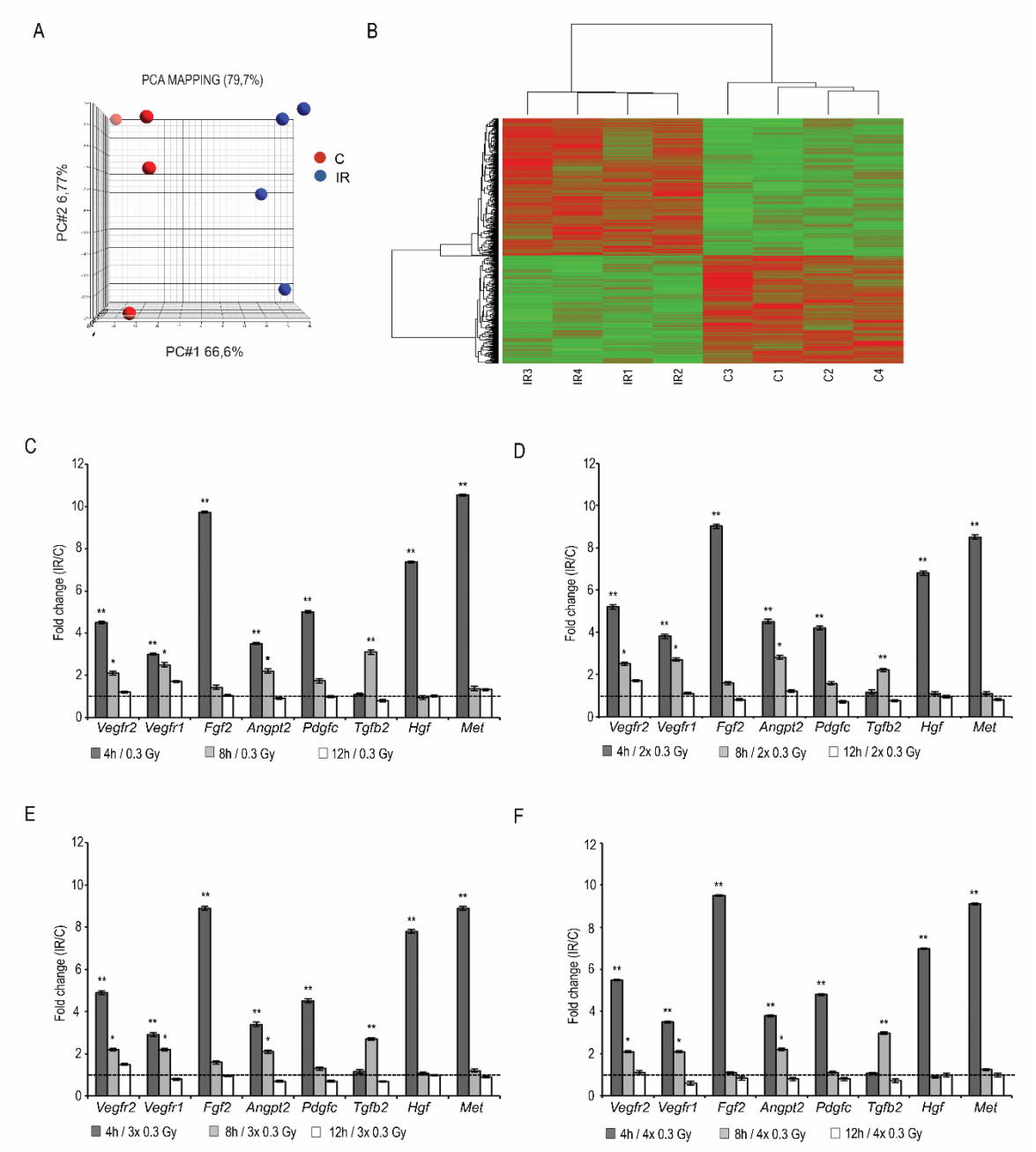

Figure 2. LDIR modulates the expression of endothelial genes involved in an angiogenic response.

Four RNA samples of irradiated (0.3 Gy) or sham-irradiated HMVEC-L were processed for hybridization to Affymetrix Human Gene 1.0 ST arrays. (**A**) Three-dimensional PCA plot. The red and blue points represent control (sham-irradiated) and irradiated samples, respectively, indicating a separation of samples based on the ionizing radiation stimulus. (**B**) Heatmap for the 2374 genes differentially expressed in LDIR vs control (one-way analysis of variance (ANOVA test) $P < 0.03$)). Columns and rows and represent biological replicates and individual genes, respectively. Red and green indicate genes up- or down-regulated compared to control cells (sham-irradiated), respectively. (**C-F**) HMVEC-L sham-irradiated or irradiated with 0.3 Gy (**C**) once; (**D**) twice, (**E**) three

or (**F**) four consecutive days. (**C-F**) Data (means ± SEM) represent the fold change in gene expression relative to the internal calibrator (sham-irradiated) in triplicate measurements and are representative of four independent experiments. Data demonstrated a significant increase in the relative expression of *Vegfr2, Vegfr1*, *Fgf2*, *Angpt2*, *Pdgfc*, *Hgf* and *Met*, at 4 hours, and of *Tgfb2* at 8 hours post-irradiation, when compared to sham-irradiated cells (dashed line). Values assumed normal distribution, equal variance and independent two-tailed t-test was used; *$P < 0.05$; ** $P < 0.002$. C, sham-irradiated; IR, irradiated.

LDIR induces the expression of pro-angiogenic genes in ECs isolated from irradiated ischemic gastrocnemius muscles

LDIR modulates the expression of angiogenic genes in a resting endothelial *in vitro* monoculture, not exposed to injury. Next, we evaluated the gene expression levels in ECs isolated from gastrocnemius muscle of mice subjected to HLI and exposed to LDIR in daily fractions of 0.3 Gy for 4 days or sham-irradiated. Forty-five days post-LDIR, mice were killed and gastrocnemius muscle sections stained for CD31 and visualized using a laser capture microdissection microscope (LCM). CD31-positive cells from ischemic and non-ischemic gastrocnemius muscles were dissected and isolated. First, we validated that these CD31-positive cells consisted primarily of ECs and not myeloid cells nor perivascular cells. We assessed the gene expression of surface and transcription markers *Pecam1* encoding CD31, *Erg* and *Etv2* that are specific for ECs; *Itgam* encoding CD11b and *Spi1* encoding PU-1 for myeloid cells and *Des* encoding Desmin, *Pdgfrb* and *Acta2* encoding smooth muscle alpha-actin for perivascular cells. The CD31+ cells isolated by LCM expressed high levels of endothelial-specific transcripts but negligible amounts (more than 10000 times less) of myeloid or perivascular-specific transcripts (Supplementary material online, *Figure S2*). Next, the same ECs were assessed by quantitative RT-PCR for the expression of *Vegfr2, Vegfr1, Fgf2, Angpt2, Pdgfc, Tgfb2, Hgf* and *Met*. Transcripts for all these genes were clearly up-regulated in ECs isolated from muscle of the ischemic limb, comparing with the contralateral limb, exclusively in mice exposed to LDIR (*Figure 3A)*. Sham-irradiated mice show the opposite, down-regulating the expression of the angiogenic genes repertoire in endothelium from the ischemic limb, comparing with the contralateral limb. Then, we questioned whether the increase of the capillary density conferred by LDIR and observed in the ischemic gastrocnemius muscle could be correlated with the increase of the

expression levels of these pro-angiogenic genes. To address this, we used the adductor muscle that does not present an increase of the capillary density at day 45 post-HLI neither in response to ischemia *per se*, nor after LDIR exposure (Supplementary material online, *Figure S3A*). Thus, the adductor muscle provides a control subjected to HLI and irradiation without increase in the capillary density. We isolated the ECs from the adductor muscles and the levels of *Vegfr2, Vegfr1, Fgf2, Angpt2, Pdgfc, Tgfb2, Hgf* and *Met* mRNA were measured. We confirmed that the transcripts are down-regulated in the irradiated ischemic limb when compared with the contralateral one (Supplementary material online, *Figure S3B*). We have previously demonstrated that VEGFR tyrosine kinase inhibition impairs the LDIR-induced pro-angiogenic response [8]. To assess the functional and clinical relevance of VEGF signaling induced by LDIR in the setting of HLI, VEGFR tyrosine kinase inhibition was achieved through oral gavage of PTK/ZK (100 mg/kg), after HLI and 2 hours before each LDIR exposure. VEGFR inhibition abrogated the LDIR-mediated gene up-regulation of pro-angiogenic factors and receptors (*Figure 3B*). Moreover, the capillary density induced by LDIR, but not by HLI, was denied by treatment with PTK/ZK (*Figure 3C*). Conversely, the collateral density induced after LDIR exposure was not affected PTK/ZK (*Figure 3D*).
Thus, 0.3 Gy administered during four consecutive days might act through VEGFR-signaling for angiogenesis, but not arteriogenesis in the ischemic gastrocnemius limb.

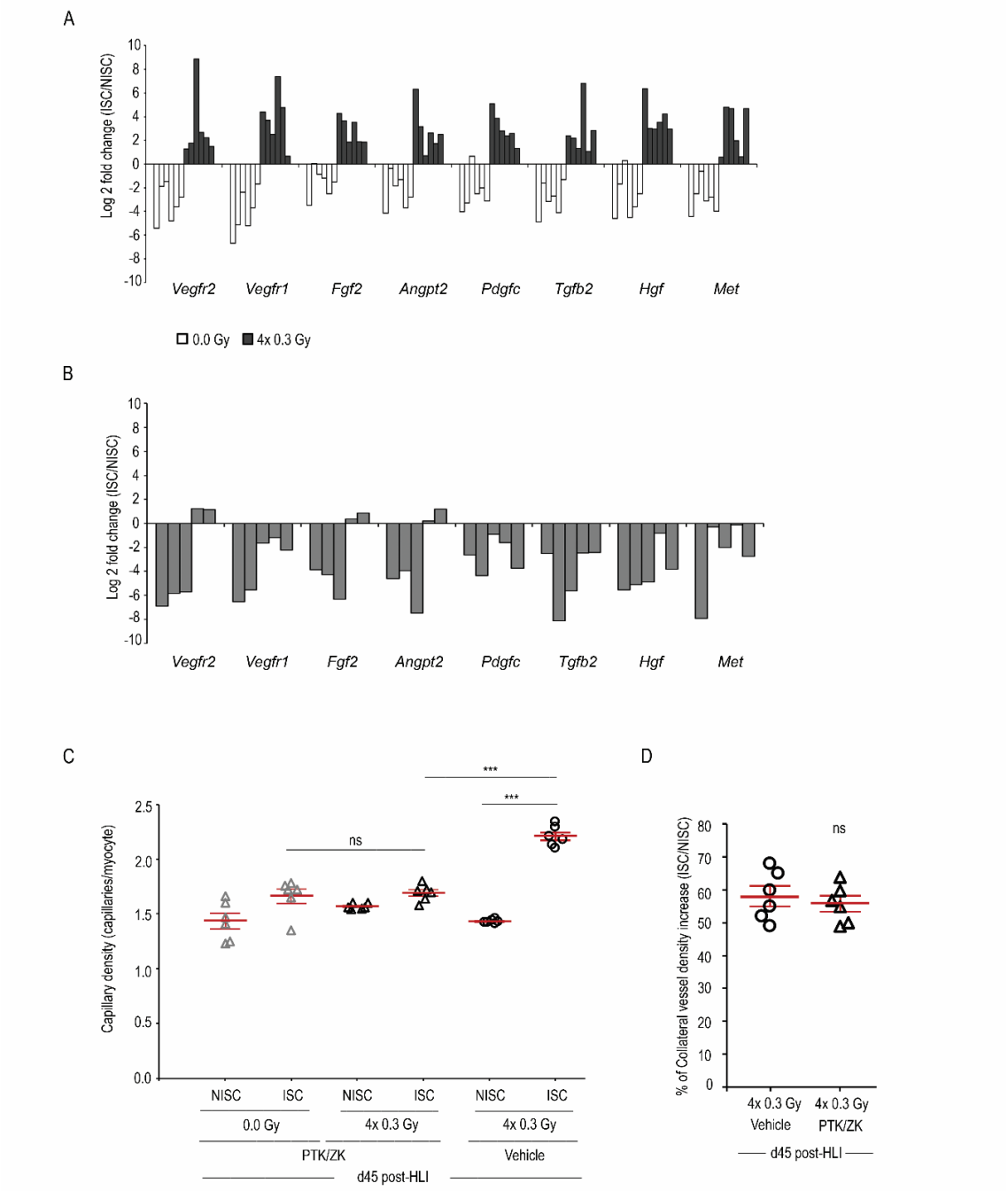

Figure 3. LDIR upregulates the expression of angiogenic genes in ECs isolated from irradiated ischemic gastrocnemius muscles.

After surgical induction of unilateral HLI, both hindlimbs of C57BL/6 mice were sham-irradiated or irradiated with four daily fractions of 0.3 Gy, in consecutive days and allowed to recover. (**A** and **B**) At day 45 post-HLI, the expression of pro-angiogenic factors and their receptors was evaluated by qRT-PCR exclusively on ECs. Gastrocnemius muscle sections were stained for CD31. Individual endothelial CD31+ cells were visualized, dissected and isolated using a laser capture microdissection microscope. ***(A)*** Each bar represents the relative gene expression in one animal.

White and gray bars represent sham-irradiated and irradiated mice, respectively. Values were normalized to 18S to obtain relative expression levels. Results expressed as log2 fold changes between ISC and NISC samples demonstrated relative abundance of the transcripts in irradiated mice; in contrast, a down-regulation is observed in sham-irradiated mice. (**B-D**) Two hours before each irradiation, ischemic mice were pretreated with PTK/ZK (100mg/Kg). (**B**) Light grey *bars* represent irradiated mice pretreated with PTK/ZK. A down-regulation in relative gene expression is found in irradiated mice treated with PTK/ZK. (**C**) Quantitative analysis, at day 45 post-HLI, revealed no difference in capillary density (capillaries/myocyte) between ISC irradiated vs ISC sham-irradiated gastrocnemius muscles, both treated with PTK/ZK. As expected a significant increase is observed between ISC irradiated and PTK/ZK treated vs ISC irradiated and treated with the control vehicle. Mixed ANOVA followed by Bonferroni post-hoc test was conducted with a within-subject factor of ISC and between-subject factors of irradiation and PTK/ZK treatment. (**D**) Data are represented as the percentage of collateral vessel density (CVD) increase of the ISC limb relatively to the NISC one. At day 45 post-HLI, no difference was observed in CVD between irradiated mice treated with PTK/ZK vs irradiated mice treated with the control vehicle. Independent two-tailed t-test was used. (**C** and **D**) Individual data and means ± SEM (in red) are shown from n=6 mice per group; *** $P < 0.001$; ns, non-significant. ISC, ischemic; NISC, non-ischemic.

LDIR does not mobilize myeloid cells to the ischemic tissue

Given that, in response to ischemia, the myeloid cells play an important role in the collateral formation [10] we questioned whether LDIR controlled the migration of myeloid cells in the ischemic tissue. Note that this process was already found for higher doses of ionizing radiation [11] (daily therapeutic doses ex: 2.0 Gy). Thus, after unilateral HLI, both hindlimbs were sham-irradiated or irradiated with four daily fractions of 0.3 Gy or 2.0 Gy as additional control. The myeloid infiltration was assessed day 4 post-HLI in ischemic and non-ischemic adductor muscles by flow cytometry (*Figure 4A*). As expected, the number of CD45+ cells increased significantly in response to HLI. Strikingly, exposure with 0.3 Gy or 2.0 Gy inhibited the CD45+ cell accumulation (*Figure 4B*). Then we went on to assess which myeloid cells were modulated in the ischemic muscles. Monocyte and macrophage numbers increased significantly after HLI in sham-irradiated ischemic muscles. A similar response was observed in ischemic muscles upon 2.0 Gy exposure. In stark contrast, low 0.3 Gy irradiation dose inhibited this monocyte and macrophage accumulation. This shows that different doses of ionizing radiation differently modulate myeloid cell infiltration in

response to ischemia (*Figure 4C and D*). Moreover, while neutrophil numbers increased substantially in response to HLI, both 0.3 Gy and 2 Gy irradiation dosages impaired this accumulation (*Figure 4E*). We also assessed whether at later time point myeloid cells could account for the increase in collateral density in response to LDIR. Fifteen days post-HLI the numbers of CD45+ cells, monocytes, macrophages and neutrophils were similar in the ischemic muscles in 0.3 Gy; 2 Gy or sham-irradiated groups (Supplementary material online, Figure S4).

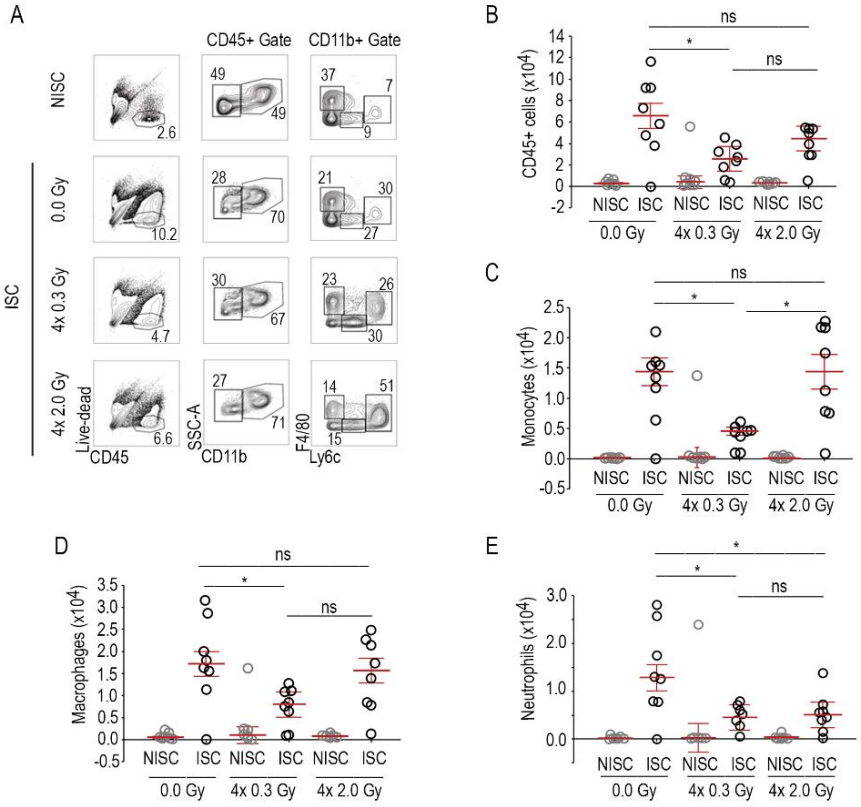

Figure 4. Profiles of leukocytes mobilized to ischemic muscles upon LDIR

After surgical induction of unilateral HLI, both hindlimbs of C57BL/6 mice were sham-irradiated or irradiated with four daily fractions of 0.3 Gy or 2.0 Gy in consecutive days. At day 4 post-HLI, analysis of $CD45^+$ immune cells that infiltrate ischemic adductor muscles was assessed. (**A**) Representative analysis of hematopoietic CD45+ cells present in ischemic muscle as assessed by flow cytometry. Analysis of the accumulation of myeloid CD11b+ cells, and in particular macrophages (CD45+CD11b+F4/80+ cells), monocytes (CD45+CD11b+LY6C+F4/80int cells), and neutrophils (CD45+CD11b+Ly6Cint). The graphs show numbers of (**B**) total CD45+ cells; (**C**) monocytes; (**D**) macrophages and (**E**) neutrophils, isolated from ISC and NISC adductor muscles and represent the data derived from two independent experiments. Mixed ANOVA followed by Bonferroni post-hoc

test was conducted with a within-subject factor of ISC and between-subject factor of irradiation. Individual data and means ± SEM are shown (in red) from n=8 mice per group; *$P < 0.05$; ns, non-significant. ISC, ischemic; NISC, non-ischemic.

LDIR enhances collateral formation through EPC recruitment in a process that is dependent of the ischemic niche irradiation

We next assessed the effect of LDIR on EPC mobilization from the bone marrow into the circulation. Total blood was collected at days 4, 5, 6 and 7 post-HLI and EPCs were identified by flow cytometry as mononuclear cells being VEGFR2+/ Sca-1+/ CD117+ cells. Consistent with the literature [12], significant increase of the percentage of EPCs occurred at day 6 in sham-irradiated mice in response to HLI (*Figure 5A*). Surprisingly, the percentage of circulating EPCs significantly increased already at day 4 post-HLI in irradiated mice, and to a level noticeably higher than in sham-irradiated mice at day 6 (*Figure 5A*). This suggests LDIR synergized with ischemia to increase EPCs in peripheral blood, a process that is not inhibited after PTK/ZK treatment (Supplementary material online, *Figure S5A*).

In addition, we confirmed that LDIR increases the circulating EPCs percentage in a process dependent of ischemia induction (Supplementary material online, *Figure S6*).

As EPC mobilization involves a complex network of migratory factors [2, 13, 14], we assessed whether LDIR modulates cytokine or chemokine concentrations synergistically with ischemia that could generate gradients that guided EPCs to areas of ischemia or/and locally induce arteriogenesis. We previously showed that *in vitro* and under hypoxia-mimicking conditions LDIR enhances VEGF expression in ECs [8].

Using a similar approach, we found that in the presence of cobalt chloride (CoCl2), which mimics hypoxic conditions, ECs significantly increased *Pgf* mRNA (encoding placental growth factor (PlGF)) expression, in a way that synergized with exposure to 0.3 Gy (Supplementary material online, *Figure S7*). However, hypoxia and irradiation do not always synergize to regulate expression of migration factors. While *Cxcl12* mRNA (encoding stroma-derived factor-1α (SDF-1α)) expression was increased by hypoxia but not by LDIR, conversely, *Csf3* mRNA (encoding granulocyte-colony stimulating factor (G-CSF)) expression was induced by LDIR but not by hypoxia (Supplementary material online, *Figure S7*). These findings were confirmed *in vivo* by ELISA. VEGF, PlGF and G-CSF concentrations in the plasma were significantly increased in the plasma of irradiated mice at day 4 post-

HLI when compared with sham-irradiated ones (*Figure 5B*). In contrast and consistent with our *in vitro* data, the levels of SDF-1α are not modulated by LDIR at least at day 4 post-HLI. Moreover, the levels of VEGF, PlGF and G-CSF were not changed in irradiated mice treated with PTK/ZK after HLI induction (Supplementary material online, *Figure S5B*).

To confirm that this process is dependent of the effect of LDIR on the ischemic/hypoxic niche, we irradiated mice outside the ischemic niche. Since technically, it is not possible to irradiate only the non-ischemic hindlimb assuring that the contralateral ischemic one was not exposed to LDIR, we irradiated the upper (above hip) part of the mouse body (Supplementary material online, *Figure S8A*). Upper body LDIR exposition was not sufficient to increase the proportion of circulating EPC (Supplementary material online, *Figure S8B*). Consistently, the VEGF, PlGF, G-CSF and SDF-1α levels did not increase upon LDIR exposure (Supplementary material online, *Figure S8C*). Importantly, the increase by LDIR of collateral density is not achieved (Supplementary material online, *Figure S8D*). This strongly suggests that the exposure of the ischemic niche to LDIR is critical for the increase of cytokines, mobilization of EPCs and collateral formation.

Next, we aimed to show that LDIR-induced circulating EPCs are functionally relevant for enhancement of their recruitment and incorporation into ischemic tissues. A bone marrow transplantation using C57Bl/6-Tg(CAG-EGFP)10sb/J donor was performed in C57Bl/6 mice and 8 weeks after, HLI was induced. Mice were sham-irradiated or irradiated with 0.3 Gy during four consecutive days and at day 15 post-HLI the adductor muscles were collected. Our results show that at day 15 post-HLI EPCs are recruited in the large vessels as identified by double-fluorescent labeling (green and red), in response to HLI (*Figure 5C*). To confirm the wide-field data, confocal images of the same ten-micron-thick section were acquired to show that green and red fluorescent signals belong to the same cells (Supplementary material online, *Figure S9).* Importantly, a quantitative evaluation of the histological sections revealed a significantly increased number of GFP+/CD31+ cells per area into irradiated ischemic thigh muscles when compared with the sham-irradiated ones (*Figure 5D*).

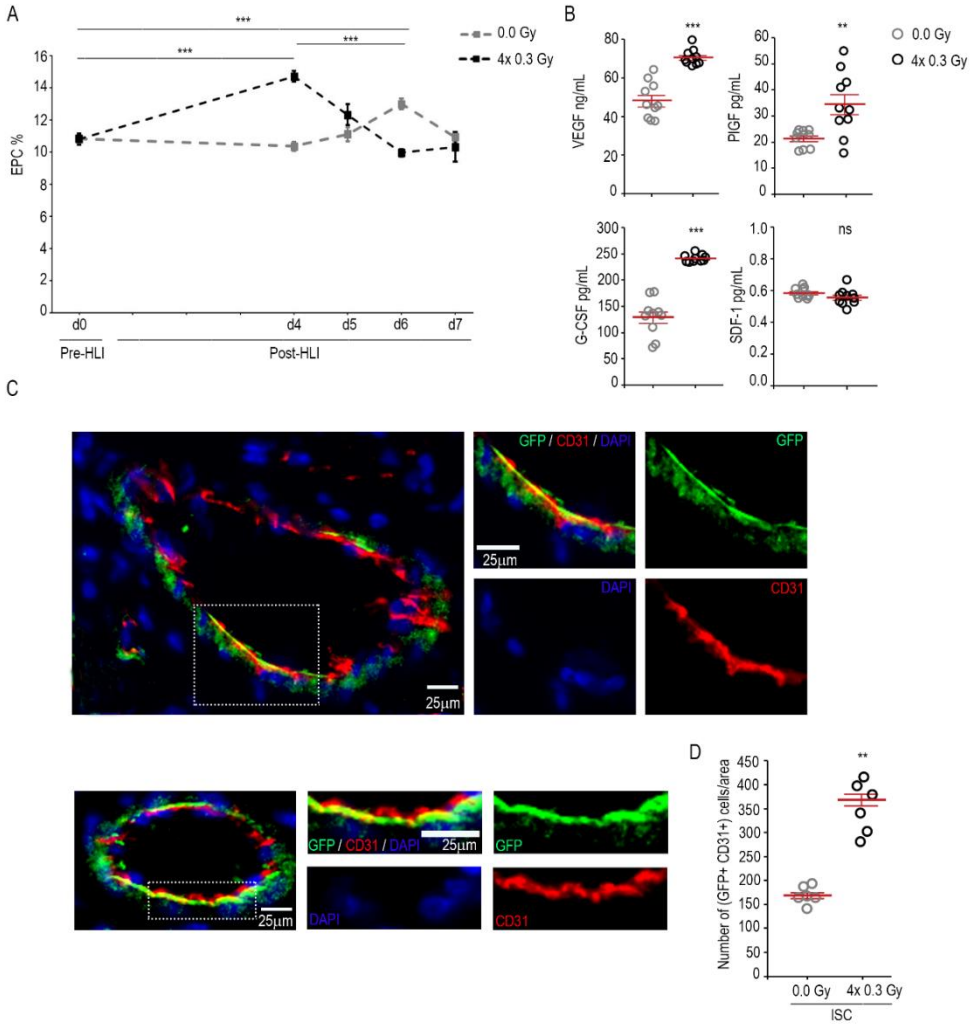

Figure 5. Post-HLI induction, LDIR increases the number of circulating EPCs, the levels of VEGF, PlFG and G-CSF and mediate EPC recruitment in ischemia.

After surgical induction of unilateral HLI, both hindlimbs of C57BL/6 mice were sham-irradiated or irradiated with four daily fractions of 0.3 Gy, in consecutive days. (**A**) Quantitative analysis of EPCs in peripheral blood demonstrated a significant increase of the percentage of EPCs in irradiated mice, at day 4 post-HLI and in sham-irradiated mice, at day 6 post-HLI when compared to the percentage before HLI induction (d0 pre-HLI). Interestingly, the increase conferred by LDIR at day 4 in response to HLI is significantly higher to the one found at day 6 post-HLI in sham-irradiated mice. Two-way ANOVA was conducted followed by Bonferroni post-hoc test with a between-subject factors of day and irradiation; n=6 mice per group. Means ± SEM are shown. (**B**) The concentrations of VEGF, PlGF, G-CSF, and SDF-1α were measured in the plasma, at day 4 post-HLI. LDIR significantly increases the VEGF, PlGF and G-CSF concentrations after HLI induction vs sham-irradiation (n=10 mice per group; values assumed normal distribution and equal or unequal (G-CSF) variance and independent two-tailed t-test was used). (**C** and **D**) Eight weeks after bone marrow transplantation,

HLI was performed in C57BL/6 mice. Mice were sham-irradiated or irradiated with 0.3 Gy during four consecutive days and at day 15 post-HLI the adductor muscles were collected. (**C**) At left, two representative images of incorporated EPCs identified by double-fluorescent labeling (green/red) in collateral vessels. Transplanted GFP:β-actin cells were identified by green fluorescence; vasculature by red fluorescence (CD31 staining) and nucleus by blue fluorescence (DAPI). Scale bar, 25 μm. At right, single and merged channels after digital zoomed of the boxed areas are shown. (**D**) Quantitative analysis revealed a significant increase of EPCs incorporation (identified as GFP+/CD31+ cells) into irradiated ischemic muscles compared to sham-irradiated ischemic ones (n = 6 mice per group; values assumed normal distribution, unequal variance and independent two-tailed t-test was used). (**B**, **D**) Individual data and means ± SEM (in red) are shown; ** $P < 0.01$; *** $P < 0.001$; ns, non-significant. ISC, ischemic; Pre-HLI, before hindlimb ischemia.

LDIR exposure is not associated with increased morbidity or mortality

To check for a possible effect of LDIR in the health status of the animals, a 52-week study was performed in a group of sham-irradiated and LDIR mice (n=140), throughout which mice were assessed for clinical signs of disease. There was no increased incidence of morbidity or mortality in the LDIR mice, compared with sham-irradiated, and there was no difference in body weight gain (at weeks 24, 36, 48 and 52 post-HLI). Fifty-two weeks post-HLI mice were killed and no significant difference was observed in organ weight, serum biochemistry (n=24), urinalysis or hematological parameters (Table 1); and the histological analysis revealed no neoplastic lesions or major changes in the liver, lung, spleen, thymus or bone marrow of these mice (n=6) (Supplementary material online, *Figure S10*).

Table 1. Clinical, hematological, biochemical and histopathological data from sham-irradiated and LDIR mice

End Point	0.0 Gy	4 x 0.3 Gy
BW gain, % (n=140; mean ± SD)	14.2 ± 3.5	21.4 ± 5.3
Mortality (n=140)	2[*]/140	1[†]/140
Blood cell counts (n=24)	WNR[A]	WNR
Clinical chemistry (n=24)	WNR	WNR
Coagulation tests (n=24)	WNR	WNR
Urinalysis (n=24)	WNR	WNR
Bone Marrow cytology: abnormalities (n=6)	0/6	0/6
Histopathological Analysis (liver; kidney; lung; bone marrow; spleen; thymus) (n=6)	0/6	0/6

[*] found dead, from unknown cause.

[†]sacrificed due to abscess formation after surgical procedure (HLI).

[A] WNR, within normal range.

Discussion

Therapeutic neovascularization aims to stimulate new blood vessel growth. Current strategies using proteins, genes or stem cells have demonstrated efficacy in animal models however, clinical translation remains challenging. We show that LDIR synergized with HLI and significantly enhance blood perfusion, capillary density in gastrocnemius muscle and collateral vessel development, tilting the angiogenic balance towards an even more pro-angiogenic phenotype, and suggesting that LDIR may favor the functional recovery of ischemic tissues. In contrast, resting vasculature, not subjected to ischemia, are unaffected by LDIR since capillary density and CVD are similar in non-ischemic muscles exposed or not to LDIR. This is in agreement with our previous work, where inter-ray capillary density remained unchanged after LDIR of non-amputated zebrafish caudal fin [8]. Our data also show that the maximal efficacy in perfusion recovery, capillary and collateral densities involves the administration of 1.2 Gy in four daily fractions of 0.3 Gy per fraction. A global gene expression analysis revealed that 2374 genes were modulated by LDIR and from those, 1344, many of which with a role in angiogenesis, were upregulated in LDIR versus control HMVEC-L. As soon as 4 hours after exposure to 0.3 Gy the expression of the majority of the pro-angiogenic molecules were increased, and returned to baseline12 hours post-LDIR. This acute short-term effect of LDIR on ECs is independent from dose fractionation since cells exposed to 0.3 Gy administered 2, 3 or 4 consecutive days presented similar gene expression pattern and magnitude. The evaluation of expression of angiogenic genes in ECs isolated from gastrocnemius muscle of mice subjected to HLI revealed that LDIR modulates the expression of angiogenic genes in the endothelium and, thus, suggested a link for the long-term advantage in blood perfusion, capillary density and collaterals in HLI. LDIR induced a sustained and prolonged pro-angiogenic response in ECs, still evident 45 days after irradiation. Because this contrasts with the transient *in vitro* response, one may hypothesize either that endothelium itself could be differently modulated by LDIR in a hypoxic microenvironment created by ischemia; some cells (ex: adipocytes) could contribute to perpetuate the effect(s) of irradiation in ways that *in vitro* cultures cannot mimic.

There is evidence that ionizing radiation can affect a variety of inflammatory processes and the composition of responding immune cells [15]. However, this highly depends on the dose, for low doses (e.g. ≤ 1Gy) promote anti-inflammatory responses [16], while high doses (e.g. ≥

2Gy) exert pro-inflammatory effects [17]. Therapeutic applicability was further demonstrated on inflammatory disease as symptomatic improvement of rheumatoid arthritis was observed when mice were irradiated with 0.5 Gy in five fractions within 1 week [18]. The hematopoietic infiltrate was monitored from inflamed and ischemic tissues to assess a potential role of immune cells upon LDIR. Ischemia *per se* induced about 20-foldsincrease in the immune CD45+ cell infiltrate recruited to the injured muscle at day 4 post-HLI. Exposure with 4x 0.3 Gy significantly inhibited the CD45+ cell accumulation with particular effects on monocytes, macrophages and neutrophils. In contrast, with 4x 2.0 Gy the total CD45+ accumulation in ischemic muscle was still reduced, and although numbers of monocytes and macrophages were restored, neutrophils were not. This is consistent with the fact that high irradiation doses have opposing effects on certain myeloid subsets, for they activate macrophages [19] while they are reported to induce rapid, but transient, neutropenia [20]. Importantly, effect of irradiation was short-lasted. Fifteen days post-HLI the profiles of myeloid cells that infiltrated non-irradiated and irradiated ischemic muscles were similar. Altogether these data pointed for a mechanism of LDIR-induced arteriogenesis independent of local myeloid cell recruitment.

In the setting of HLI we showed that LDIR boosts the induction of a sustained VEGFR-mediated pro-angiogenic program in ECs from ischemic gastrocnemius muscle. These results corroborate our previous findings [8] and suggest a new mechanism: LDIR under HLI induces capillary density. Consistently, the capillary density induced by LDIR, but not by HLI, was abrogated by treatment with PTK/ZK. Conversely, the enhancement promoted in collateral density by LDIR was not affected by PTK/ZK, suggesting that this process is regulated by a mechanism independent of the VEGF receptor signaling.

Consistent with our previous results showing that in hypoxic mimicking conditions, LDIR increases the expression of VEGF in ECs [8], here we found that the expression of *Pgf* and *Csf3* is also increased in ECs. Importantly, these results were confirmed *in vivo* as VEGF, PlGF and G-CSF concentrations significantly increase in the plasma at day 4, upon LDIR exposure. Of note, beside VEGF, the upregulation of other cytokines (such as PlGF and G-CSF), might explain why circulating EPCs are insensitive to PTK/ZK inhibition. It is plausible that the effects of VEGF, PlGF and G-CSF are redundant on EPCs, and may explain why PTK/ZK does not affect the enhancement promoted in collateral density by LDIR. These cytokines were reported as being involved in the guidance of EPC to ischemic tissue [2, 13, 14].

In line with this, we observed EPC mobilization and recruitment to the ischemic tissue upon LDIR. In the absence of ischemia, LDIR *per se* does not induce that effect and notably the irradiation of the ischemic tissue is critical for the mobilization of EPCs and collateral formation. Of note, in our transplantation model, all hematopoietic cells are GFP+ (including circulating and extravasated/tissue leucocytes, erythrocytes and platelets), but EPC, forming the inner lining of blood vessels, exhibit both green (GFP+) and red (CD31+). Thus, our results suggest that LDIR increases these growth factor concentrations synergistically with HLI and given the fact that this happens only if the ischemic tissue is irradiated, we hypothesize that a hypoxic niche is critical for this process. Although we cannot exclude that other cells could modulate the levels of these cytokines upon LDIR, our results strongly suggest the involvement of ECs.

We propose a model of enhanced and sustained angiogenesis induction by *in situ* LDIR administration as a promising therapeutic approach for ischemic diseases (*Figure 6*).

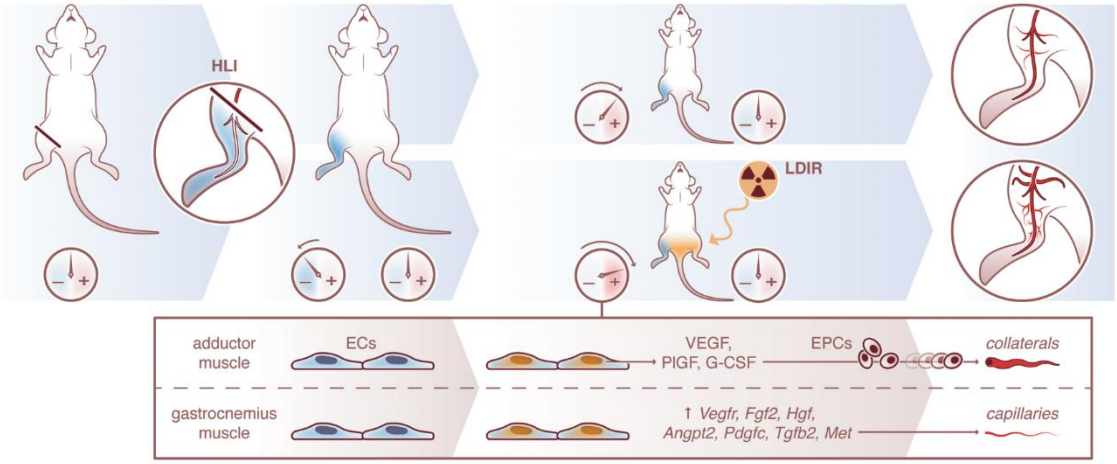

Figure 6. Proposed model of LDIR effect after HLI.

After unilateral HLI (represented by a thick brown line), the flow to the ischemic limb is dramatically decreased (in blue) and vascular function is compromised as represented by a reduction in the dial. After LDIR exposure of both hindlimbs (in orange), we propose a synergistic effect occurs with the ischemic insult, tilting the dial towards an improvement of the vascular function by stimulating neovascularization. Then, ECs in an hypoxic microenvironment secrete VEGF, PlGF and G-CSF leading to the recruitment of EPCs and consequently to collateral density increase. Simultaneously, the up-regulation of several pro-angiogenic target genes namely *Vegfr (Vegfr-2 and -1)*, *Fgf2*, *Angpt2*, *Pdgfc, Tgfb2*, *Hgf* and *Met* in ECs induces capillary density. The vascular function of

nonischemic hindlimbs was not affected by LDIR exposure as represented by the dial in an equilibrium status before, during and after ischemia recovery. (© Diogo Guerra. 2016).

LDIR applied as one daily irradiation of 0.3 Gy, administered for four consecutive days, synergistically act with the ischemic insult, exacerbating the local pro-angiogenic response. Our results suggest that this is achieved through (i) increased capillary density accompanied by an up-regulation of several pro-angiogenic target genes in ECs localized in gastrocnemius muscles, a process that is dependent of VEGF signaling and (ii) the mobilization and recruitment of EPCs by increasing the concentrations of VEGF, PlGF and G-CSF that may explain the collateral density increase in the ischemic limb leading to blood perfusion improvement.

One important concern when addressing ionizing radiation is its toxic effect. According to the linear no-threshold (LNT) hypothesis, the dose-response is linear and no threshold exists where damage begins to show. Recent advances in radiobiology challenge the validity of the LNT suggesting that it overestimates radiation risks [21]. We performed a 52-week and LDIR had no significant impact in the morbidity and mortality of the mice, although the possibility of LDIR long-term toxicity cannot be ruled out. Importantly, the LDIR proposed herein is usually absorbed by healthy tissues during radiotherapy, in areas where no adverse effects were found during the follow-up of the patient for several years. The angiogenic potential of ionizing radiation has already been shown [22]. We and others have shown that LDIR favors angiogenesis by promoting EC proliferation and migration, accelerating wound healing [8, 22]. However, there is no consensus about the doses described as pro-angiogenic, as different radiation schemes are used. Herein, ionizing radiation was delivered through a linear accelerator producing photon beams, currently used in the clinical practice. The use of conventional radiotherapy dose (2-10 Gy, administered once, Caesium-137 source) has been shown to induce neovascularization in HLI through VEGF release from mast cells and MMP-9-mediated progenitor cell mobilization; however potential adverse effects were seen [11] and so, to the best of our knowledge, to date the use of those high doses has not been proposed for therapeutic neovascularization.

Our data supports the use of LDIR in enhancing ischemia-induced neovascularization *in vivo*, which is achieved through the increase of cytokines, mobilization and recruitment of EPC to the ischemic tissue and simultaneous activation of a repertoire of pro-angiogenic

factors and resulting in enhanced recovery of blood flow. LDIR may therefore have a clinical significant impact in the treatment of peripheral arterial disease that represents a growing health problem worldwide, with high economic burden and limited therapeutic options. We currently have an ongoing exploratory clinical trial to determine the clinical and molecular effects in “non-option” CLI patients. The success of this clinical trial will lead to the development of new trials to propose a novel and effective therapeutic tool with worldwide impact to peripheral arterial disease.

Funding

P.O. is supported by a fellowship (SFRH/BD/80483/2011) from Fundação para a Ciência e Tecnologia. K.S. received a Postdoctoral fellowship (SFRH/BPD/78039/2011) and an Investigator Program (IF/00004/2014) from Fundação para a Ciência e Tecnologia.

Acknowledgments

We thank to the Department of Radiotherapy, Centro Hospitalar Lisboa Norte, Lisbon, Portugal, particularly to I. Diegues, C. Raimundo, A. Borges, D. Parreira, M. Pereira, C. Moreira, A. Curto, C. Mestre, A. Momede, H. Silva, I. Lima, T. Mouro and V. Quintino for help in irradiation delivery. We thank to A. Duarte and R. Malveiro for help in the treatment planning and dosimetry. We thank to I. Monteiro Grillo and M. Jorge in the quality of ex-directors of the department of radiotherapy for opening the doors when this work started, for their unconditional support and for all the discussions we had. We gratefully acknowledge A. Portêlo for statistical advice and D. Guerra for the illustration of the proposed model.

Conflict of Interest

None declared.

References

1. Sanada F, Taniyama Y, Azuma J, Yuka, II, Kanbara Y, Iwabayashi M, Rakugi H, Morishita R. Therapeutic Angiogenesis by Gene Therapy for Critical Limb Ischemia: Choice of Biological Agent. *Immunol Endocr Metab Agents Med Chem* 2014;**14**:32-39.
2. Luttun A, Tjwa M, Moons L, Wu Y, Angelillo-Scherrer A, Liao F, Nagy JA, Hooper A, Priller J, De Klerck B, Compernolle V, Daci E, Bohlen P, Dewerchin M, Herbert JM, Fava R, Matthys P, Carmeliet G, Collen D, Dvorak HF, Hicklin DJ, Carmeliet P. Revascularization of ischemic tissues by PlGF treatment, and inhibition of tumor angiogenesis, arthritis and atherosclerosis by anti-Flt1. *Nat Med* 2002;**8**:831-840.
3. Collinson DJ, Donnelly R. Therapeutic angiogenesis in peripheral arterial disease: can biotechnology produce an effective collateral circulation? *Eur J Vasc Endovasc Surg* 2004;**28**:9-23.
4. Davies MG. Critical limb ischemia: cell and molecular therapies for limb salvage. *Methodist Debakey Cardiovasc J* 2012;**8**:20-27.
5. Isner JM, Asahara T. Angiogenesis and vasculogenesis as therapeutic strategies for postnatal neovascularization. *J Clin Invest* 1999;**103**:1231-1236.
6. Rivard A, Fabre JE, Silver M, Chen D, Murohara T, Kearney M, Magner M, Asahara T, Isner JM. Age-dependent impairment of angiogenesis. *Circulation* 1999;**99**:111-120.
7. Hill JM, Zalos G, Halcox JP, Schenke WH, Waclawiw MA, Quyyumi AA, Finkel T. Circulating endothelial progenitor cells, vascular function, and cardiovascular risk. *N Engl J Med* 2003;**348**:593-600.
8. Sofia Vala I, Martins LR, Imaizumi N, Nunes RJ, Rino J, Kuonen F, Carvalho LM, Ruegg C, Grillo IM, Barata JT, Mareel M, Santos SC. Low doses of ionizing radiation promote tumor growth and metastasis by enhancing angiogenesis. *PLoS One* 2010;**5**:e11222.
9. Couffinhal T, Silver M, Zheng LP, Kearney M, Witzenbichler B, Isner JM. Mouse model of angiogenesis. *Am J Pathol* 1998;**152**:1667-1679.
10. Carmeliet P. Mechanisms of angiogenesis and arteriogenesis. *Nat Med* 2000;**6**:389-395.
11. Heissig B, Rafii S, Akiyama H, Ohki Y, Sato Y, Rafael T, Zhu Z, Hicklin DJ, Okumura K, Ogawa H, Werb Z, Hattori K. Low-dose irradiation promotes tissue revascularization

through VEGF release from mast cells and MMP-9-mediated progenitor cell mobilization. *J Exp Med* 2005;**202**:739-750.

12. Asahara T, Masuda H, Takahashi T, Kalka C, Pastore C, Silver M, Kearne M, Magner M, Isner JM. Bone marrow origin of endothelial progenitor cells responsible for postnatal vasculogenesis in physiological and pathological neovascularization. *Circ Res* 1999;**85**:221-228.
13. Sennikov SV, Temchura VV, Trufakin VA, Kozlov VA. Effects of granulocyte-macrophage colony-stimulating factor produced by intestinal epithelial cells on functional activity of hemopoietic stem cells. *Bull Exp Biol Med* 2002;**134**:548-550.
14. Asahara T, Takahashi T, Masuda H, Kalka C, Chen D, Iwaguro H, Inai Y, Silver M, Isner JM. VEGF contributes to postnatal neovascularization by mobilizing bone marrow-derived endothelial progenitor cells. *EMBO J* 1999;**18**:3964-3972.
15. Rodel F, Frey B, Gaipl U, Keilholz L, Fournier C, Manda K, Schollnberger H, Hildebrandt G, Rodel C. Modulation of inflammatory immune reactions by low-dose ionizing radiation: molecular mechanisms and clinical application. *Curr Med Chem* 2012;**19**:1741-1750.
16. Rodel F, Keilholz L, Herrmann M, Sauer R, Hildebrandt G. Radiobiological mechanisms in inflammatory diseases of low-dose radiation therapy. *Int J Radiat Biol* 2007;**83**:357-366.
17. Williams J, Chen Y, Rubin P, Finkelstein J, Okunieff P. The biological basis of a comprehensive grading system for the adverse effects of cancer treatment. *Semin Radiat Oncol* 2003;**13**:182-188.
18. Frey B, Gaipl US, Sarter K, Zaiss MM, Stillkrieg W, Rodel F, Schett G, Herrmann M, Fietkau R, Keilholz L. Whole body low dose irradiation improves the course of beginning polyarthritis in human TNF-transgenic mice. *Autoimmunity* 2009;**42**:346-348.
19. Klug F, Prakash H, Huber PE, Seibel T, Bender N, Halama N, Pfirschke C, Voss RH, Timke C, Umansky L, Klapproth K, Schakel K, Garbi N, Jager D, Weitz J, Schmitz-Winnenthal H, Hammerling GJ, Beckhove P. Low-dose irradiation programs macrophage differentiation to an iNOS(+)/M1 phenotype that orchestrates effective T cell immunotherapy. *Cancer Cell* 2013;**24**:589-602.

20. Romero-Weaver AL, Wan XS, Diffenderfer ES, Lin L, Kennedy AR. Kinetics of neutrophils in mice exposed to radiation and/or granulocyte colony-stimulating factor treatment. *Radiat Res* 2013;**180**:177-188.

21. Tubiana M, Feinendegen LE, Yang C, Kaminski JM. The linear no-threshold relationship is inconsistent with radiation biologic and experimental data. *Radiology* 2009;**251**:13-22.

22. Madani I, De Neve W, Mareel M. Does ionizing radiation stimulate cancer invasion and metastasis? *Bull Cancer* 2008;**95**:292-300.

Supplementary Material

Supplementary Methods

Cell Culture

Lung human microvascular endothelial cells (HMEC-L) were purchased from Lonza and cultured according to manufacturer's instructions. While different batches of primary cells were used over the course of the work, cells from the same batch were used in individual experiments (e.g. control vs. an experimental condition). Cells were used at passages 4 to 6.

Mice and Reagents

Twenty–two-week-old C57BL/6 female mice, purchased from Charles River Laboratories, Spain, were used in all HLI experiments; and nine-week-old C57Bl/6-Tg(CAG-EGFP)10sb/J female mice (Instituto Gulbenkian de Ciência) were used as a donor mice in for bone marrow transplantation. Briefly, for the HLI procedure and in vivo imaging, animals were anesthetized with ketamine-medetomidine (75mg/Kg BW and 1 mg/Kg BW, respectively) and the anaesthesia was reverted with atipamezole (5mg/kg BW). Postoperatively, analgesia was administered (buprenorphine 100µl/15-30g BW q8-12 hours) and the animals were closely monitored. Mice were euthanized by cervical dislocation. PTK787/ZK222584 (PTK/ZK) (100 mg/Kg) was kindly provided by Novartis Pharma AG, Basel, Switzerland. PTK/ZK, polyethylene glycol-300 was used as vehicle (Sigma) and administered by oral gavage. The animals were randomly assigned to each experimental group.

HLI Model

A surgical procedure was performed to induce unilateral HLI in the mice. Briefly, an incision in the skin overlying the thigh of the right hindlimb of each mouse was made and the distal external iliac artery and the femoral artery and veins were ligated and excised. The vein was ligated both to increase the severity of the ischemia as well as to increase the technical reproducibility of the model, as isolation of the femoral artery alone often results in tearing of the vein resulting in hemorrhage.

Irradiation

The radiotherapy plan was devised on a dedicated 3D treatment planning system (XiO, Elekta) using an isocentric dose distribution of two opposite fields (0°, 180°) at 6 MV photon energy, normalized to a reference point. Ionizing radiation was delivered, at room temperature, using a linear accelerator that produces x-rays photon beam (Synergy S, Elekta) operating at a dose rate of 500 MU/min.

Mice were transferred to an acrylic phantom in order to achieve the adequate thickness to improve homogeneity during the radiation therapy. A computed tomography scan (Somatom Sensation, Siemens) was performed and a volumetric acquisition was carried out; acquired images were reconstructed with axial slices width of 2 mm, and cross sectional data was transferred to the image processing system work station for contouring the planning target volume.

A 0.6 cm^3 PTW farmer ionizing chamber, connected to UNIDOS electrometer, was used to validate the IR doses calculated by the treatment planning system (TPS), according to the IAEA TRS-398 protocol. We obtained, in average, differences lower than 2% between the experimental and the XiO TPS dose values. The irradiation field included mice entire legs (pelvic girdle down to the feet) or the upper (above hip) part of the mouse body with a dose of 0.3 Gy administered for 4 consecutive days, starting 12 hours after ischemia induction. Control mice were sham-irradiated (0.0 Gy) following the same procedure for the irradiated experimental groups. The irradiation procedure was performed in a non-blinded manner. During this protocol the mice were anesthetized.

Laser Doppler perfusion imaging

The laser Doppler perfusion imager (MoorLDI-V6.0, Moor Instruments Ltd, Axminster, UK) was used to assess limb perfusion. Hair was removed one day before laser Doppler analysis using an electrical shaver followed by depilatory cream. Blood flow was measured both in the ischemic and non-ischemic legs, before HLI induction (Pre-HLI), immediately post-HLI (Post-HLI), and at days 7, 15 and 45 post-HLI (d7 Post-HLI, d15 Post -HLI and d45 Post -HLI, respectively). According to the analysis performed immediately post-HLI, mice are randomized assuring an equal reduction of blood flow in the different experimental groups. Color-coded images of tissue perfusion were recorded and poor or no perfusion was displayed as darkblue, and the highest perfusion level was displayed as red. Mean flux

values were calculated using the Moor LDI V5.3 image processing software. To account for variables such as temperature and ambient light, blood perfusion is expressed as the ratio of ischemic to non-ischemic limb. The mice were placed on a 37°C heating pad to reduce heat loss during measurements.

Immunohistochemistry and Capillary density analysis

Mice were sacrificed at days 15 and 45 post-HLI. The gastrocnemius or adductor muscles of both legs were harvested, placed in transverse orientation on a small cork disc with the help of 10% tragacanth, snap frozen in liquid nitrogen cooled isopentane and stored at -80ºC until sectioned. Seven-micrometer sections were labeled with CD31 monoclonal antibody (Pharmingen). After fixation in acetone, for 10 minutes, hydrogen peroxidase (0.3% diluted in methanol) was added, for 30 minutes, at room temperature, followed by 2 washes in PBS, for 10 minutes. Blocking solution (5% rabbit serum in PBS) was applied, for 30 minutes, at room temperature, and then slides were incubated, for 1 hour, at room temperature, with rat monoclonal antibody against mouse CD31 at 1:500, diluted in PBS-1% BSA. After 3 washes in PBS, for 30 minutes, a secondary biotinylated rabbit anti-rat IgG antibody was added at 1:200 in PBS-1% BSA plus 5% rabbit serum, for 30 minutes, at room temperature. Washes were performed as before and labeled avidin-conjugated peroxidase complex (Vectastain ABC kit; Vector Laboratories) was used for color development according to the manufacturer's recommendations, for 30 minutes, at room temperature. After rinsing in PBS (3 times, for 5 minutes), DAB peroxidase substrate kit (Vector Laboratories) was added, for 5 minutes to localize the immune complexes. The sections were counterstained with Hematoxylin (Bio-Optica), for 10 seconds, and mounted with Entelan (Merck). Omission of the primary antibody was run in parallel as a negative control. Analysis of tissue samples was conducted using Leica DM2500 upright brightfield microscope (Leica Microsystems). Capillary densities, i.e. number of capillaries per number of muscle fibers, were measured in 2 different sections of 4 distinct anatomic areas of each specimen using the ImageJ® software.

Contrast Agent Perfusion and Diaphonization

Fifteen, forty-five and ninety days post-HLI induction, when mice were well stabilized from the ischemic injury, they were deeply anesthetized and the torso and limbs were shaved. A medial thoracotomy was performed to expose the heart and a needle (26 Gauge), attached to an automatic injector, was introduced in the left ventricle. An incision was performed in the right atrium to allow venous drainage. Mice were primarily perfused with heparinized serum (3000 IU/L) until the blood was completely removed from circulation. A vasodilatation mixture of adenosine (3.7 μmol/L) and papaverine (11.8 μmol/L) was subsequently administered, right before the contrast agent, for 2 minutes. The contrast used was a mixture of barium sulfate (50%) and gelatin (5%). This solution was kept warm until the injection time to avoid thickening. Contrast agent was perfused manually until the feet blanched. Right after the injection the mice were transferred to a cold chamber, so that the contrast agent became solidified. All the solutions were injected with a perfusion rate of 0.01 cm^3/s. Then, the skin of each mouse was removed from the lower body and diaphonization was performed by using a modified version of Spalteholz technique. Briefly, the mice were fixated, decalcified, whitened, washed, dehydrated by freeze substitution and placed into a vacuum pump with Spalteholz solution (benzyl benzoate and methyl salicylate) until transparency was acquired. Diaphonization allows the visualization of effective lumen diameter, vessel angulation and emergence position.

Collateral vessels quantification

Mice were kept in Spalteholz solution during image acquisition, in order to achieve a homogenous density between the tissues and the media, with minimal absorption or reflection of light. Mice entire limbs were photographed in a magnifier with a light source. After acquisition, images were aligned and stitched together using Adobe Photoshop CS6® and entire limb photographs were obtained. Collateral vessels were manually segmented by highlighting them using Adobe Photoshop CS6®. We considered collateral vessels according to Longland's definition, a defined stem, mid-zone and re-entrant. According to this definition, collateral vessels with a diameter between 20 and 300 μm were included in our quantification excluding femoral, saphenous and popliteal arteries and all venous structures. Since arteriogenesis occurs primarily around the occluded blood vessel segment, the region of interest (ROI) in every mouse was in the same anatomic region in

the adductor, surrounding and bellow the surgical occlusion. Collateral vessel density (CVD) was quantified in equivalent ROIs corresponding to 20% of the total limb area. The CVD was calculated as the ratio between the vascular area and the ROI areas. All density measurements were performed using ImageJ® software. To exclude variations in the anatomy, perfusion or diaphonization procedures, the CVD value of the non-ischemic limb for each mouse was assumed to correspond to 100%. According to this assumption, the CVD percentage in the ischemic limb was calculated relatively to the non-ischemic one. The percentage of CVD increase was determined as the difference between the CVD percentage among the ischemic and non-ischemic limbs.

Laser capture microdissection of capillaries

Mice were sacrificed at day 45 post-HLI. Twelve-micrometer sections of the gastrocnemius or adductor muscles were labeled with CD31 monoclonal antibody (Pharmingen). The sections were stored at –80°C until microdissection. The immunohistochemistry protocol described above was modified to improve RNA preservation[1] by using high salt buffer, 2 mol/L NaCl in PBS (at 4ºC) in all incubation and washing steps. After immunohistochemistry, sections were dehydrated in ice cold 90% ethanol followed by 100% ethanol and allowed to dry. Ten thousand capillaries were microdissected using a Zeiss PALM MicroBeam Laser Microdissection System (Carl Zeiss Microscopy, Germany) equipped with a pulsed solid-state 355 nm laser. Dissected capillaries were catapulted into a microfuge tube adhesive-cap.

Isolation of immune cell infiltrate from muscle and FACS analysis

Adductor muscles were excised after perfusing the mice with 30ml PBS. Muscles were cut in small pieces and digested for 30 minutes with collagenase I (1.5 mg/ml, Worthington) and DNase I (10 µg/ml, Sigma) diluted in DMEM. The digested product was filtered through a 70 µm mesh cell-strainers (Becton Dickinson) using a plunger to disrupt undigested tissue and washed with RPMI supplemented with serum. To isolate the leukocyte fraction, the cells were resuspended in 40% Percoll, overlayed on 80% Percoll and spun for 25 minutes at 2400 rpm without brake. The interphase containing leukocytes was recovered, washed and erythrocytes were osmotically lysed in red blood cell lysis buffer (BioLegend). For cell surface staining, single-cell suspensions were incubated, in presence 5% normal mouse

serum, for 30 minutes with saturating concentrations of combination of the following monoclonal antibodies that were purchased from BD Biosciences, eBiosciences or Biolegend: FITC anti-CD3ε (145-2C11), PE anti-CD69 (H1-2F3), PerCP-Cy5.5 anti-Ly6G (1A8), PE-Cy7 anti-F4/80 (BM8), APC anti-CD11b (M1/70), APC-Cy7 anti-CD19 (1D3), brilliant violet 510 anti-CD45 (30-F11), brilliant violet 605 anti-Ly6C (HK1.4), brilliant violet 711 anti-4 (N418). Zombie violet dye (BioLegend) was then added to the final suspension for 10 minutes, at 4ºC in order to stain and exclude dead cells. Cells were then immediately analyzed by flow cytometry on LSR Fortessa (BD Biosciences). All graphical output was performed using FlowJo® 10 (Tree Star, Costa Mesa, CA).

Endothelial progenitor cells and FACS analysis

Terminal peripheral blood collection was performed transcardially, to an EDTA-coated tube, and erythrocytes were osmotically lysed in red blood cell lysis buffer (BioLegend). Then, cells were incubated, in presence of PBS - 5% BSA, for 30 minutes with saturating concentrations of combination of the following monoclonal antibodies purchased from Invitrogen, eBioscience or BD Pharmingen: TOPRO 3, biotin anti-Ter119, PE-Cy7 anti-CD117, FITC anti-Sca-1, PE anti-VERGFR2. For Ter119, a secondary eFluor 450 streptavidin was used. Cells were then immediately washed with PBS and analyzed by flow cytometry on LSR Fortessa (BD Bioscience). All graphical output was performed using FlowJo 10 (Tree Star, Costa Mesa, CA).

Endothelial progenitor cells (EPCs) were quantified within the monocytic cell population, by a dual expression of VEGFR2 and Sca-1 in the CD117 gate.

Circulating Cytokine Quantification

Peripheral blood was obtained by cardiac puncture at day 4 post-HLI induction. Blood was centrifuged 30 minutes and plasma separated from the cellular fraction and stored at -20ºC. In plasma, vascular endothelial growth factor (VEGF), granulocyte-colony stimulating factor (G-CSF), placenta growth factor (PlGF) and stroma-derived factor-1α (SDF-1α) were measured via ELISA (R&D Systems) according to manufacturer's instructions.

Bone Marrow Transplantation Model and Immunofluorescence

Bone marrow cells were obtained by flushing the tibia and femur of eight-week-old C57BL/6 female mice C57Bl/6-Tg(CAG-EGFP)10sb/J (donor mice). Mononuclear cells were isolated by density centrifugation and filtered in a 70 μm cell strainer (BD).

The transplantation was done in ten-week-old C57BL/6 female mice (recipient mice), lethally irradiated with 900 rads (Gammacell® 3000Elan). After irradiation, the recipient mice received unfractionated bone marrow cells ($5x10^6$) from the donor mice by tail vein injection. Eight weeks after, HLI was induced and mice were sacrificed at day 15 post-HLI. The adductor muscles of both hindlimbs were harvested, placed in transverse orientation on a small cork disc with the help of 10% tragacanth, snap frozen in liquid nitrogen cooled isopentane and stored at -80ºC until sectioned. Ten-micrometer sections were labeled with CD31 monoclonal antibody (Pharmingen) and purified rabbit anti-GFP (Torrey Pines BioLabs Inc). After fixation in acetone, for 10 minutes, 0.5%Triton x-100 was added, for 10 minutes, at room temperature followed by 2 washes in PBS, for 10 minutes. Blocking solution (10% goat (DakoCytomation) plus 10% donkey (Sigma-Aldrich) serum in PBS-1% BSA) was applied, for 30 minutes, at room temperature, and the slides were then incubated for 1 hour, at room temperature, with a rat monoclonal antibody against mouse CD31 and rabbit anti-GFP in PBS-1% BSA. After 3 washes in PBS-0.1%Tween, for 15 minutes, secondary antibodies goat anti-rat Alexa fluor 594 (Invitrogen) and goat anti-donkey Alexa fluor 488 (Invitrogen) were added in PBS-1% BSA, for 1hour, at room temperature. Washes were performed as before. Sections were incubated with Dapi (Sigma-Aldrich), for 10 minutes, washed in PBS, for 5 minutes, mounted with vectashield mounting medium (Vector Laboratories) and seal with nail polish. Omission of the primary antibodies was run in parallel as a negative control. Analysis of tissue samples was conducted using a Motorized Widefield Fluorescence Microscope (Zeiss Axiovert 200M) with a 20x/0.8 objective or confocal microscope (Zeiss LSM 880) with a 63x/1.4 oil immersion objective, with the pinhole set to 1 Airy unit (optical slice thickness = 0.7 micron). The number of EPC, defined as GFP+ CD31+, was measured on an area of 4.30 mm^2 into 5 different sections of the adductor muscle for each specimen. All measurements were performed using ImageJ® software.

RNA extraction, cDNA synthesis and pre-amplification

Total RNA from the microdissected capillaries or HMEC-L was isolated using an RNeasy Micro or Mini Kit (QIAGEN) including DNase treatment, respectively. For synthesis and preamplification of cDNA RT^2 PreAMP cDNA Synthesis kit (QIAGEN) was used with two rounds of pre-amplification using the following murine primers:

*Vegfr1*_F (5'-TTGAGGAGCTTTCACCGAACTCCA-3')
*Vegfr1*_R (5'-TATCTTCATGGAGGCCTTGGGCTT-3')
V*egfr2*_F (5'-AGGCCCATTGAGTCCAACTACACA-3')
V*egfr2*_R (5'-AGACCATGTGGCTCTGTTTCTCCA-3')
*Fgf2*_F (5'-ACTCCAGTTGGTATGTGGCACTGA-3')
*Fgf2*_R (5'-AACAGTATGGCCTTCTGTCCAGGT-3')
*Tgfb2*_F (5'-GCTTTGGATGCGGCCTATTGCTTT-3')
*Tgfb2*_R (5'-CTCCAGCACAGAAGTTGGCATTGT-3')
*Ang2*_F (5'-ATCCAACACCGAGAAGATGGCAGT-3')
*Ang2*_R (5'-AACTCATTGCCCAGCCAGTACTCT-3')
*Pdgf-c*_F (5'-ATGCCACAAGTCACAGAAACCACG-3')
*Pdgf-c*_R (5'-AAGGCAGTCACAGCATTGTTGAGC-3')
*Hgf*_F (5'-GCATTCAAGGCCAAGGAGAAGGTT-3')
*Hgf*_R (5'-TCATGCTTGTGAGGGTACTGCGAA-3')
*C-met*_F (5'-ACGTTGAAATGCACAGTTGGTCCC-3')
*C-met*_R (5'-TTGCGTCGTCTCTCGACTGTTTGA-3')
*Pecam*_F (5'-CCCATCACTTACCACCTTTATG-3')
*Pecam*_R (5'-TGTCTCGGTGGGCTTAT-3')
*Etv2*_F (5'-CACCGATCACACCAATGAA-3')
*Etv2*_R (5'-GTACGTCTTCGTGAGGTAAAG-3')
*Erg1*_F (5'-CCAAACTGGAGGAGATGATG-3')
*Erg 1*_R (5'-GTGCTGCTGCTGCTATTA-3')
*Spi1*_F (5'-GCGCTGGCACCTTTTTGTAT-3')
*Spi1*_R (5'-CAATAATTTTACTTGTCTTTAGTGGTTA-3')
*Itgam*_F (5'-TCTACTACCCATCTGGCTTATC-3')
*Itgam*_R (5'-TGGACTCAGCAGGCTTTA-3')

*Des*_F (5’-GCCACCTACCGGAAGCTACT-3’)

*Des*_R (5’-GCAGAGAAGGTCTGGATAGGAA-3’)

*Pdgfr*_F (5’-GTGGTGAACTTCCAATGGACG-3’)

*Pdgfr*_R (5’-GTCTGTCACTGGCTCCACCAG-3’)

*Acta2*_F (5’-CCAGCACCATGAAGATCAAG-3’)

*Acta2*_R (5’-TGGAAGGTAGACAGCGAAGC -3’)

*18s*_F (5’-GCCCTATCAACTTTCGATGGTAGT-3’)

*18s*_R (5’-CCGGAATCGAACCCTGATT-3’)

Real-time PCR was performed according to the manufacturer’s protocol using Power SYBR® Green (Applied Biosystems) and an Applied Biosystems 7500 Fast Real-Time PCR for the same targets described above. Human primer sequences are as follows:

*Vegfr1*_F (5’-CCCTCGCCGGAAGTTGTAT-3’)

*Vegfr1*_R (5’-GTCAAATAGCGAGCAGATTTCTCA-3’)

V*egfr2*_F (5’-ATTCCTCCCCCGCATCA-3’)

V*egfr2*_R (5’-GCTCGTTGGCGCACTCTT-3’)

*Fgf2*_F (5’-GCAGTGGCTCATGCCTATATT-3’)

*Fgf2*_R (5’-GGTTTCACCAGGTTGGTCTT-3’)

*Tgfb2*_F (5’-GCTTTGGATGCGGCCTATTGCTTT-3’)

*Tgfb2*_R (5’-CTCCAGCACAGAAGTTGGCATTGT-3’)

*Ang2*_F (5’-AGGACACACCACGAATGGCATCTA-3’)

*Ang2*_R (5’-TGAATAATTGTCCACCCGCCTCCT-3’)

*Pdgf-c*_F (5’-AGGTCTTCAATCGTGGAAAGAA-3’)

*Pdgf-c*_R (5’-CAGAACCCAGCTAGTGGAATAC-3’)

*Hgf*_F (5’-GGTAAAGGACGCAGCTACAA-3’)

*Hgf*_R (5’-AGCTGTGTTCGTGTGGTATC-3’)

*C-met*_F (5’-CTGGTTCCTGGGCACCGAAAGATAAA-3’)

*C-met*_R (5’-CCATTGCTCCTCTGCACCAAGGTAAA-3’)

*Pgf*_F (5’-CATGCAGCTCCTAAAGATCC-3’)

*Pgf*_R (5’-CTTTCCGGCTTCATCTTCTC-3’)

*Cxcl12*_F (5’-TCTCAACACTCCAAACTGTG-3’)

*Cxcl12*_R (5'-TCTCCAGGTACTCCTGAATC-3')

*Csf3*_ F (5'-GATGGAAGAACTGGGAATGG-3')

*Csf3*_R (5'-AAGCTCTGCAGATGGGA-3')

*18s*_F (5'-GCCCTATCAACTTTCGATGGTAGT-3')

*18s*_R (5'-CCGGAATCGAACCCTGATT-3')

The housekeeping gene used to normalize was 18S. The RT-PCR program consisted of an initial denaturation step, at 95ºC, for 10 minutes followed by 50 cycles, at 95ºC, for 15 seconds and, at 60ºC, for 1 minute. The relative quantification was performed according to the comparative method ($2^{-\Delta\Delta Ct}$; Applied Biosystems User Bulletin no. 2P/N 4303859), with non-ischemic muscle as internal calibrator. The formula used is $2^{-\Delta\Delta Ct} = 2^{-[\Delta Ct\ (sample) - \Delta Ct\ (calibrator)]}$, where ΔCt (sample) =Ct (sample) –Ct (reference gene). For the internal calibrator, $\Delta\Delta$Ct=0 and 2^0=1. For the remaining samples, the value of $2^{-\Delta\Delta Ct}$ indicates the fold change in gene expression relative to the calibrator. ΔCt value for each sample is the average of triplicates.

Clinical Pathology and Histological Analyses

Fifty-two weeks post-HLI, body weight was recorded and mice were sacrificed with anesthetic overdose. Blood was collected by cardiac puncture and assessed for complete blood cell count, serum biochemistry (urea, creatinine, alanine aminotransferase, aspartate amino transferase, alkaline phosphatase, phosphorus and albumin) and coagulation tests (prothrombin time, activated partial thromboplastin time, thrombin time and fibrinogen assay). Urine was collected by urinary bladder puncture for urinalyses.

Necropsy was performed and several organs and tissues were collected for routine cytological and histopathology analysis: bone marrow smears were performed from flushed bone marrow (femur), and lung, liver, kidney, thymus, spleen, lymph nodes and long bone (femur) were collected, formalin-fixed and paraffin embedded. Hematoxylin and eosin-stained 3 µm sections were analyzed by a pathologist blinded to experimental groups.

RNA Isolation, Target Synthesis and Hybridization to Affymetrix GeneChips

Total RNA was extracted using the RNeasy Micro Kit (QIAGEN) including DNase treatment. Concentration and purity was determined by spectrophotometry and integrity was confirmed using an Agilent 2100 Bioanalyzer with a RNA 6000 Nano Assay (Agilent Technologies, Palo Alto, CA).

RNA was processed for use on Affymetrix (Santa Clara, CA, USA) GeneChip HuGene 1.0 ST Arrays, according to the manufacturer's Whole Transcript Sense Target Labeling Assay. Briefly, 100 ng of total RNA containing spiked in Poly-A RNA controls (GeneChip Expression GeneChip Eukaryotic Poly-A RNA Control Kit; Affymetrix) was used in a reverse transcription reaction (GeneChip® WT cDNA Synthesis Kit; Affymetrix) to generate first-strand cDNA. After second-strand synthesis, double-stranded cDNA was used in an in vitro transcription (IVT) reaction to generate cRNA (GeneChip® WT cDNA Amplification Kit; Affymetrix). 15 µg of this cRNA was used for a second cycle of first-strand cDNA synthesis (GeneChip® WT cDNA Synthesis Kit; Affymetrix). 5.5 µg of single stranded cDNA was fragmented and end-labeled (GeneChip® WT Terminal Labeling Kit; Affymetrix). Size distribution of the fragmented and end-labeled cDNA, respectively, was assessed using an Agilent 2100 Bioanalyzer with a RNA 6000 Nano Assay. 5 µg of end-labeled, fragmented cDNA was used in a 100 µl hybridization cocktail containing added hybridization controls. 80 µl of mixture was hybridized on arrays for 17 hours, at 45ºC. Standard post hybridization wash and double-stain protocols (FS450_0007; GeneChip HWS kit, Affymetrix) were used on an Affymetrix GeneChip Fluidics Station 450. Arrays were scanned on an Affymetrix GeneChip scanner 3000 7G.

GeneChip Data Analysis

Scanned arrays were analyzed first with Affymetrix Expression Console software for quality control. Subsequent analysis was carried out using Partek Genomics Suite 6.4. Here the 8 arrays were normalized and modeled using Robust Multichip Averaging RMA. Probe sets showing differential expression were determined using 1-way Analysis of Variance (ANOVA) with a p-value cut-off of 0.03. Expression values of these 2374 well-annotated genes were imported into Chipster 3.7.2. Arrays and genes were clustered using Pearson correlation as a distance measure and average linkage for constructing a dendrogram, subsequently visualized as a heatmap. Microarray data are available in the Gene Expression

Omnibus database (http://www.ncbi.nlm.nih.gov/geo/) under accession number GSE73341. Reviewer access: (http://www.ncbi.nlm.nih.gov/geo/query/acc.cgi?token=afybsswgdfmlrsp&acc=GSE73341).

References

1. Brown AL, Smith DW. Improved RNA preservation for immunolabeling and laser microdissection. *RNA* 2009;**15**:2364-2374.

Supplementary figures

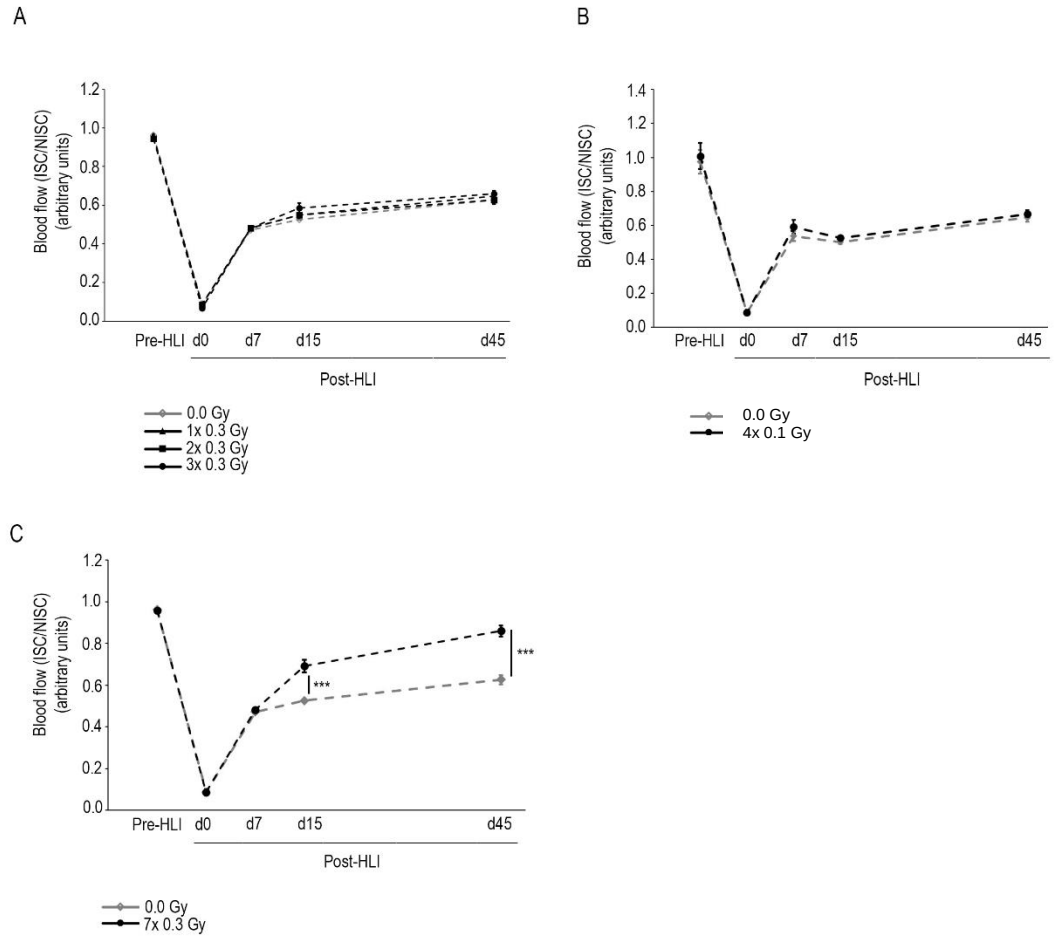

Supplementary Figure 1: Perfusion recovery after exposure to different doses of IR.

After surgical induction of unilateral HLI, both hindlimbs of C57BL/6 mice were sham-irradiated or irradiated with (**A**) 0.3 Gy, once, twice or three consecutive days (**B**) 0.1 Gy for four consecutive days (**C**) 0.3 Gy for seven days. Quantitative evaluation of blood flow expressed as a ratio of ISC to NISC limb was assessed before (Pre-HLI) and at days 0, 7, 15 and 45 post-HLI induction. At days 15 and 45 post-HLI, blood perfusion is significantly induced in mice exposed to 0.3 Gy during seven days. Between-group changes were assessed by two-away repeated measurements ANOVA followed by Bonferroni post-hoc test (n=6 mice per group). Means ± SEM are shown. *** $P < 0.001$. ISC, ischemic; NISC, non-ischemic; Pre-HLI, before hindlimb ischemia.

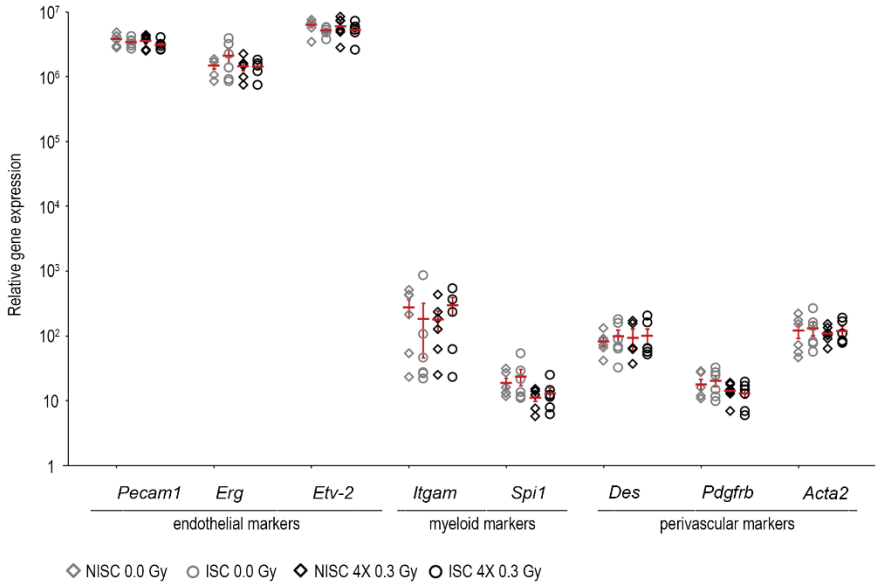

Supplementary Figure 2: The CD31+ cells isolated from laser capture microdissection microscope express consisted primarily of ECs and no myeloid nor perivascular cells

After surgical induction of unilateral HLI, both hindlimbs of C57BL/6 mice were sham-irradiated or irradiated with four daily fractions of 0.3 Gy, in consecutive days and allowed to recover. At day 45 post-HLI, gastrocnemius muscles were harvested sectioned, and stained for CD31. Individual endothelial CD31+ cells were and visualized, dissected and isolated using a laser capture microdissection microscope. To ensure that only ECs were isolated, the expression of markers specific for endothelium, myeloid or perivascular cells was assessed at the gene levels by qRT-PCR exclusively on ECs. The cell markers *Pecam1* encoding CD31, *Erg* and *Etv2* that are specific for ECs; *Itgam* encoding CD11b and *Spi1* encoding PU-1 for myeloid cells; and *Des* encoding Desmin, *Pdgfrb* and *Acta2* encoding smooth muscle alpha-actin for perivascular cells were assessed. The relative mRNA levels were determined by real time qRT-PCR relative to the level of 18S RNA expression. Each symbol represents data obtained from isolated individual ECs pooled from one mouse and means ± SEM (in red) are shown from n=6 mice per group; ns, non-significant. ISC, ischemic; NISC, non-ischemic.

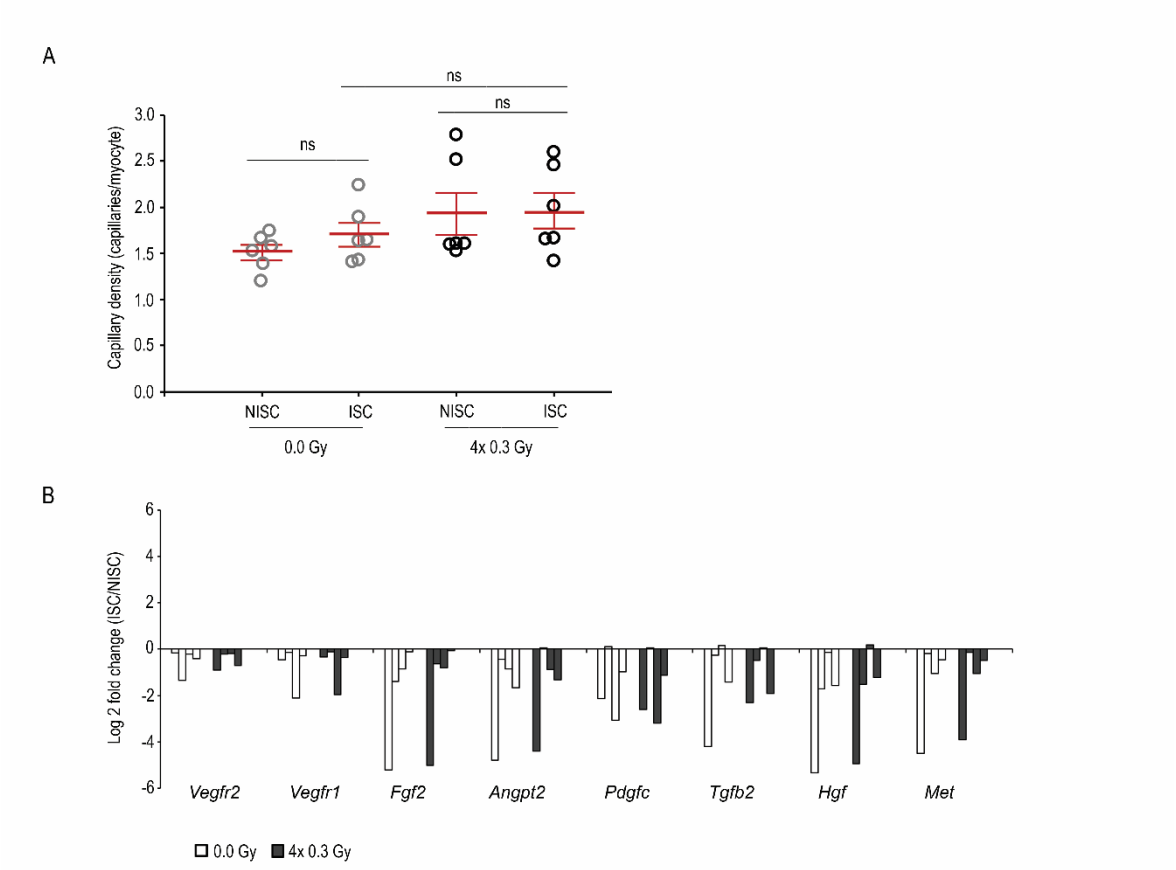

Supplementary Figure 3: Capillary density is not increased in the adductor muscles neither in response to ischemia nor upon LDIR and ECs do not present an up-regulation of pro-angiogenic genes.

After surgical induction of unilateral HLI, both hindlimbs of C57BL/6 mice were sham-irradiated or irradiated with four daily fractions of 0.3 Gy, in consecutive days and allowed to recover. (**A**) At day 45 post-HLI, quantitative analysis does not show an increase in capillary density (capillaries/myocyte) in irradiated ischemic adductor muscles compared to sham-irradiated ischemic ones. Furthermore, capillary density is not increased in adductor muscles in response to ischemia *per se*. Mixed ANOVA followed by Bonferroni post-hoc test was conducted with a within-subject factor of ISC and between-subject factor of irradiation. Individual data and means ± SEM (in red) are shown from n=6 mice per group; ns, non-significant. (**B**) At day 45 post-HLI, the expression of pro-angiogenic factors and their receptors was evaluated by qRT-PCR exclusively on ECs isolated from the adductor muscles. Each bar represents the relative gene expression in one animal. White and gray bars represent sham-irradiated and irradiated mice, respectively. Values were normalized to 18S to obtain relative expression levels. Results expressed as log2 fold changes between ISC and NISC samples demonstrated a down-regulation of the transcripts in both experimental groups. ISC, ischemic; NISC, non-ischemic.

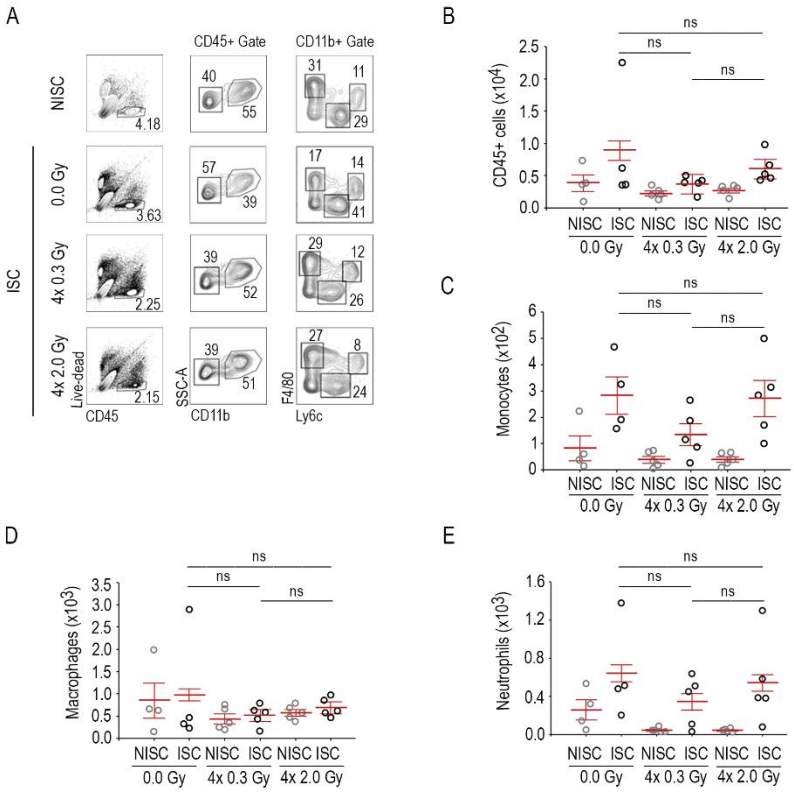

Supplementary Figure 4: Profiles of leukocytes mobilized to ischemic muscles upon LDIR. After surgical induction of unilateral HLI, both hindlimbs of C57BL/6 mice were sham-irradiated or irradiated with four daily fractions of 0.3 Gy or 2.0 Gy in consecutive days. At day 15 post-HLI, analysis of $CD45^{+}$ immune cells that infiltrate ischemic adductor muscles was assessed. (**A**) Representative analysis of hematopoietic CD45+ cells present in ischemic muscle as assessed by flow cytometry. Analysis of the accumulation of myeloid CD11b+ cells, and in particular macrophages (CD45+CD11b+F4/80+ cells), monocytes (CD45+CD11b+LY6C+F4/80int cells), and neutrophils (CD45+CD11b+Ly6Cint). The graphs show numbers of (**B**) total CD45+ cells; (**C**) monocytes; (**D**) macrophages and (**E**) neutrophils, isolated from ISC and NISC adductor muscles. Mixed ANOVA followed by Bonferroni post-hoc test was conducted with a within-subject factor of ISC and between-subject factor of irradiation. Individual data and means ± SEM (in red) are shown from n=4 mice per group; ns, non-significant. ISC, ischemic; NISC, non-ischemic.

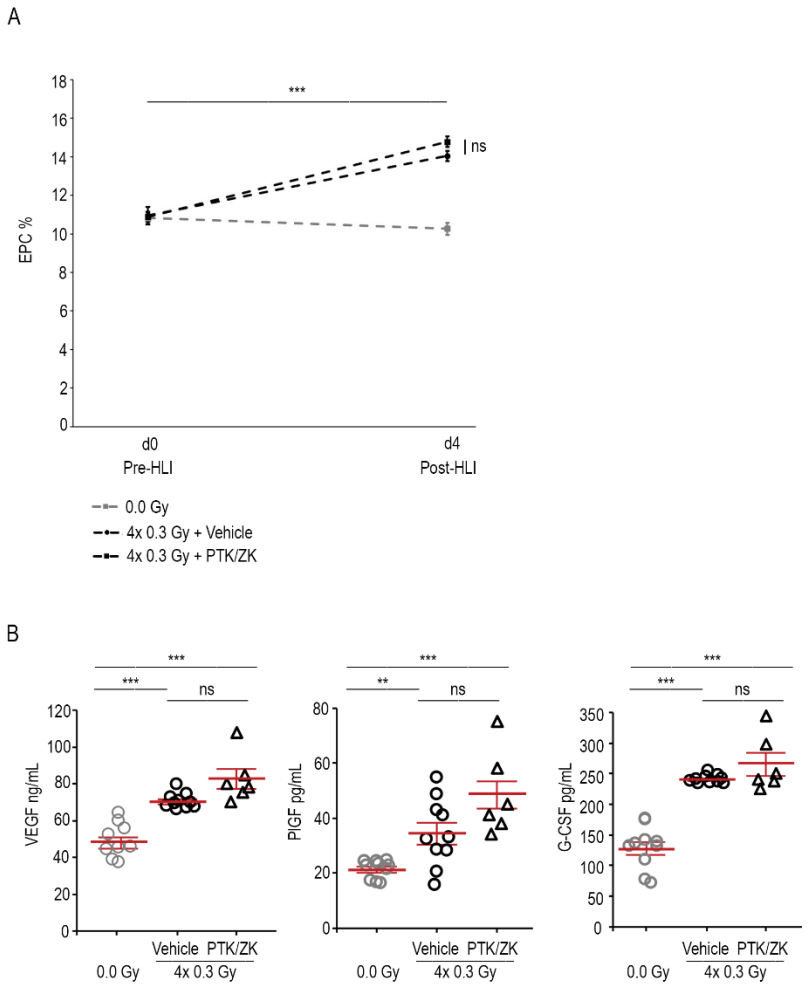

Supplementary Figure 5: PTK/ZK treatment does not change the effect of LDIR in increasing the number of circulating EPCs or the levels of VEGF, PlGF and GCSF in plasma after HLI induction.

After surgical induction of unilateral HLI both hindlimbs of C57BL/6 mice were sham-irradiated or irradiated with four daily fractions of 0.3 Gy, in consecutive days and allowed to recover. Two hours before each irradiation, ischemic mice were pretreated with PTK/ZK (100mg/Kg) or with the control vehicle. (**A**) Quantitative analysis of EPCs in peripheral blood demonstrated no differences at day 4 in irradiated mice pretreated with PTK/ZK vs irradiated mice pretreated with the control vehicle. As expected a significant increase of EPC at day 4 post-HLI is observed in both experimental groups when compared to day 0 pre-HLI or when compared to sham-irradiated mice at day 4. Two-way ANOVA was conducted followed by Bonferroni post-hoc test with a between-subject factors of day, irradiation and PTK/ZK treatment (n=6 mice per group). Means ± SEM are shown. (**B**) The concentrations of VEGF, PlGF and G-CSF were measured in the plasma, at day 4 post-HLI. The levels of VEGF, PlGF and G-CSF are not changed in irradiated mice pretreated with PTK/ZK treatment vs irradiated mice pretreated with the control vehicle. Two-way ANOVA was conducted followed by

Bonferroni post-hoc test with a between-subject factors of irradiation and PTK/ZK pre-treatment. Individual data and means ± SEM are shown (in red) from n=10 or 6 mice per group; ns, non-significant. ISC, ischemic; NISC, non-ischemic; Pre-HLI, before hindlimb ischemia.

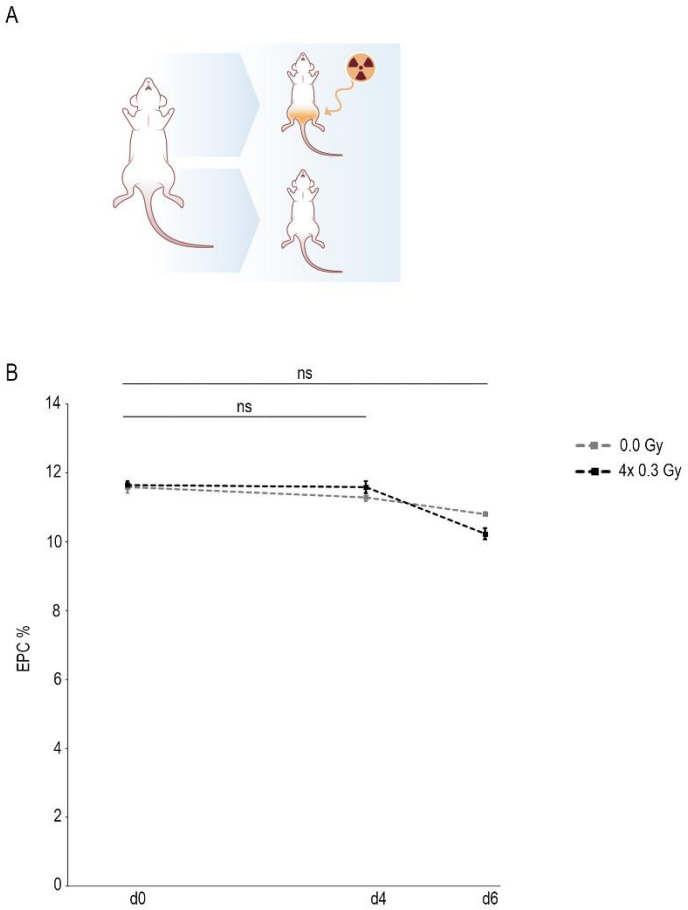

Supplementary Figure 6: In the absence of HLI, LDIR *per se* do not increase the number of circulating EPC.

Both hindlimbs of C57BL/6 mice were sham-irradiated or irradiated with four daily fractions of 0.3 Gy, in consecutive days. (**A**) A schematic illustration of our experimental design. Both hindlimbs are irradiated (in orange) or sham-irradiated. (**B**) Quantitative analysis of EPCs in peripheral blood demonstrated no differences at day 4 in irradiated mice and at day 6 in sham-irradiated mice when each group is compared to the percentage at day 0, before irradiation. Two-way ANOVA was conducted followed by Bonferroni post-hoc test with a between-subject factors of day and irradiation. Means ± SEM are shown from n=6 mice per group; ns, non-significant.

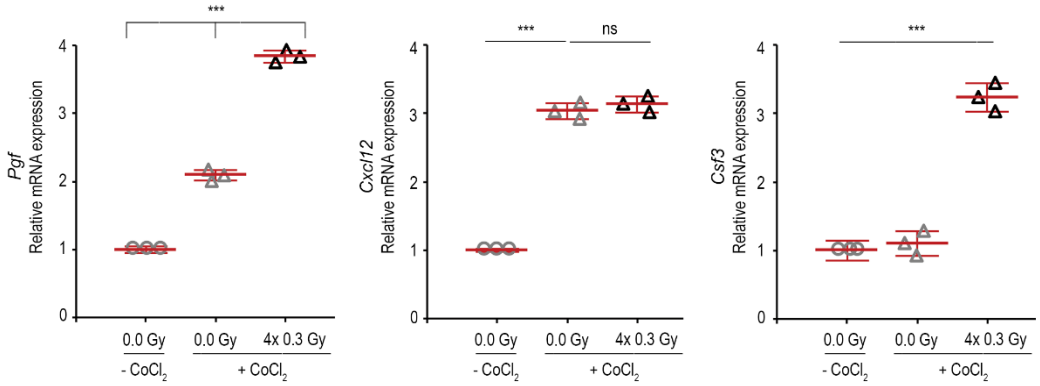

Supplementary Figure 7: LDIR enhance hypoxia-induced *Pgf* and *Csf3* expression.

Cells were cultured with or without $CoCl_2$ (150 µM) in normoxia to mimic hypoxic conditions and immediately exposed to 0.3 Gy. Eight hours post-irradiation, *Pgf* and *Cxcl12* mRNA was quantified by qRT-PCR and 16 hours after *Csf3*. LDIR significantly increase *Pgf* and *Csf3* mRNA expression. Two-way ANOVA was conducted followed by Bonferroni post-hoc test with a between-subject factors of irradiation and $CoCl_2$ treatment. Individual data represent the fold change in gene expression relative to the internal calibrator (−CoCl2) in three independent experiments. Individual data and means ± SEM are shown (in red); ***$P < 0.001$; ns, non-significant.

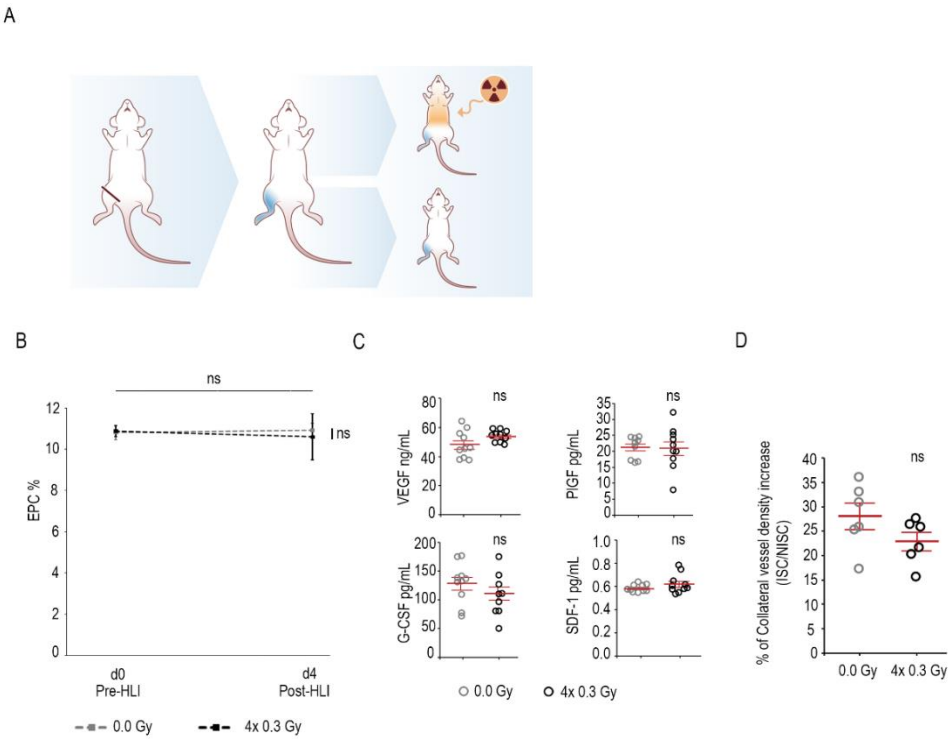

Supplementary Figure 8: The exposure of the ischemic niche to LDIR is critical for the increase of cytokines, mobilization of EPCs and collateral formation.

After surgical induction of unilateral HLI, C57BL/6 mice were irradiated but not in the ischemic niche with four daily fractions of 0.3 Gy, in consecutive days. As a control C57BL/6 mice were sham-irradiated. (**A**) A schematic illustration of our experimental design. After unilateral HLI (represented by a thick brown line), the flow to the ischemic limb is dramatically decreased (in blue). Mice are irradiated (in orange) or sham-irradiated but both hindlimbs are not exposed to LDIR. (**B**) Quantitative analysis of EPCs in peripheral blood demonstrated no differences at day 4 in irradiated mice and in sham-irradiated mice when compared to the percentage at day d0 pre-HLI. Two-way ANOVA was conducted followed by Bonferroni post-hoc test with a between-subject factors of day and irradiation (n=6 mice per group). Means ± SEM are shown. (**C**) The concentrations of VEGF, PlGF, G-CSF, and SDF-1α were measured in the plasma, at day 4 post-HLI. The VEGF, PlGF, G-CSF and SDF-1α concentrations are not changed by LDIR after HLI induction (*n* = 10 mice per group; for VEGF, PlGF, G-CSF values assumed normal distribution and equal variance and independent two-tailed t-test was used; for SDF-1 values not assumed normal distribution, Mann-Whitney test was used). (**D**) Data are represented as the percentage of collateral vessel density (CVD) increase of the ISC limb relatively to the NISC one. At day 45 post-HLI, no difference in CVD upon LDIR was observed. (n=6 mice per group; values assumed normal distribution, equal variance and independent two-tailed t-test was used). (**C, D**) Individual data and means ± SEM (in red) are shown; ns, non-significant. Pre-HLI, before hindlimb ischemia; ISC, ischemic; NISC, non-ischemic.

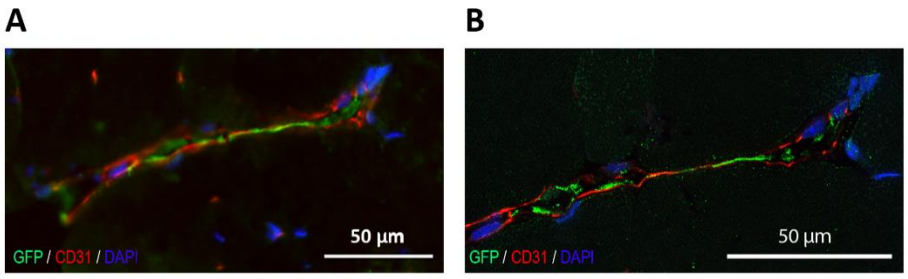

Supplementary Figure S9. Confocal and widefield images of the same ten-micron-thick section show that green and red fluorescent signals belong to the same cells.

(**A**) corresponds to a widefield image acquired with a 20x/0.8 objective on a Zeiss Axiovert 200M microscope, with the same acquisition settings that were used for the images in Figure 5C. (**B**) corresponds to the same section imaged on a Zeiss LSM 880 confocal microscope with a 63x/1.4 oil immersion objective, with the pinhole set to 1 Airy unit (optical slice thickness = 0.7 micron). Notice that even when imaging a single plane, cells show both green and red signals.

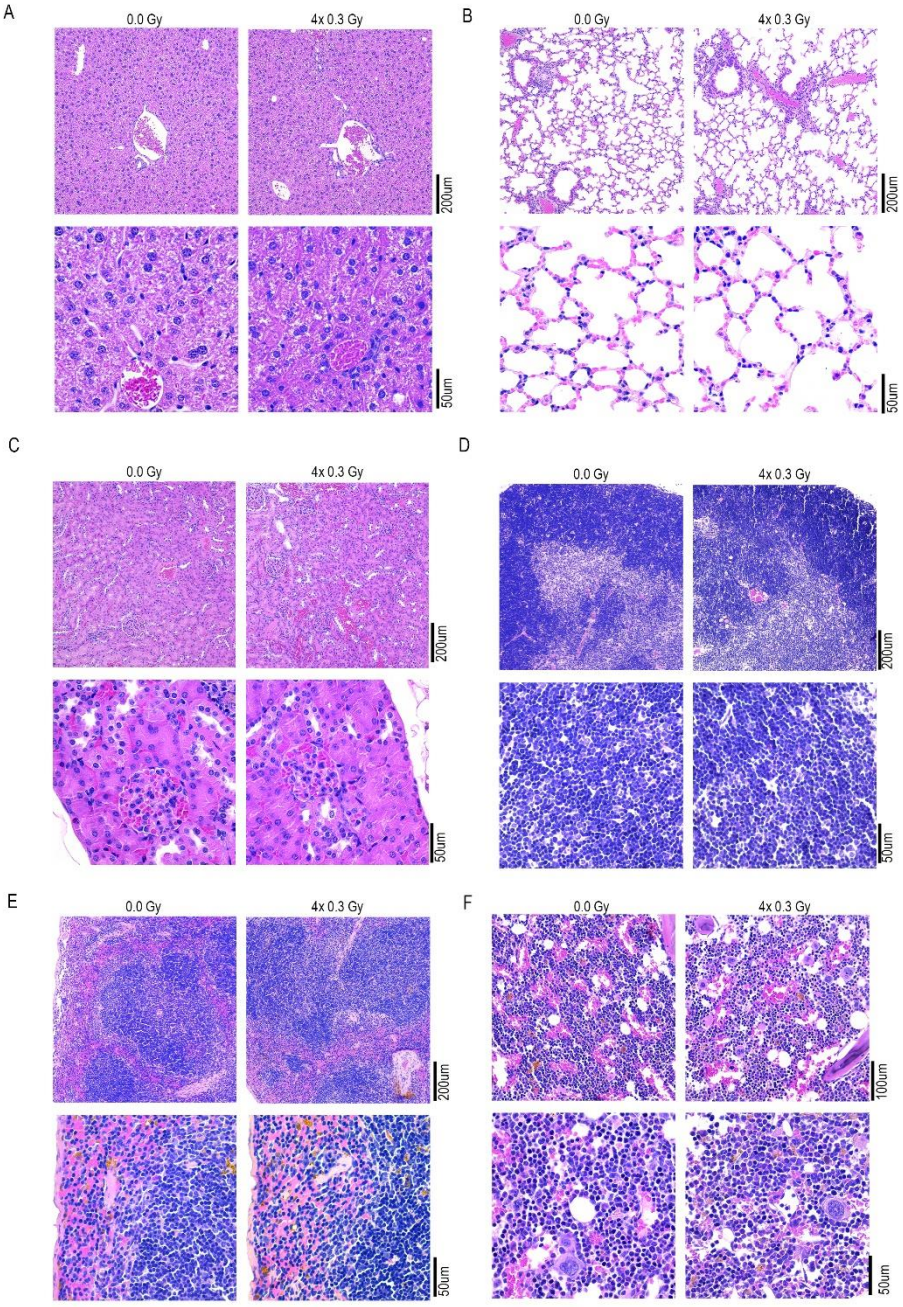

Supplementary Figure S10. Representative microphotographs of selected organs and tissues from sham-irradiated mice and mice irradiated with LDIR.

No significant changes were observed for liver (A), lung (B) and kidney (C); and no signs of immunotoxicity, altered cell distribution/density or neoplasia were seen in lympho-hematopoietic organs, namely thymus (D), spleen (E) and bone marrow (F). Hematoxylin and eosin stain; original objective magnification 5x (upper panels) and 40x (lower panels).

Chapter IV

Low-dose ionizing radiation promotes neovascularization in experimentally induced diabetic mice subjected to hindlimb ischemia.

Paula de Oliveira, Augusto Ministro, Andreia Pena, J. Goyri-O'Neill, Filomena Pina, Esmeralda Poli and Susana Constantino Rosa Santos.

Unpublished data

Abstract

Lower limb ischemia is a major health problem. Due to the absence of effective treatment in the advanced stages of the disease, limb amputation is required. Recently, we demonstrated that low-dose ionizing radiation (LDIR) induces therapeutic neovascularization in a pre-clinical model of hindlimb ischemia (HLI). Accordingly to our previous data, LDIR induces angiogenesis and arteriogenesis and consequently improves blood perfusion in a mice model of HLI. Since almost 50% of the patients with limb ischemia are diabetic, in this work we assessed whether LDIR induces neovascularization in response to HLI in diabetic mice. Our results suggest that LDIR promotes blood perfusion and increases both capillary and collateral densities in diabetic ischemic mice. However, further studies are needed to propose the use of LDIR as an innovative pro-angiogenic strategy in the treatment of critical limb ischemia in diabetic patients.

Keywords

Angiogenesis, Low-doses ionizing radiation, Diabetes, Hindlimb ischemia

Introduction

Peripheral arterial disease (PAD) is characterized by lower limb arterial obstruction due to atherosclerosis. From a pathophysiologic perspective, PAD can be classified as functional or critical. While the functional ischemia occurs when blood flow becomes insufficient during exercise but is normal at rest, the critical one occurs when blood flow is insufficient, even at rest, and is typically characterized by the presence of trophic lesions in the feet or pain while resting. The prevalence of PAD is increasingly recognized as a health burden worldwide. Diabetes, smoking, dyslipidaemia and hypertension are important risk factors for PAD. Decreasing these risk factors may improve the prognosis[1,2]. The severity of the symptoms is dependent on the extent of the obstructive process and collateral circulation[2]. It is known that after being diagnosed with PAD, 25% of the patients will have a worsening ischemic condition with 5 to 10% progressing to critical limb ischemia (CLI). CLI patients have chronic ischemic rest pain, ulcers or gangrene. It is the end-stage of PAD and occurs when blood flow and distal perfusion pressure are insufficient to satisfy the nutritive needs of the limb at rest. CLI is associated with endothelial dysfunction, white blood cell activation and inflammation[2-4]. The primary goals of the treatment of CLI are to relieve ischemic pain, heal ulcers, prevent limb loss, improve patient function and quality of life and prolong overall survival. However, approximately 20%–30% of patients with CLI can not be treated with conventional techniques and still require amputation[5]. Currently, amputation continues to be the recommended solution to the disabling symptoms, even when associated with morbidity and mortality[2,3].

Almost 50% of the patients with limb ischemia have diabetes and this factor increases approximately 3- to 5-fold the risk of PAD[6]. Furthermore, the duration of diabetes and use of insulin are associated with increased risk. PAD is more aggressive in patients with diabetes than in non-diabetic ones. This finding is probably due to diabetes-associated sensory neuropathy, microangiopathy, and infection, as well as a specific pattern of PAD affecting more-distal arteries with fewer possibilities for revascularization. The need for a major amputation is 5 to 10 times higher in patients with diabetes than in individuals without diabetes[2]. In patients with CLI, progression to gangrene occurs in 40% of diabetics when compared to 9% of non-diabetic patients[7]. Further, limb salvage rates in diabetic

patients with CLI have been reported to be lower than in non-diabetic ones, being diabetes an independent risk factor for postoperative amputation and complications in CLI[2].

Diabetes is a metabolic disorder of multifactorial etiology characterized by chronic hyperglycemia and changes in the metabolism of carbohydrates, lipids and proteins, resulting in absolute or relative impairment of insulin secretion and/ or reduction of its biological activity[8]. This disease is associated with a marked impairment in collateral formation. However, angiogenesis is markedly increased in several vascular beds in this disease, particularly in retina. This pathological angiogenesis is linked to an excess of growth factors production, such as VEGF. Diabetes is also correlated with peripheral neuropathy and decreased resistance to infection, which leads to an increased risk of foot ulcers and infections[2,8]. We previously showed that LDIR (lower or equal to 0.8 Gy) induces a pro-angiogenic phenotype in ECs *in vitro,* and promote angiogenesis *in vivo* during regeneration[9]. Moreover, we recently found that 0.3 Gy, administered during 4 consecutive days, induces angiogenesis and collateral development and thereby improves blood perfusion in experimentally induced hindlimb ischemia (HLI)[10]. In the present work, we aim to demonstrate that LDIR also promotes neovascularization in diabetic mice after HLI induction. The obtained results may have the potential to propose an innovative strategy using LDIR for pro-angiogenic therapy, which could provide a significant contribution to the management of CLI disease.

Methods

Study Approval

All animal experiments were performed according to EU regulations and approved by the Animal Ethics Committee of Instituto de Medicina Molecular (iMM) and by the Direção Geral de Alimentação e Veterinária (DGAV; license number 023861/2013). The animal facility of iMM complies with the Portuguese law for the use of laboratory animals (Decreto-Lei 113/2013); and follows the European Directive 2010/63/EU and the FELASA (Federation of European Laboratory Animal Science Associations) guidelines and recommendations concerning laboratory animal welfare.

Mice and Reagents

Eleven-week-old C57BL/6 female mice, purchased from Charles River Laboratories, Spain, were used in all HLI experiments. Mice were group-housed in filter-top cages under controlled conditions (22±2°C; 12h light/12h dark cycle) and with ad libitum access to water and chow.

Briefly, for the HLI procedure and *in vivo* imaging, animals were anesthetized by intraperitoneal (i.p.) injection with a mixture of ketamine (75 mg/Kg BW; Imalgene® 1000, Merial, France) and medetomidine (1 mg/Kg BW; Domitor®, OrionPharma, Espoo, Finland). The anaesthesia was reverted with atipamezole (5mg/kg BW, i.p.; Antisedan®, OrionPharma). Postoperatively, analgesia was administered for pain relief purposes (buprenorphine 100 µl/15-30 g BW q8-12 h; Bupaq®, RichterPharma AG,Wels, Austria) and the animals were closely monitored until the end of the experiments. Mice were euthanized by cervical dislocation.

Diabetes Induction

Streptozotocin (STZ) (50 mg/Kg) (Sigma) was administrated daily by i.p. injection during 5 consecutive days and glucose levels were measured 7 days after. Mice with glucose levels above 300 mg/dL were considered diabetic. In some experiments (collateral and capillary density at 30 days post-HLI), glucose levels were controlled with administration of 1U of Insulin Glargine (Lantus Solostar 5064571)[11,12].

HLI Model

A surgical procedure was performed to induce unilateral HLI in the mice. Briefly, an incision in the skin overlying the thigh of the right hindlimb of each mouse was made and the distal external iliac artery and the femoral artery and veins were ligated and excised. The vein was ligated both to increase the severity of the ischemia as well as to increase the technical reproducibility of the model, since isolation of the femoral artery alone often results in tearing of the vein and consequent hemorrhage. Animals were kept on a 37°C heating pad during surgery and recovery period.

Irradiation

The radiotherapy plan was devised on a dedicated 3D treatment planning system (XiO, Elekta) using an isocentric dose distribution of two opposite fields (0°, 180°) at 6 MV photon energy, normalized to a reference point. Ionizing radiation was delivered, at room temperature, using a linear accelerator that produces X-rays photon beam (Synergy S, Elekta) operating at a dose rate of 500 MU/min.

Anesthetized mice were transferred to an acrylic phantom in order to achieve the adequate thickness to improve homogeneity during the radiation therapy. A computed tomography scan (Somatom Sensation, Siemens) was performed and a volumetric acquisition was carried out. Acquired images were reconstructed with axial slices of 2 mm width, and cross sectional data was transferred to the image processing system work station for contouring the planning target volume.

A 0.6 cm^3 PTW farmer ionizing chamber, connected to UNIDOS electrometer, was used to validate the IR doses calculated by the treatment planning system (TPS), according to the IAEA TRS-398 protocol. We obtained, in average, differences lower than 2% between the experimental and the XiO TPS dose values. The irradiation field included mice entire legs (pelvic girdle down to the feet) or the upper (above hip) part of the mouse body with a single-daily dose of 0.3 Gy administered for four consecutive days, starting 12 hours after ischemia induction. Control mice were sham-irradiated (0.0 Gy) following the same procedure as for the irradiated experimental groups. The irradiation procedure was performed in a non-blinded manner. During this protocol the mice were anesthetized.

Laser-Doppler Perfusion Imaging

The laser-Doppler perfusion imager (MoorLDI-V6, Moor Instruments Ltd, Axminster, UK) was used to assess limb perfusion. Hair was removed one day before laser Doppler analysis using an electrical shaver followed by depilatory cream. Blood flow was measured both in the ischemic and non-ischemic legs, before HLI induction (pre-HLI), immediately post-HLI (post-HLI), and at days 7, 15 and 21 post-HLI (d7 Post-HLI, d15 Post-HLI and d21 Post-HLI, respectively). According to the analysis performed immediately post-HLI, mice were randomized assuring an equal reduction of blood flow in the different experimental groups. Color-coded images of tissue perfusion were recorded: poor or no perfusion was displayed as darkblue, and the highest perfusion level was displayed as red. Mean flux values were calculated using the Moor LDI V5.3 image processing software. To account for variables, such as temperature and ambient light, blood perfusion was expressed as the ratio of ischemic to non-ischemic limb. The mice were kept on a 37°C heating pad to reduce heat loss during measurements.

Immunohistochemistry (IHC) and Capillary Density Analysis

Mice were sacrificed at day 30 post-HLI. The gastrocnemius muscle of both legs were harvested, placed in transverse orientation on a small cork disc with the help of 10% tragacanth (Sigma, Steinheim, Germany), snap frozen in liquid nitrogen cooled isopentane and stored at -80°C until sectioned. Seven-micrometer thick sections were cut on a cryostat (Leica CM 3050S, Nussloch, Germany), mounted on glass slides (Menzel-Glaser Super frost® Plus; Thermo Scientific, Braunschweig, USA) and then processed to IHC to stain ECs with anti-CD31 antibody (Pharmingen). After fixation in acetone, for 10 minutes, hydrogen peroxidase (0.3% diluted in methanol) was added, for 30 minutes, followed by 2 washes in PBS, for 10 minutes. Blocking solution (5% rabbit serum in PBS) was applied, for 30 minutes, and then slides were incubated, for 1 hour, with rat monoclonal antibody against mouse CD31 at 1:500, diluted in PBS-1% BSA. After 3 washes in PBS, for 30 minutes, a secondary biotinylated rabbit anti-rat IgG antibody (Vectastain ABC kit; Vector Laboratories, Inc, Burlingame, CA) was added at 1:200 in PBS-1% BSA plus 5% rabbit serum, for 30 minutes. Washes were performed as before and labeled the avidin-conjugated peroxidase complex (Vector Laboratories, Inc) was used for color development, according to the manufacturer's

recommendations. After PBS washing (3 times of 5 minutes each), DAB peroxidase substrate kit (Vector Laboratories, Inc) was added, for 5 minutes, to localize the immune complexes. The sections were counterstained with Harri's Hematoxylin solution (Bio-Optica, Milan, Italy), for 10 seconds, to visualize nuclei and then mounted with Entellan® (Merck Millipore). Omission of the primary antibody was run in parallel as negative control. All procedure was performed at room temperature. Tissue samples were observed with a Leica DM2500 upright brightfield microscope (Leica Microsystems,) using a 10X objective and images acquired with a digital camera Leica DFC420 (Software Leica FireCam version 3.4.1;). Capillary densities, i.e. number of capillaries per number of muscle fibers, were measured in 2 sections with 200 µm apart. In each section, 4 distinct anatomical areas were measured using the ImageJ®1.48 software.

Contrast Agent Perfusion and Diaphonization

Thirty days post-HLI induction, when mice were well stabilized from the ischemic injury, they were deeply anesthetized and the torso and limbs were shaved. A medial thoracotomy was performed to expose the heart, after which a needle (26 Gauge), attached to an automatic injector, was introduced in the left ventricle. An incision was performed in the right atrium to allow venous drainage. Mice were primarily perfused with heparinized serum (Braun) (3000 IU/L) until the blood was completely removed from circulation. A vasodilatation mixture of adenosine (3.7 µmol/L) and papaverine (11.8 µmol/L) was subsequently administered, for 2 minutes, just before the contrast agent, which consisted of a mixture of barium sulfate (50%) and gelatin (5%). This solution was kept warm until the injection time to avoid thickening. Contrast agent was perfused manually until the feet blanched. Immediately after the injection, mice were transferred to a cold chamber to allow the solidification of the contrast agent. All the solutions were injected with a perfusion rate of 0.01 cm^3/s. Then, the skin of each mouse was removed from the lower body and diaphonization was performed by using a modified version of Spalteholz technique. Briefly, mice were fixated, decalcified, whitened, washed, dehydrated by freeze substitution and placed into a vacuum pump with Spalteholz solution (benzyl benzoate and methyl salicylate), until transparency was acquired. Diaphonization allows the visualization of effective lumen diameter, vessel angulation and emergence position.

Collateral vessels quantification

In order to achieve a homogenous density between the tissues and the media, with minimal absorption or reflection of light, mice were kept in Spalteholz solution during image acquisition. Mice entire limbs were photographed in a magnifier with a light source. After acquisition, images were aligned and stitched together using Adobe Photoshop CS6® and entire limb photographs were obtained. Collateral vessels were manually segmented by highlighting, using Adobe Photoshop CS6®. According to Longland's definition, collateral vessels were considered a defined stem-, mid- and re-entrant zone. According to this definition, collateral vessels with a diameter between 20 and 300 µm were included in our quantification, excluding femoral, saphenous and popliteal arteries and all venous structures. Since arteriogenesis primarily occurs around the occluded blood vessel segment, the region of interest (ROI) in every mouse was in the same anatomic region as in the adductor, surrounding and bellow the surgical occlusion. Collateral vessel density (CVD) was quantified in equivalent ROIs corresponding to 20% of the total limb area. The CVD was calculated as the ratio between the vascular and the ROI areas. All density measurements were performed using ImageJ® software. To exclude variations in the anatomy, perfusion or diaphonization procedures, the CVD value of the non-ischemic limb for each mouse was assumed to correspond to 100%. According to this assumption, the CVD percentage in the ischemic limb was calculated relatively to the non-ischemic one. The percentage of CVD increase was determined as the difference between the CVD percentage among the ischemic and non-ischemic limbs.

Statistics

Experimental results are shown as the mean ± SEM. Data were analyzed with SPSS 20.0 software for Windows. Statistical test employed are detailed described in figure legends. The different analyses were performed in a blinded manner.

Results

LDIR increase perfusion recovery and capillary and collateral densities in diabetic mice

Diabetes were induced with STZ in order to evaluated the effect of LDIR in the restoration of blood flow in a diabetic model. Our preliminary experiments using a diabetic model showed that animals presented high glucose levels (600 mg/dL), lost body weight and most of them also presented signs of cachexia. No differences between ischemic and non-ischemic muscles were observed, even for the sham-irradiated group, which suggests that capillary density is not increased in response to ischemia in diabetic mice. In order to stabilize the glucose levels during the experiments and minimize side effects, insulin Gargine was administrated whenever mice presented glucose levels higher than 300 mg/dL.

Blood flow was analyzed before and after STZ administration to evaluate whether this compound *per se* modulates blood perfusion. Our results shown that STZ does not affect blood flow in mice, since values were similar in both experimental groups (Figure 1A). Then, by using a model of HLI, diabetic mice were irradiated or not (sham-irradiated) with daily fractions of 0.3 Gy, for four consecutive days and perfusion was measured overtime. As shown in Figure 1B and quantified in Figure 1C, a dramatic reduction in blood flow was observed in the ischemic limb immediately after surgery, in comparison with the contralateral limb, and as expected, a gradual improvement in perfusion was observed overtime. Interestingly, the blood flow recovery significantly increased in irradiated diabetic mice when compared to sham-irradiated ones at 7, 15 and 21 days post-HLI. These results demonstrate a benefit of LDIR in diabetic mice with HLI induction. Subsequently, we quantified capillary density and collateral vessel development in hindlimb muscles, since blood flow recovery depends on both angiogenesis and arteriogenesis. In order to quantify the capillary density, diabetic mice were sacrificed at day 30 post-HLI and gastrocnemius muscles were collected. Our results showed that capillary density in irradiated ischemic muscles was increased when compared to sham-irradiated ones. Also as expected, sham-irradiated ischemic muscles showed an increase in capillary density when compared to their contralateral non-ischemic muscles (Figure 1D). The CVD was evaluated, at day 30 post-HLI. Mice were diaphonized and an equivalent ROI, corresponding to 20% of the limb

area, was selected for CVD quantification. A greater increase in CVD was observed for the ischemic limbs of mice exposed to LDIR, versus the sham-irradiated ones (Figure 1E). Noteworthy, no difference in these parameters was seen in non-ischemic muscle, either exposed to LDIR or sham-irradiated, showing that irradiation *per se* does not have an effect on resting vasculature.

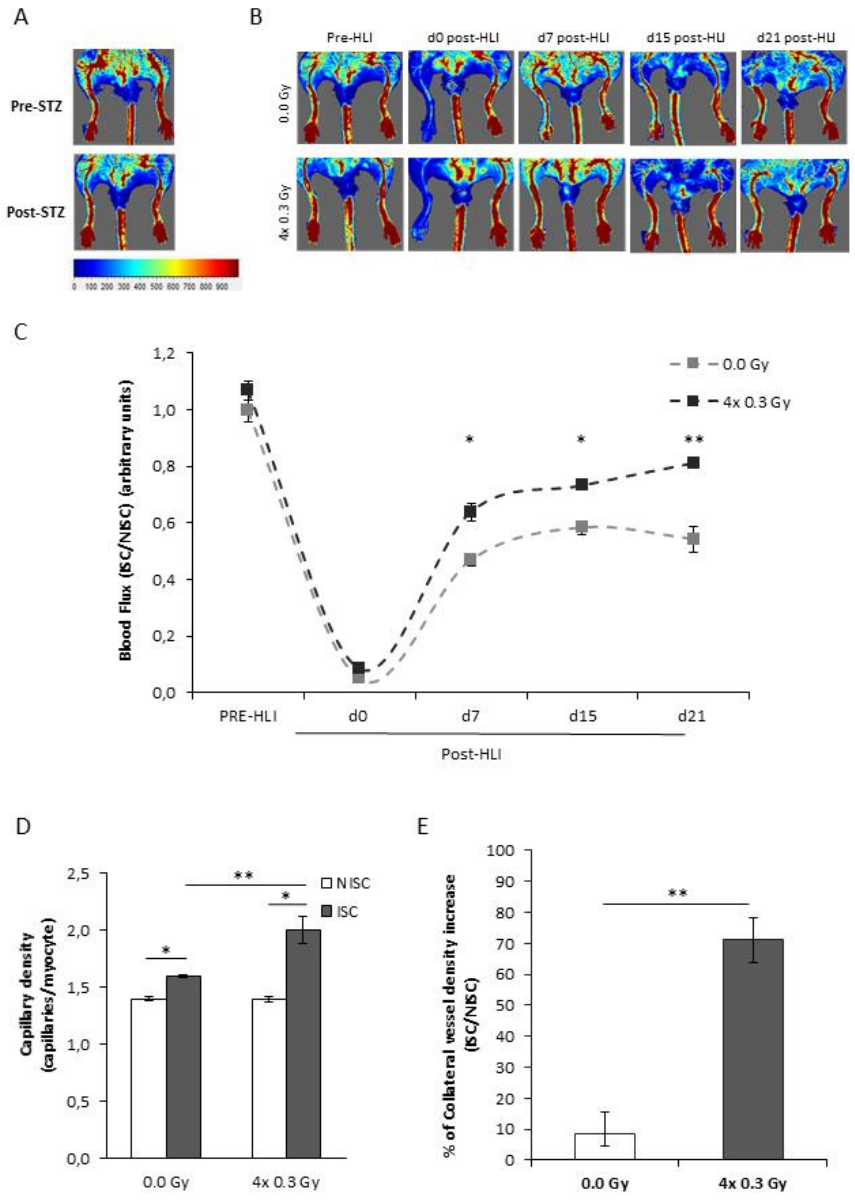

Figure 1. LDIR increases perfusion recovery, capillary and collateral densities in diabetic mice.

After diabetic and surgical induction of unilateral HLI, both hindlimbs of C57BL/6 mice were sham-irradiated or irradiated with daily fractions of 0.3 Gy, for four consecutive days, and allowed to recover. (**A**) Representative laser Doppler flow images pre- and post- STZ induction (**B**)

Representative laser Doppler flow images pre-HLI, and at days 0 (d0), 7 (d7), 15 (d15) and 21 (d21) post-HLI induction. (**C**) Quantitative evaluation of blood flow expressed as a ratio of ISC to NISC limb demonstrated significantly enhanced limb blood perfusion in irradiated mice vs sham-irradiated ones both at days 7 (d7), 15 (d15) and 21 (d21) post-HLI. Changes between groups were assessed by two-way repeated measurements ANOVA followed by Bonferroni post-hoc test (n=5 mice per group). Means ± SEM are shown. (**D**) Quantitative analysis revealed increased capillary density (capillaries/myocyte) in irradiated ischemic gastrocnemius muscles compared with sham-irradiated ischemic ones at day 30 post-HLI. Mixed ANOVA followed by Bonferroni post-hoc test was conducted with a within-subject factor of ISC and the irradiation factor between-subject (n=3 mice per group). (**E**) Data are represented as the percentage of collateral vessel density (CVD) increase of the ISC limb relatively to the NISC one. At day 30 post-HLI, irradiated mice presented significantly higher CVD increase (%) versus sham-irradiated mice. Unpaired two-tailed *t*-test was performed. Values are represented as means ± SEM (n=3 mice per group). *$P < 0.05$; ** $P < 0.01$; HLI, hindlimb ischemia; ISC, ischemic; NISC, non-ischemic; Pre-HLI, before hindlimb ischemia; Pre-STZ, before STZ administration; post-STZ, after STZ administration.

Discussion

CLI represents the most severe clinical manifestation of PAD. This disease involves a severe disturbance of both macro and microcirculation. Patients with diabetes have 3 to 5 times increased risk of suffering from PAD. The lack of available medical therapy for patients with CLI implies that many patients may face amputation as the sole therapeutic option[2]. Amputation is associated with high morbidity and mortality. Therefore, novel therapies are required to treat these patients. Therapeutic angiogenesis aims to induce, augment and control the host angiogenic response in order to re-vascularize the ischemic tissues. Experimental studies are encouraging, while the randomized controlled clinical trials have produced less consistent results[13].

We have previously found that LDIR induces angiogenesis. It promotes EC proliferation and migration, accelerating wound healing and thereby inducing angiogenesis *in vitro* and *in vivo*[9]. Moreover, recently published results show that LDIR promotes therapeutic neovascularization in an experimental model of HLI[10]. In the present work, we aimed to validate these results in a diabetic mice model of HLI. Thus, after surgical induction of unilateral ischemia, both mouse hindlimbs were irradiated with daily fractions of 0.3 Gy, administered during four consecutive days, and a significant increase of blood perfusion and capillary and collateral densities was observed.

However, it is important to refer that the glucose levels were not stable after inducing diabetes by STZ administration. Accordingly, we found that in long term evaluations, it is crucial to administrate insulin after diabetes induction in order to prevent glucose levels higher than 300 mg/dL and consequently minimize the side effects. Our results also suggest that the angiogenic response to HLI is affected by the glucose levels, since mice presenting high glucose levels (600 mg/dL) and consequently signs of cachexia, did not show an increase in capillary density in response to ischemia. Moreover, independently of insulin administration in the course of the experiment, an evaluation of diabetic mice during 4 or more weeks is very difficult to achieve due to the high mortality rate observed in this experimental model, either with or without the LDIR stimuli or ischemia induction and/or recovery. On the other side, the sacrifice of the animals could not be performed before 30 days post-HLI, since the muscles must be recovered and the putative presence of adipocytes that characterize the regenerative phase impedes the measurement of the capillary density. Similarly, the assessment of arteriogenesis should only be performed

after regeneration, when collateral density is already developed and stabilized. To overcome the main limitations of the designed model further studies using a larger number of animals are required.

Overall, we believe that this work has the potential to propose a new strategy for angiogenic therapy using LDIR, providing a significant contribution to CLI disease treatment, particularly in diabetic patients.

References

1 Gornik, H. L. & Beckman, J. A. Cardiology patient page. Peripheral arterial disease. *Circulation* **111**, e169-172, doi:10.1161/01.CIR.0000160581.58633.8B (2005).

2 Norgren, L. *et al.* Inter-Society Consensus for the Management of Peripheral Arterial Disease (TASC II). *Journal of vascular surgery* **45 Suppl S**, S5-67 (2007).

3 Jones, W. S. *et al.* Comparative effectiveness of endovascular and surgical revascularization for patients with peripheral artery disease and critical limb ischemia: systematic review of revascularization in critical limb ischemia. *American heart journal* **167**, 489-498 e487, doi:10.1016/j.ahj.2013.12.012 (2014).

4 Kobayashi, N. *et al.* Prognosis of critical limb ischemia patients with tissue loss after achievement of complete wound healing by endovascular therapy. *Journal of vascular surgery* **61**, 951-959, doi:10.1016/j.jvs.2014.11.065 (2015).

5 Varu, V. N., Hogg, M. E. & Kibbe, M. R. Critical limb ischemia. *Journal of vascular surgery* **51**, 230-241, doi:10.1016/j.jvs.2009.08.073 (2010).

6 Wahlberg, E. Angiogenesis and arteriogenesis in limb ischemia. *Journal of vascular surgery* **38**, 198-203 (2003).

7 Kannel, W. B. Risk factors for atherosclerotic cardiovascular outcomes in different arterial territories. *Journal of cardiovascular risk* **1**, 333-339 (1994).

8 Kolluru, G. K., Bir, S. C. & Kevil, C. G. Endothelial dysfunction and diabetes: effects on angiogenesis, vascular remodeling, and wound healing. *International journal of vascular medicine* **2012**, 918267, doi:10.1155/2012/918267 (2012).

9 Sofia Vala, I. *et al.* Low doses of ionizing radiation promote tumor growth and metastasis by enhancing angiogenesis. *PloS one* **5**, e11222, doi:10.1371/journal.pone.0011222 (2010).

10 Ministro, A. *et al.* Low-dose ionizing radiation induces therapeutic neovascularization in a pre-clinical model of hindlimb ischemia. *Cardiovascular research*, doi:10.1093/cvr/cvx065 (2017).

11 McEvoy, R. C., Andersson, J., Sandler, S. & Hellerstrom, C. Multiple low-dose streptozotocin-induced diabetes in the mouse. Evidence for stimulation of a cytotoxic cellular immune response against an insulin-producing beta cell line. *The Journal of clinical investigation* **74**, 715-722, doi:10.1172/JCI111487 (1984).

12 Graham, M. L., Janecek, J. L., Kittredge, J. A., Hering, B. J. & Schuurman, H. J. The streptozotocin-induced diabetic nude mouse model: differences between animals from different sources. *Comparative medicine* **61**, 356-360 (2011).

13 Dragneva, G., Korpisalo, P. & Yla-Herttuala, S. Promoting blood vessel growth in ischemic diseases: challenges in translating preclinical potential into clinical success. *Disease models & mechanisms* **6**, 312-322, doi:10.1242/dmm.010413 (2013).

Chapter V

Concluding Remarks and Future Perspectives

Concluding Remarks and Future Perspectives

The circulatory system is a network of specialized blood vessels that carry oxygen and nutrients to the organs and tissues of the body[1]. Diseases of the vascular system, including peripheral, cardiac and cerebrovascular diseases, pose a major health burden[2]. More than 25 million people have PAD in Europe and The United Stated and its incidence has been increasing[3]. Particularly, PAD is characterized by the narrowing of blood vessels, which leads to impaired blood supply to the organs[4]. PAD may first exist without symptoms, but with further progression it may lead to intermittent claudication and advanced disease is characterized by pain at rest and ulceration or gangrene of ischemic tissues[5]. Approximately 1% of patients with PAD presents this advanced state of disease resulting in CLI with serious prognosis[3]. Thus, CLI is considered the "end stage" of PAD[6]. Furthermore, in case of CLI, options for vascular interventions, such as stenting or bypass surgery, become limited and amputation of ischemic toes, foot or limbs remains the only option in 50% of patients with CLI within 1 year, because of insufficient response to treatments[5]. Consequently, the development of alternative therapeutic strategies for these high-risk patients is strongly needed.

The concept of "therapeutic angiogenesis", which can be induced by the delivery of specific proteins, genes or cells to ischemic tissue, offers the possibility of blood flow recovery in ischemic limbs. Despite substantial evidence of its efficacy in preclinical studies, as well as some promising phase I/II human trials, larger randomized clinical trials of angiogenic therapies for CLI have been negative. Moreover, there is insufficient knowledge about angiogenic agents, namely regarding dose, frequency of administration and method of delivery in patients with CLI[7].

Therefore, the present PhD thesis aimed to contribute with new insights into therapeutic angiogenesis/neovascularization using LDIR as novel strategy for HLI (Chapter III) as well as for diabetes associated with HLI (Chapter IV), using mouse models.

In our first data (Chapter III), we show that LDIR synergized with HLI significantly enhances blood perfusion, capillary density in gastrocnemius muscle and collateral vessel development. Furthermore, we observe that in vasculature not subjected to ischemic injury, capillary and collateral densities in irradiated mice are similar to those found in the

sham-irradiated ones, suggesting that in non-pathological conditions LDIR *per se* does not have an effect in vascularization. These data are in agreement with our previous results where the inter-ray capillary density was not changed by LDIR after irradiation of an intact zebrafish caudal fin[8]. However, when caudal fin was amputated at mid-fin level, we demonstrated that LDIR significantly increases the inter-ray capillary density. According to our finding, we may hypothesize that LDIR shifts the angiogenic balance towards activation, being this effect dependent of the state of the balance. If in equilibrium, LDIR alone does not tip the balance towards angiogenesis. However, if the balance is deregulated by ischemia, a daily dose of 0.3 Gy, administered for 4 consecutive days, tilts the balance in favor of angiogenesis in a HLI mice model.

In order to understand which genes were significantly modulated by LDIR, a gene expression array was carried out and candidates associated with a pro-angiogenic response were analyzed. Our molecular results showed that the expression of several pro-angiogenic genes including, *Vegfr2, Vegfr1, Fgf2, Angpt2, Pdgfc, Tgfb2, Hgf* and *Met* were clearly up-regulated in ECs isolated from mice muscle subjected to HLI, when comparing with the contralateral limb exclusively exposed to LDIR. The ability of LDIR to increase the expression of the pro-angiogenic genes repertoire in endothelium from the ischemic limb suggests a pro-angiogenic response. LDIR modulates the gene expression of molecular mediators involved in the angiogenic response. It is described that the activation of VEGFR2 leads to a rapid activation of different cellular proteins and consequently to *de novo* mRNA and protein expression of mediators involved in the angiogenic response[8]. Although some of these pro-angiogenic genes are frequently used in clinical trials, only one or two are often reported, while here we achieved a “cocktail” of angiogenic factors, which may be a therapeutic advantage.

The angiogenic potential of ionizing radiation has already been shown for doses equal to or above 2 Gy[9,10]. A study from Heissing lab demonstrated an increase in vascular regeneration using doses of ionizing radiation between 2-10 Gy through recruitment and activation of mast cells[9]. Moreover, Thanik *at al* showed that a single dose of 5 Gy delivered to an ischemic full-thickness cutaneous flap improves vascularity. This study suggests that ionizing radiation creates a stimulus for systemic response leading to pro-angiogenic effects[10]. In addition, we have shown that a lower ionizing radiation dose (0.8 Gy) also

improves angiogenesis by promoting EC proliferation and migration, accelerating wound healing[8]. These doses, lower than the conventional ones used in radiotherapy, have been particularly used in the treatment of benign diseases, due to the anti-inflammatory properties of ionizing radiation[11]. Doses of 0.5 Gy/fraction are especially efficient at the beginning of the inflammatory process, characterized by vasodilatation, edema and leukocyte infiltration. Data from inflamed and ischemic tissues show that ischemia *per se* increases the immune $CD45^+$ cell infiltrate. However, in our results exposure to 0.3 Gy during four consecutive days significantly inhibited the $CD45^+$ cell accumulation, with particular effect on monocytes, macrophages and neutrophils. On the other hand, with doses of 2.0 Gy during four consecutive days the total $CD45^+$ accumulation in ischemic muscle was still reduced; although numbers of monocytes and macrophages were restored but neutrophils were not. These results corroborate previous studies that describe ionizing radiation with both pro- and anti-inflammatory properties[12]. Moreover, these properties depend on the dose of ionizing radiation, since LDIR (<1 Gy) reveals anti-inflammatory properties while doses higher than 2 Gy exert pro-inflammatory effects[13].

Besides the use of ionizing radiation as a potential angiogenic therapy, other strategies have emerged. Several years ago, a step forward was taken in the understanding of the mechanisms of neovascularization. In 1997, Asahara *et al* identified a class of bone marrow-derived circulating EPCs that contribute to vasculogenesis in ischemic tissue. After that, the term "therapeutic neovascularization" was no longer restricted to angiogenesis, but included postnatal vasculogenesis as well. EPCs are primitive bone marrow cells with the capacity to proliferate, migrate and differentiate into ECs. During the last two decades, several studies have demonstrated the capability of EPCs to reduce ischemic damage effects[14,15]. Based on the literature, we also know that EPCs enhance collateral formation[16]. EPC recruitment to sites of arteriogenesis is regulated either by interactions between SDF-1 and its receptor or by several factors secreted by EPCs, both contributing to collateral formation[17,18]. Studies from Shintani *et al* show that cells derived from BMNCs contributed to collateral formation, detected by angiography in a rabbit model of HLI [19].

Our work validates previous studies reporting that EPCs are present in the systemic circulation and are augmented in response to ischemic damage[20,21]. Our results also show that LDIR, synergistically with HLI, enhances the response of EPCs. It is known that the

mobilization of EPCs involves a complex cytokine system. In this way, our results confirm that, in response to HLI induction, the concentration of VEGF, PIGF and G-CSF is significantly increased in the plasma upon LDIR exposure. This cytokine gradient contributes to the mobilization and incorporation of EPCs into ischemic tissues after LDIR exposure and may explain the increase in collateral density observed in our work. However, in the absence of ischemia, LDIR *per se* does not induce that effect, suggesting that the pre-existence of an ischemic tissue/damage is critical for the mobilization of EPCs upon irradiation. The use of EPCs has also been successfully tested in other ischemic diseases. Jackson *et al* demonstrated the incorporation of labeled EPCs in regions of myocardial infarction and[22] Grant *et al* also demonstrated that the recruitment of EPCs to sites of ischemic injury plays a significant role in neovascularization using a mouse model of retinopathy[23].
Moreover, the use of EPCs-based therapies in patients affected by PAD and/or CLI emerged as a new approach for the treatment of ischemic conditions. In this context, results of several clinical studies have rapidly demonstrated the beneficial effect of autologous BM-MNC transplantation to patients affected by ischemic diseases[14,24].

Nevertheless, for the success of pro-angiogenic therapy, it is essential that long-term safety data becomes available. Thus, experimental therapies must be administered with safety monitoring. Some aspects related with the impact of angiogenesis on physiological or pathological processes and the specific adverse effects associated with each therapy should be considered[25]. In this way, we assessed the potential toxicological effects of LDIR, and no significant impact on the morbidity and mortality of the mice was observed after a 52-week follow-up study.

To complement the research work developed in Chapter III, we evaluated the potential of LDIR in promoting neovascularization after HLI in diabetic mice.
The discordance between the promising preclinical studies and the disappointing clinical trials in angiogenic therapies may be due to problems with the animal model. The mice model used in these studies does not totally resemble the human pathology, since patients with PAD frequently have additional diseases/risk factors (such as cardiovascular conditions, diabetes, hypertension, tobacco). Thus, the addition of at least one of these factors to the animal model of HLI will have a great impact in the study of PAD, better

mimicking this disease. Diabetes, which is a very common disease in patients with PAD, is known to impair angiogenesis. Accordingly, our work shows that LDIR synergized with HLI significantly enhance blood perfusion, capillary density in gastrocnemius muscle and collateral vessel development in diabetic mice. However, regarding the use of a diabetic model, STZ administration for diabetes induction and associated problems together with animal welfare will lead us, in the future, to look for a better animal model of diabetes, namely transgenic mice. Also, we believe it is crucial to further validate our experimental work by increasing the number of animals per group.

In summary, this research work proposes a model of enhanced and sustained angiogenesis induction by *in situ* LDIR administration as a promising therapeutic approach for ischemic diseases. LDIR applied as one daily dose of 0.3 Gy, administered for four consecutive days, acts synergistically with the ischemic injury, exacerbating the local pro-angiogenic response. Our results suggest that this is achieved through (i) increased capillary density accompanied by an up-regulation of several pro-angiogenic target genes in ECs localized in the gastrocnemius muscles, a process that is dependent on VEGF signaling and (ii) the mobilization and recruitment of EPCs by increasing the concentrations of VEGF, PIGF and G-CSF, that may explain the collateral density increase in the ischemic limb leading to blood perfusion improvement. We also found that, in response to HLI induction, 0.3 Gy applied during four consecutive days significantly promote blood perfusion, capillary and collateral vessel densities in diabetic mice. Therefore, our data suggest that LDIR may have clinical use in the treatment of CLI, particularly in the case of diabetic patients. Additionally, we have an ongoing exploratory clinical trial to determine the clinical and molecular effects of LDIR in “non-option” CLI patients. The success of this clinical trial will lead to the development of new trials to propose a novel and effective therapeutic tool with worldwide impact to PAD.

Overall, the present PhD work improves the knowledge on the biological effects of LDIR, in a context of HLI and diabetes, and proposes an innovative and non-invasive strategy for pro-angiogenic therapy using LDIR. This could provide a significant contribution to the management of CLI disease, which will be further corroborated by the ongoing clinical trial.

References

1 Gornik, H. L. & Beckman, J. A. Cardiology patient page. Peripheral arterial disease. *Circulation* **111**, e169-172, doi:10.1161/01.CIR.0000160581.58633.8B (2005).

2 Sen, S., McDonald, S. P., Coates, P. T. & Bonder, C. S. Endothelial progenitor cells: novel biomarker and promising cell therapy for cardiovascular disease. *Clinical science* **120**, 263-283, doi:10.1042/CS20100429 (2011).

3 Suzuki, H. & Iso, Y. Clinical application of vascular regenerative therapy for peripheral artery disease. *BioMed research international* **2013**, 179730, doi:10.1155/2013/179730 (2013).

4 Samura, M. *et al.* Therapeutic strategies for cell-based neovascularization in critical limb ischemia. *J Transl Med* **15**, 49 (2017).

5 van Weel, V., van Tongeren, R. B., van Hinsbergh, V. W., van Bockel, J. H. & Quax, P. H. Vascular growth in ischemic limbs: a review of mechanisms and possible therapeutic stimulation. *Annals of vascular surgery* **22**, 582-597, doi:10.1016/j.avsg.2008.02.017 (2008).

6 Varu, V. N., Hogg, M. E. & Kibbe, M. R. Critical limb ischemia. *Journal of vascular surgery* **51**, 230-241, doi:10.1016/j.jvs.2009.08.073 (2010).

7 Cooke, J. P. & Losordo, D. W. Modulating the vascular response to limb ischemia: angiogenic and cell therapies. *Circulation research* **116**, 1561-1578, doi:10.1161/CIRCRESAHA.115.303565 (2015).

8 Sofia Vala, I. *et al.* Low doses of ionizing radiation promote tumor growth and metastasis by enhancing angiogenesis. *PloS one* **5**, e11222, doi:10.1371/journal.pone.0011222 (2010).

9 Heissig, B. *et al.* Low-dose irradiation promotes tissue revascularization through VEGF release from mast cells and MMP-9-mediated progenitor cell mobilization. *The Journal of experimental medicine* **202**, 739-750, doi:10.1084/jem.20050959 (2005).

10 Thanik, V. D. *et al.* Cutaneous low-dose radiation increases tissue vascularity through upregulation of angiogenic and vasculogenic pathways. *Journal of vascular research* **47**, 472-480, doi:10.1159/000313875 (2010).

11 Luis, A. M. Radiotherapy for non-malignant diseases. *Reports of Practical Oncology and Radiotherapy* **18**, S14-S15, doi:10.1016/j.rpor.2013.04.004 (2013).

12 Di Maggio, F. M. *et al.* Portrait of inflammatory response to ionizing radiation treatment. *Journal of inflammation* **12**, 14, doi:10.1186/s12950-015-0058-3 (2015).

13 Rodel, F. *et al.* Modulation of inflammatory immune reactions by low-dose ionizing radiation: molecular mechanisms and clinical application. *Current medicinal chemistry* **19**, 1741-1750 (2012).

14 Schiavetta, A. *et al.* A phase II trial of autologous transplantation of bone marrow stem cells for critical limb ischemia: results of the Naples and Pietra Ligure Evaluation of Stem Cells study. *Stem cells translational medicine* **1**, 572-578, doi:10.5966/sctm.2012-0021 (2012).

15 Murasawa, S. & Asahara, T. Endothelial progenitor cells for vasculogenesis. *Physiology* **20**, 36-42, doi:10.1152/physiol.00033.2004 (2005).

16 Tongers, J., Roncalli, J. G. & Losordo, D. W. Role of endothelial progenitor cells during ischemia-induced vasculogenesis and collateral formation. *Microvascular research* **79**, 200-206, doi:10.1016/j.mvr.2010.01.012 (2010).

17 Carmeliet, P. & Luttun, A. The emerging role of the bone marrow-derived stem cells in (therapeutic) angiogenesis. *Thrombosis and haemostasis* **86**, 289-297 (2001).

18 Schaper, W. & Scholz, D. Factors regulating arteriogenesis. *Arteriosclerosis, thrombosis, and vascular biology* **23**, 1143-1151, doi:10.1161/01.ATV.0000069625.11230.96 (2003).

19 Shintani, S. *et al.* Augmentation of postnatal neovascularization with autologous bone marrow transplantation. *Circulation* **103**, 897-903 (2001).

20 Crosby, J. R. *et al.* Endothelial cells of hematopoietic origin make a significant contribution to adult blood vessel formation. *Circulation research* **87**, 728-730 (2000).

21 Murohara, T. *et al.* Transplanted cord blood-derived endothelial precursor cells augment postnatal neovascularization. *The Journal of clinical investigation* **105**, 1527-1536, doi:10.1172/JCI8296 (2000).

22 Jackson, K. A. *et al.* Regeneration of ischemic cardiac muscle and vascular endothelium by adult stem cells. *The Journal of clinical investigation* **107**, 1395-1402, doi:10.1172/JCI12150 (2001).

23 Grant, M. B. *et al.* Adult hematopoietic stem cells provide functional hemangioblast activity during retinal neovascularization. *Nature medicine* **8**, 607-612, doi:10.1038/nm0602-607 (2002).

24 Raval, Z. & Losordo, D. W. Cell therapy of peripheral arterial disease: from experimental findings to clinical trials. *Circulation research* **112**, 1288-1302, doi:10.1161/CIRCRESAHA.113.300565 (2013).

25 Tongers, J., Roncalli, J. G. & Losordo, D. W. Therapeutic angiogenesis for critical limb ischemia: microvascular therapies coming of age. *Circulation* **118**, 9-16, doi:10.1161/CIRCULATIONAHA.108.784371 (2008).